ESTIMATION OF STRESS AND DEFORMATION PARAMETERS AT SALT FORK RIVER BRIDGES ON US 177

By

ARTHUR J. SCHWIDDER

Bachelor of Science

Oklahoma State University

Stillwater, Oklahoma

1993

Submitted to the Faculty of the Graduate College of the Oklahoma State University in partial fulfillment of the requirements for the Degree of MASTER OF SCIENCE July, 1994

ESTIMATION OF STRESS AND DEFORMATION PARAMETERS AT SALT FORK RIVER BRIDGES ON US 177

Thesis Approved:

Donald R. Snethen

Thesis Adviser

Thomas C. Collins

Dean of the Graduate College

ACKNOWLEDGEMENTS

I would like to thank my adviser, Dr. Don Snethen, for hiring me to work on this research project and for all his help on the research. I would also like to thank Dr. Snethen for his help in getting me a scholarship to help pay for tuition. My sincere appreciation also extends to my other committee members, Dr. Mike Ayers and Dr. Vernon Mast, for their help on this research project. I also wish to express my sincere appreciation to the Oklahoma Department of Transportation for funding this research.

Also, there were many people in the Oklahoma Department of Transportation who provided some much needed assistance for this research. Among them were Dr. Jim Nevels, who let me spend time out in the field with his drilling crew as they performed the geotechnical testing for this project. I would also like to thank Mr. Bruce Fraker for his help in finding old bridge plans, as well as Anthony Apple and Mike Kahn, for getting me in touch with Mr. Fraker. Finally, I would like to thank Mr. Curt Hayes in the Research Division for his help.

TABLE OF CONTENTS

LIST OF TABLES

Table Page

LIST OF FIGURES

Figure | Page

CHAPTER 1

INTRODUCTION

Stress and deformation within approach embankments of highway bridges cause many problems for state transportation departments. The end result of these deformations is often a bump at the end of the bridge, which requires expensive repairs. There are many reasons for these deformations, including lateral earth pressures on the abutment wall, settlement of the embankment and foundation soil, and lateral movement of the embankment soil as it settles.

Description of Research Project

This research project addresses some of these issues. It tests five methods of constructing approach embankments with respect to how each one performs with regard to deformations. This project involves three bridges planned for construction on US highway 177 in Noble County, Oklahoma, across the Salt Fork River 8 miles south of Ponca City. The main bridge and two overflow bridges are labeled from south to north, bridge "A", bridge "B", and bridge "C". The south approach embankment of bridge A is twice as high as the other approaches, so it will not be used in the research project. However, the approaches on the north end of bridge A and both ends of bridges B and C are all between 13 and 17 feet high. Therefore, the differences in height will not be enough to appreciably affect the settlements from one approach to the next.

Each of the five approaches in the study will be built using a different construction method. The north approach of bridge A will be constructed using unclassified borrow, which is a widely used method of constructing bridge approaches in Oklahoma and will serve as the control embankment. The south approach of bridge B will be constructed using a geotextile reinforced retaining wall with granular backfill, while the north approach of bridge B will be constructed using controlled low strength backfill material, which is a mixture of portland cement, fly ash, sand, and water. The south embankment of bridge C will be constructed using dynamic compaction of the foundation and embankment materials, with the backfill for this embankment being granular backfill. The north abutment of bridge C will be constructed using granular backfill with routine construction practices. The material specifications for granular backfill and typical sections of embankments and underdrains may be found in appendix B.

In order to evaluate the performance of each approach embankment, instrumentation will be placed in each embankment. The layout of these instruments is shown in appendix B. An open tube piezometer will be placed at the center of the embankment, with two inclinometer casings placed in the center of each traffic lane and midway longitudinally on the embankment. Two settlement gauges will be placed beneath the center of the approach fill section being treated, and three total pressure cells will be placed on the centerline of the abutment wall. There will be surface settlement points located on a grid pattern over the embankment surface, and their exact locations will be based on embankment heights, treatment methods, and material properties. The type of settlement gauges, pressure cells, piezometers, and inclinometers will be based on anticipated settlement and lateral earth pressures. Also, an instrumentation specialist will review the final instrumentation plans. Once construction is completed, these instruments will be monitored over a two year period.

This data will be evaluated in two ways. First, the data will be compared with values predicted for these embankments using conventional settlement prediction methods. This will be used to determine the accuracy and reliability of these equations. Second, this data will be used to evaluate the performance of each embankment construction method.

Purpose of this Thesis

The purpose of this thesis is to estimate the settlement of each of the five approach embankments at the Salt Fork River site, as well as lateral earth pressures on the abutment walls. This will allow proper instrumentation to be chosen for these embankments, and it will form the basis on which current settlement and lateral earth pressure prediction methods can be tested. Eventually, the settlement and lateral earth pressures measured from the instruments will be compared with these calculated results.

In order to estimate lateral earth pressures on the abutment wall and settlement of the embankment, several steps were taken. First, a thorough search of the literature was done in order to get background information on this subject. This included looking into problems associated with approach embankments, reviewing methods for estimating stress and deformation parameters for such embankments, and reviewing embankment settlement prediction methods based on the cone penetration test. Next, several settlement prediction methods were evaluated. The University of Oklahoma had done an extensive study on bridge approach settlement, and they developed a statistical model for estimating bridge approach settlement. This was reviewed, and the statistical method was compared to Schmertmann's and Sanglerat's methods for predicting settlement from cone penetration test results. For Schmertmann's and Sanglerat's methods, several different equations were used for calculating changes in stress in the foundation soil. These different methods were tested on the approach embankments at 12 of the OU sites throughout Oklahoma. Cone penetration test data and settlement data were available at each of these sites, so the predicted settlement was compared to the measured settlement at each site. From this, the most accurate method was chosen to calculate settlement at the Salt Fork River research site. In order to calculate the settlement of the embankments, a detailed boring and in situ testing program was performed. From this, foundation soil profiles and properties were obtained, and estimates were made for the properties of the embankment materials. Once this was done, settlement and lateral earth pressure calculations were made for the approach embankments at the Salt Fork site.

CHAPTER 2

BACKGROUND INFORMATION

Many state transportation departments have problems with bridge approaches. In most cases, the approach fill is placed on the existing ground surface, while the bridge itself is founded on deep foundations. When the approach slab settles, the bridge does not, and this creates a bump at the end of the bridge. This requires frequent and expensive maintenance, and it creates extra wear on the bridge structure. The following sections discuss problems associated with this bump at the end of the bridge, as well as methods to estimate stress and deformation parameters and settlement prediction methods.

Bump at the End of the Bridge

Most bridges are founded on deep foundations, and the approaches consist of fill placed on the existing ground surface. Therefore, when the approach slab settles, the bridge does not. This creates a bump, which can cause several problems. First, it creates discomfort for those who must drive over the bridge, and it causes extra wear on these vehicles. Second, it is a potential safety problem if the differential settlement is more than about two inches. Next, such a bump causes impact loads on the bridge itself, causing premature wear on the bridge deck and the bridge structure. Bridges are generally not designed to handle such repeated loadings. Finally, maintenance must be done on these bridges, which is often expensive and inconvenient, as traffic must be rerouted. Figure 1 shows examples of bridges where approach fill settlement is a problem.

Next, it is logical to ask what causes the approach embankments to settle. In a report published by the Colorado Department of Highways, the following causes of bridge approach settlement were identified (1):

- time dependent consolidation of the embankment foundation,
- time dependent consolidation of the approach embankment,
- poor compaction of the abutment backfill caused by restricted access of standard compaction equipment,
- erosion of soil at the abutment face, and
- poor drainage of the embankment and abutment backfill.

In another report published by the University of Oklahoma (15), the researchers surveyed 52 agencies that have had problems with settlement of bridge approaches. The results of this survey were similar to the conclusions of the Colorado Department of Highways study. The OU report states that the differential settlement is due to settlement of the embankment foundation, type of embankment material, and technique and quality of embankment construction. It also sites erosion of soil from the abutment sides and embankment. Of all of these causes, though, settlement or consolidation of the foundation soil was considered by far to be the most significant (10).

Horizontal Displacement of Abutment Wall

Another problem that can occur at the ends of the bridge is lateral displacement of the abutment wall. This can happen in one of two ways. First, lateral earth pressure from the fill can push the wall away from the fill, and this can either cause the abutment wall to

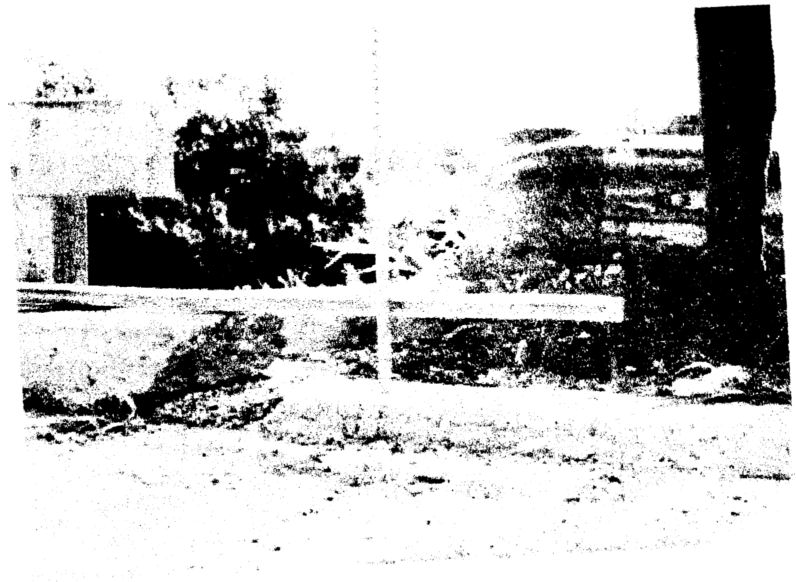

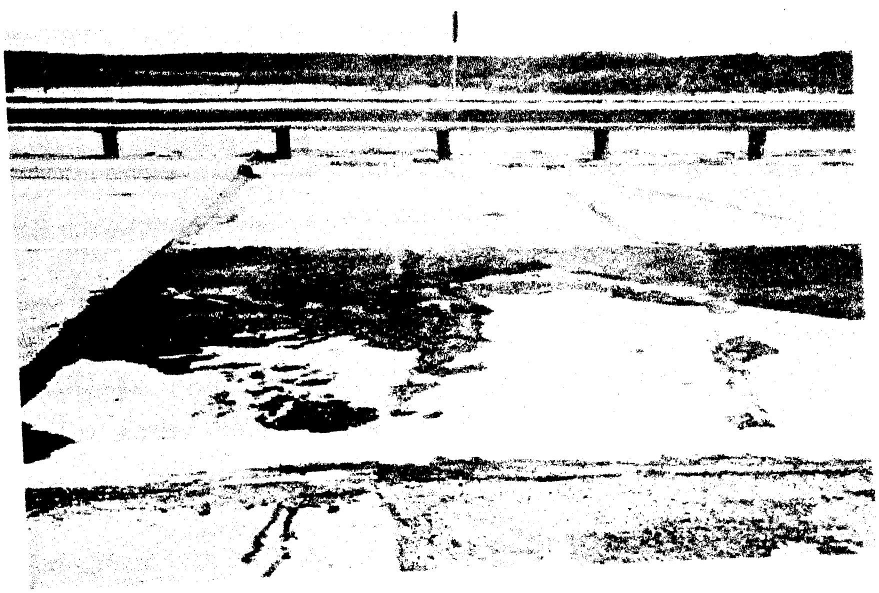

Figure 1. Examples of Approach Embankments with Settlement Problem (After Laguros, Zaman, and Mahmood, 1990)

tilt about the base of the wall or about the base of the piles supporting the wall (7). Another more common way for the wall to tilt occurs when the foundation soil is soft and excessive settlement occurs in this soil. As it settles, it also "squeezes" laterally. This bends the piles that support the abutment wall, forcing them away from the fill side of the wall. The abutment wall is then tilted backwards toward the fill, as shown in Figure 2, (7).

Methods for Estimating Stress and Deformation Parameters

In order to design a proper bridge approach, it is necessary to first estimate the stress and deformation parameters in the embankment. First, the lateral earth pressure on the abutment wall is calculated, which is used to design the abutment wall and the drain system behind the abutment wall. Next, settlement of the embankment is calculated, which generally includes settlement of the embankment itself and the foundation soil. Finally, lateral movement at the wall and embankment is calculated. All of these procedures are described in the next three sections.

Lateral Earth Pressures

The abutment wall behaves as a normal retaining wall, except that it is generally built on deep foundations. The most widely used methods for calculating lateral earth pressures behind abutment walls utilize either the Coulomb method or the Rankine method. There is also a more recent method developed by Caquot and Kerisel in 1948.

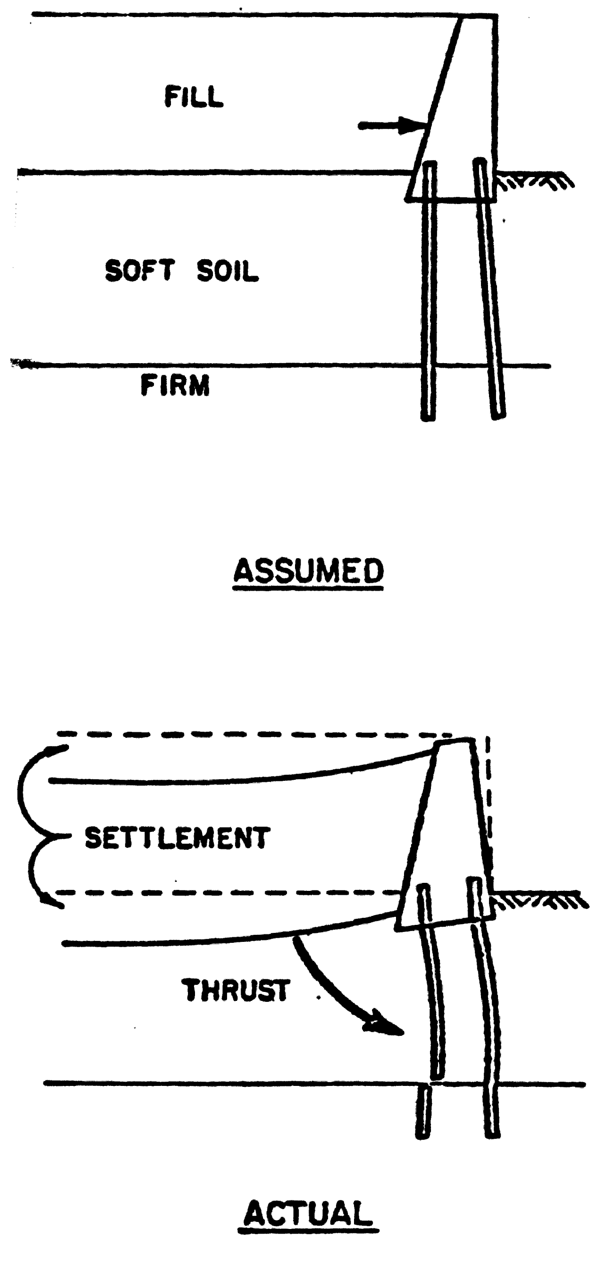

Figure 2. Lateral Squeezing of Soft Foundation Soil
(after Cheny and Chassie, 1982)

In the Coulomb the equations for the active case are as follows (3):

$$P_a = \frac{\gamma H^2}{2} K_a \tag{1}$$

and

$$K_a = \frac{\sin^2(\phi - \beta)}{\sin^2\beta \sin(\beta - \delta)\left[1 + \sqrt{\frac{\sin(\phi+\delta)\sin(\phi+i)}{\sin(\alpha-\delta)\sin(\alpha-i)}}\right]^2} \tag{2}$$

where

ϕ = angle of internal friction,

β = slope of the back of the retaining wall,

δ = angle of soil to wall friction,

i = slope of the backfill soil,

γ = unit weight of soil, and

H = height of wall.

This active case corresponds to a situation where the soil pushes against the wall, pushing the wall away from the soil. On the other hand, the passive case corresponds to the wall being pushed into the soil mass. The equations for the passive case are as follows (3):

$$P_p = \frac{\gamma H^2}{2} K_p \tag{3}$$

where

$$K_p = \frac{\sin^2(\phi + \beta)}{\sin^2\beta \sin(\beta - \delta)\left[1 - \sqrt{\frac{\sin(\phi+\delta)\sin(\phi+i)}{\sin(\beta-\delta)\sin(\alpha-i)}}\right]^2}. \tag{4}$$

Also, figure 3 defines i, β, δ, and ϕ and shows the wall configuration that was used to develop Coulomb's equations.

Several Assumptions were made by Coulomb when he developed these equations (4). First, the soil was assumed to be isotropic and homogeneous, having both internal friction and cohesion. Second, the rupture surface was assumed to be planar, and the friction resistance was assumed to be distributed uniformly along that surface. Next, the

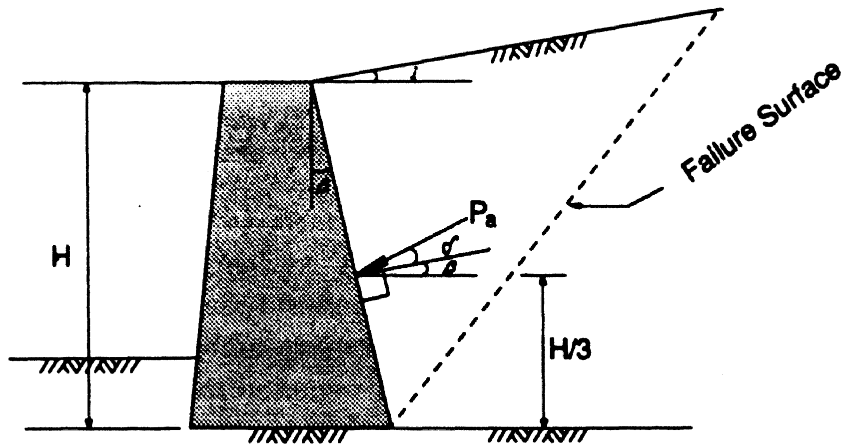

(a) Active Pressure Force

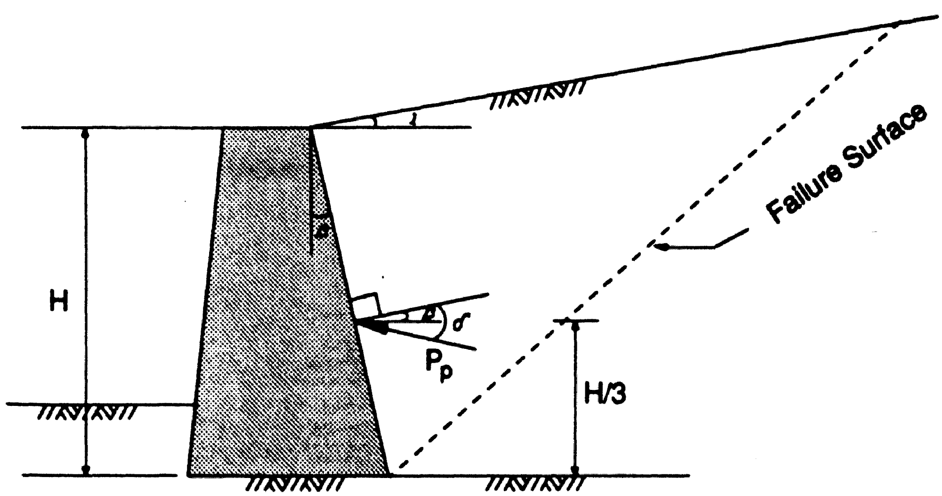

(b) Passive Pressure Force

Figure 3. Wall Configuration for Coulomb Theory for Active and Passive Earth Pressures (After Barker, Duncan, Roijani, Ooi, Tan, and Kim, 1991)

failure wedge was assumed to be a rigid body undergoing translation. Also, wall friction was assumed to develop as the failure wedge moves with respect to the wall, and the backfill surface was assumed to be planar. Finally, failure was assumed to be a plane strain problem.

In 1857, Rankine developed his equations for lateral earth pressure. The equations for active pressure are as follows (4):

$$P_a = \tfrac{1}{2}\gamma H^2 K_a \qquad (5)$$

where
$$K_a = \frac{\cos i - \sqrt{\cos^2 i - \cos^2 \phi}}{\cos i + \sqrt{\cos^2 i - \cos^2 \phi}}. \qquad (7)$$

The equations for passive earth pressure are as follows:

$$P_p = \tfrac{1}{2}\gamma H^2 K_a \qquad (7)$$

where
$$K_p = \frac{\cos i + \sqrt{\cos^2 i - \cos^2 \phi}}{\cos i - \sqrt{\cos^2 i - \cos^2 \phi}}. \qquad (8)$$

The assumptions for these equations are similar to the assumptions for the Coulomb equations, except that the Rankine equations assume no wall friction or soil cohesion. A situation where Rankine's method works well is when the wall friction angle, δ is equal to the slope of the backfill surface, i (3).

In 1948, Caquot and Kerisel (6)developed a method for finding lateral earth pressure that assumes a log spiral failure surface, and the shape of this failure surface is shown in Figure 4 . The equations for P_a and P_p are the same as Coulomb's method and Rankine's method. However K_a and K_p are found from Table 1. This method gives results that are very similar to Rankine's method when the ground surface is horizontal and the β angle is 0.

Settlement of the Embankment

There are two separate settlements that are calculated for a bridge approach. The first is settlement of the foundation soil underneath the embankment. This is where the majority of the approach settlement comes from (20). The other is settlement within the approach embankment itself. This settlement is small compared to the settlement of the foundation soil (20), and it can be mostly eliminated with proper placement and compaction of the approach fill. The following sections describe the various methods available for calculating approach settlement.

Settlement of the Foundation Soil The first step in calculating the settlement of the foundation soil is to determine the soil profile from the ground surface to bedrock. This can be done using continuous tube sampling with laboratory testing, Standard Penetration Tests, Cone Penetration Tests, Dilatometer testing, or Pressuremeter testing. The type of test used depends upon the soil type at the site. General information on the soil type can be obtained from county soil maps or from other published material or by using geophysical exploration techniques. The number of test holes depends upon the type of construction. Also, if extreme irregularities in soil type or depth to bedrock are encountered, more test holes can be ordered by the engineer.

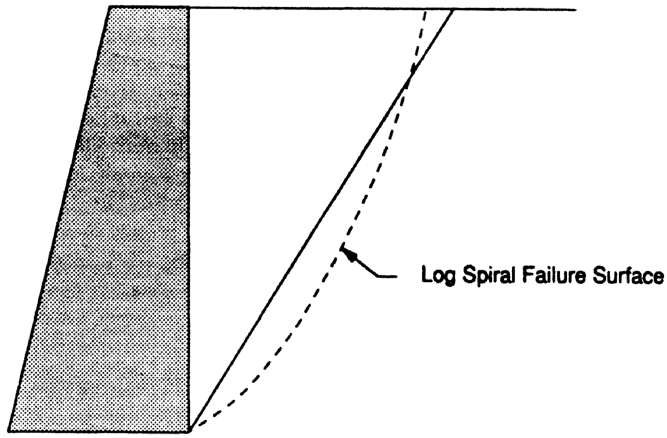

Figure 4. Comparison of the Log Spiral and Straight Line Failure Surfaces for Active Conditions (after Barker, Duncan, Roijiani, Ooi, Tan, and Kim, 1991)

K_a

δ	i	β	$\phi_f{}^\circ$					
			20	25	30	35	40	45
		-10	0.37	0.3	0.24	0.19	0.14	0.11
	-15	0	0.42	0.35	0.29	0.24	0.19	0.16
		10	0.45	0.39	0.34	0.29	0.24	0.21
		-10	0.42	0.34	0.27	0.21	0.16	0.12
0	0	0	0.49	0.41	0.33	0.27	0.22	0.17
		10	0.55	0.47	0.4	0.34	0.28	0.24
		-10	0.55	0.41	0.32	0.23	0.17	0.13
	15	0	0.65	0.51	0.41	0.32	0.25	0.2
		10	0.75	0.6	0.49	0.41	0.34	0.28
		-10	0.31	0.26	0.21	0.17	0.14	0.11
	-15	0	0.37	0.31	0.26	0.23	0.19	0.17
		10	0.41	0.36	0.31	0.27	0.25	0.23
		-10	0.37	0.3	0.24	0.19	0.15	0.12
ϕ_f	0	0	0.44	0.37	0.3	0.26	0.22	0.19
		10	0.5	0.43	0.38	0.33	0.3	0.26
		-10	0.5	0.37	0.29	0.22	0.17	0.14
	15	0	0.61	0.48	0.37	0.32	0.25	0.21
		10	0.72	0.58	0.46	0.42	0.35	0.31

K_p

δ	i	β	$\phi_f{}^\circ$					
			20	25	30	35	40	45
		-10	1.32	1.66	2.05	2.52	3.09	3.95
	-15	0	1.09	1.33	1.56	1.82	2.09	2.48
		10	0.87	1.03	1.17	1.3	1.33	1.54
		-10	2.33	2.96	3.82	5	6.68	9.2
0	0	0	2.04	2.46	3	3.69	4.59	5.83
		10	1.74	1.89	2.33	2.7	3.14	3.69
		-10	3.36	4.56	6.3	8.98	12.2	20
	15	0	2.99	3.86	5.04	6.72	10.4	12.8
		10	2.63	3.23	3.97	4.98	6.37	8.2
		-10	1.95	2.9	4.39	6.97	11.8	22.7
	-15	0	1.62	2.31	3.35	5.04	7.99	14.3
		10	1.29	1.79	2.5	3.58	5.09	8.86
		-10	3.45	5.17	8.17	13.8	25.5	52.9
$-\phi_f{}^\circ$	0	0	3.01	4.29	6.42	10.2	17.5	33.5
		10	2.57	3.5	4.98	7.47	12	21.2
		-10	4.95	7.95	13.5	24.8	50.4	11.5
	15	0	4.42	6.72	10.8	18.6	39.6	73.6
		10	3.88	5.62	8.51	13.8	24.3	46.9

Table 1. Values of K_a and K_p for Log Spiral Failure Surface (After Caquot and Kerisel, 1948)

Once the subsurface profile is defined, the change in stress in each soil layer due to the embankment is calculated. Several methods exist for doing this, including Schmertmann's method for CPT results or elastic theory equations such as the Boussinesq equations, Newmark's chart (9), or Perloff's method for stress due to a trapezoidal embankment (17). Schmertmann's method was developed to find the settlement of a shallow footing on sand. It assumes either a square or rectangular footing, i.e. a footing with a finite length and width. His method uses influence factors to find the change in stress at a given depth below the footing, and these influence factors are shown in Figure 5. Boussinesq equations are used to find the vertical stress below the center of a uniformly loaded circular or rectangular footing. Distribution of vertical stress under a rectangular load may be found from the following equation:

$$\Delta p = q[I_1 + I_2 + I_3 + I_4] \tag{9}$$

where I_1, I_2, I_3, and I_4 are influence values for each individual rectangle

q = uniform rectangular load

The influence factors each give the load (for a given depth) at the corner of a rectangular uniformly loaded area. Therefore, for a uniformly loaded rectangle, one must divide it into four equal parts (1, 2, 3, and 4) and calculate the influence factor for each part. The individual influence factors are found by defining m = B/z and n = L/z, where B and L are the width and length of the foundation. The Boussinesq method, like Schmertmann's method is limited in that the footing has to be a finite length. Newmark, on the other hand, developed a method to find the change in stress at any depth under a footing of any shape, provided that the area is uniformly loaded. This method involves placing a scale

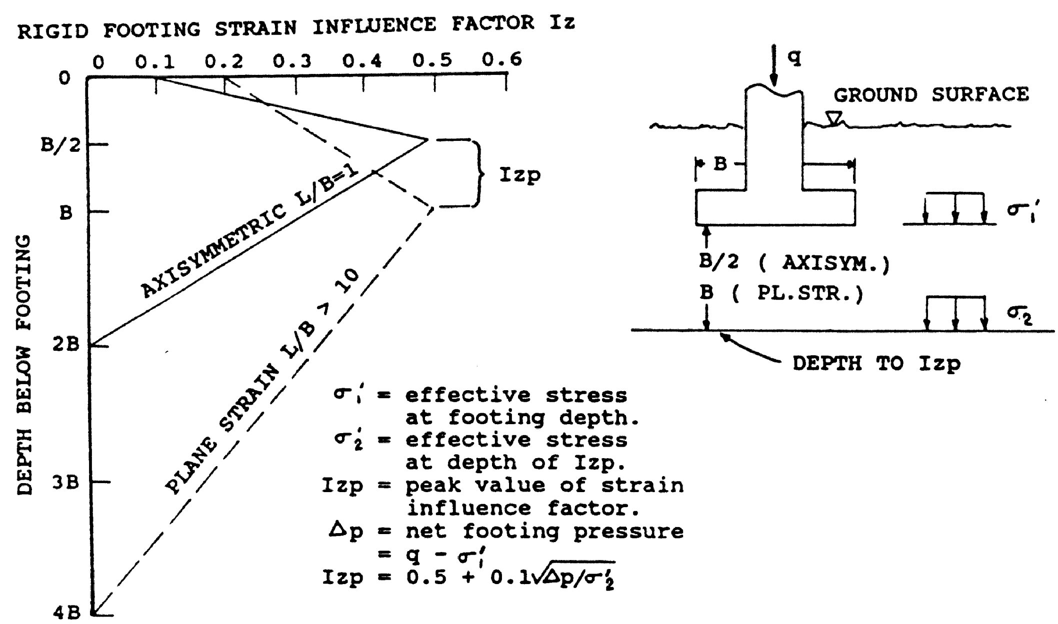

Figure 5. Schmertmann's Influence Values (after Schmertmann, 1974)

drawing of the footing on a chart, which is shown in Figure 7. The steps for determining the influence values are as follows:

1. Determine the depth (z) below the load at which the stress increase is needed.
2. Plot the plan view of the loaded area at a scale of z = the unit length of the chart. This unit length is given in the lower left hand corner of the chart (0.005).
3. Place the plot on the influence chart so that the point at which stress is to be calculated is located at the center of the chart.
4. Count the number of squares (M) that are inside the plot of the loaded area.

The change in stress is then calculated from:

$$\Delta p = (IV)qM \qquad (10)$$

where IV = influence value given on chart

q = pressure on loaded area

M = number of squares

Another method to calculate the change in stress due to an infinite strip load, which overcomes the limitations of Schmertmann's method and the Boussinesq equations in that a finite length is not required. This load can be found from the following equation (9):

$$\Delta p = \frac{q}{\pi}[\beta + \sin\beta\cos(\beta + 2\delta)] \qquad (11)$$

The variables are defined by figure 13. The final method of calculating changes in stress was developed by Perloff, and is for an embankment with a trapezoidal cross section. The plot in Figure 9 shows contours of vertical stress, assuming an elastic foundation and a weightless foundation soil. This can be used to find the change in stress at any depth (z)

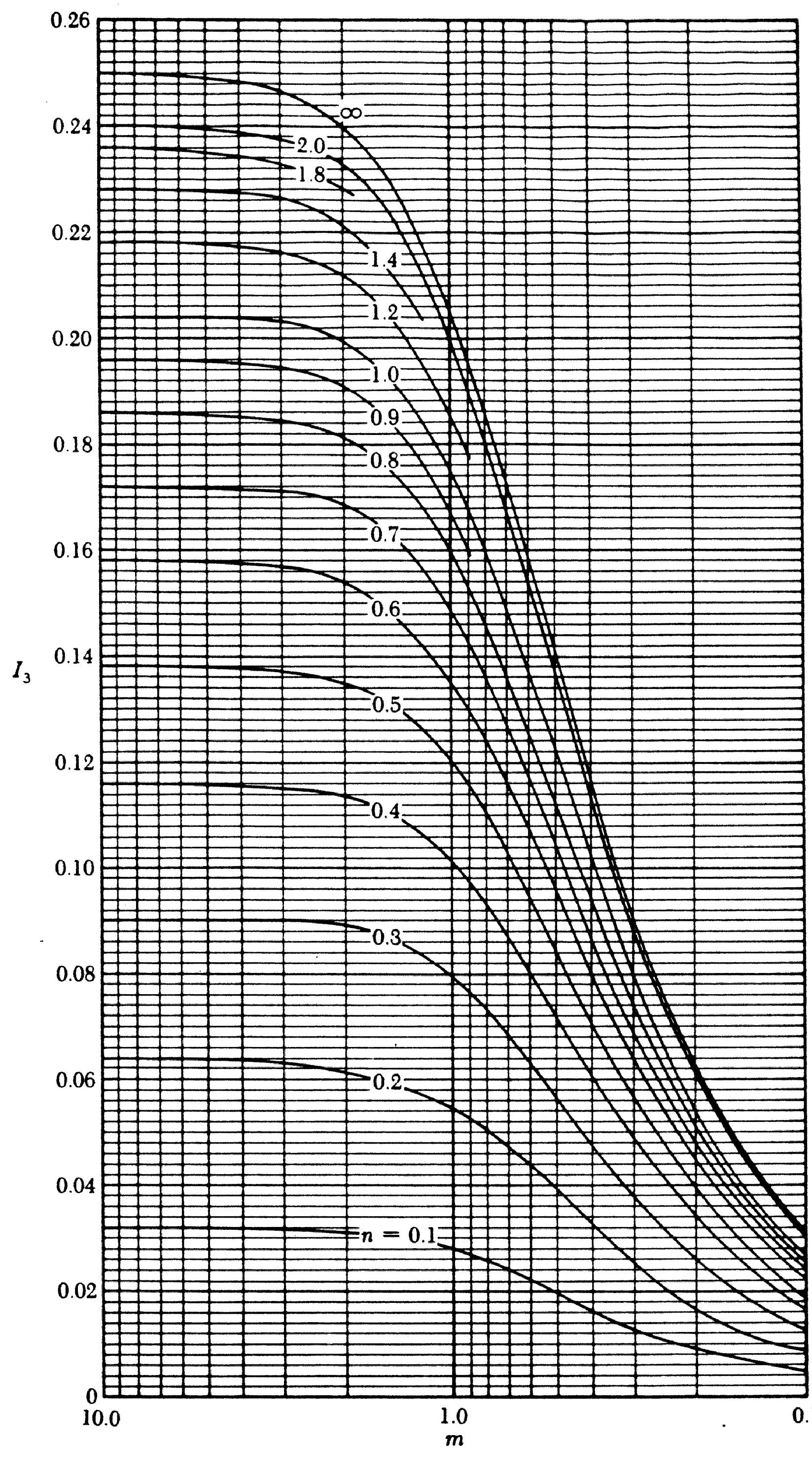

Figure 6. Charts for Calculating the Boussinesq Influence Value
(after Das, 1990)

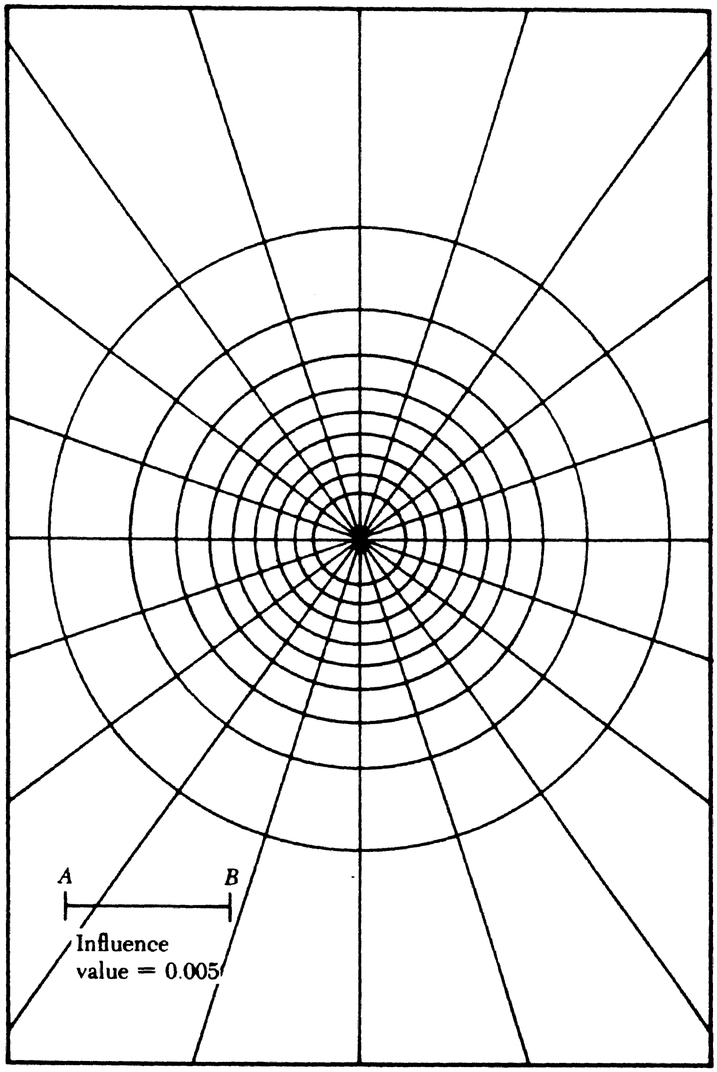

Figure 7. Newmark's Chart (after Newmark, 1942)

and any horizontal distance (x) from the centerline of the embankment. Each contour is given as a fraction of the embankment loading (17). The Perloff solution tends to give lower vertical stresses for trapezoidal embankments than conventional methods of calculating stress distribution. Conventional methods usually overestimate settlement when used with embankments, as they usually assume uniform loading (17).

The next step is to calculate settlement, which is due to either immediate settlement or consolidation settlement, depending upon the type of foundation soil. Figure 10 shows how the immediate settlement and consolidation settlement are related. Consolidation occurs as pore water is squeezed out of the soil, the soil compresses. This happens rapidly in sands and gravels and slowly in clays and silts, where the permeability is lower. For clays, consolidation theory is used to determine settlement. First, one dimensional consolidation tests are done on undisturbed samples of the soil. After the tests are performed, the settlement from consolidation for normally consolidated clays can be calculated as follows:

$$s = \frac{C_c H}{1+e_0}\log\left(\frac{p_0+\Delta p}{p_c}\right) \qquad (12)$$

C_c = compression index (from lab test)

e_0 = initial void ratio of sample,

p_0 = existing effective overburden pressure at given depth,

Δp = increase in pressure, and

H = thickness of soil layer.

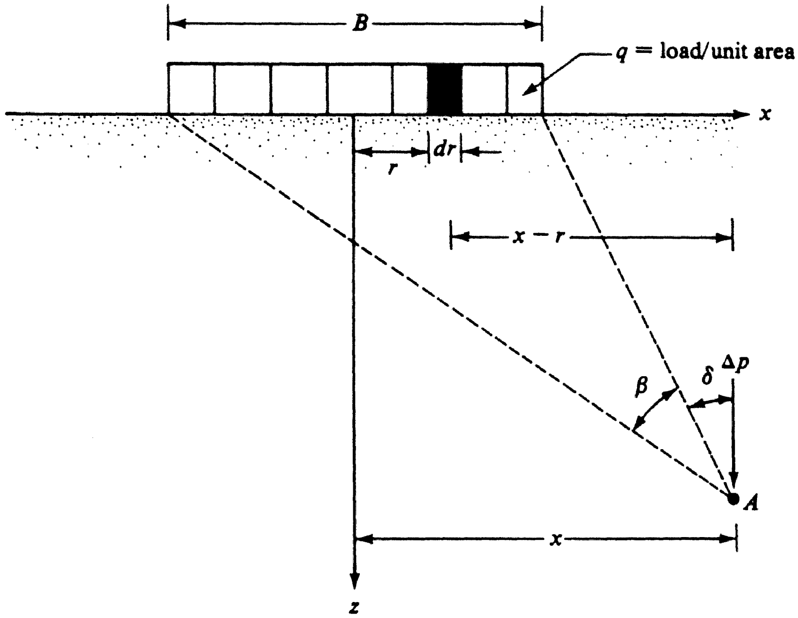

Figure 8. Vertical Stress Due to an Infinite Strip Load
(after Das, 1990)

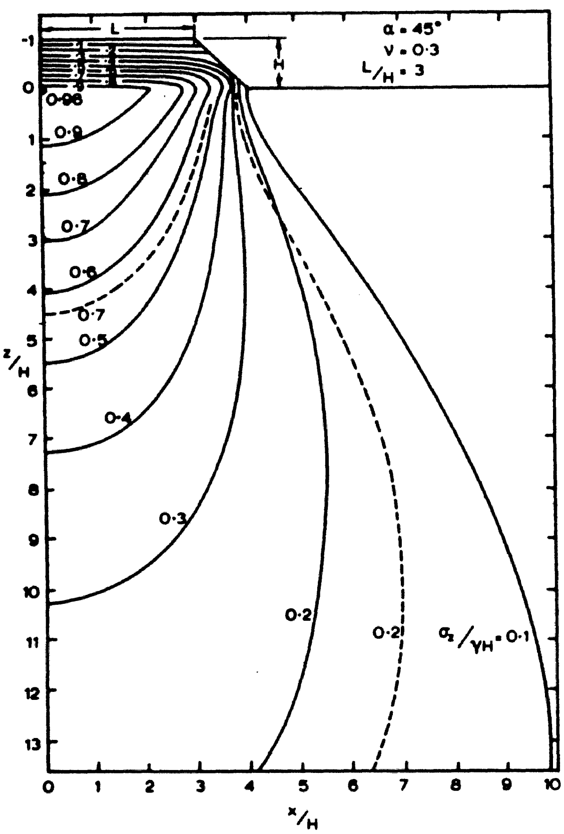

Figure 9. Vertical Stress Under a Trapezoidal Embankment
(after Perloff, 1967)

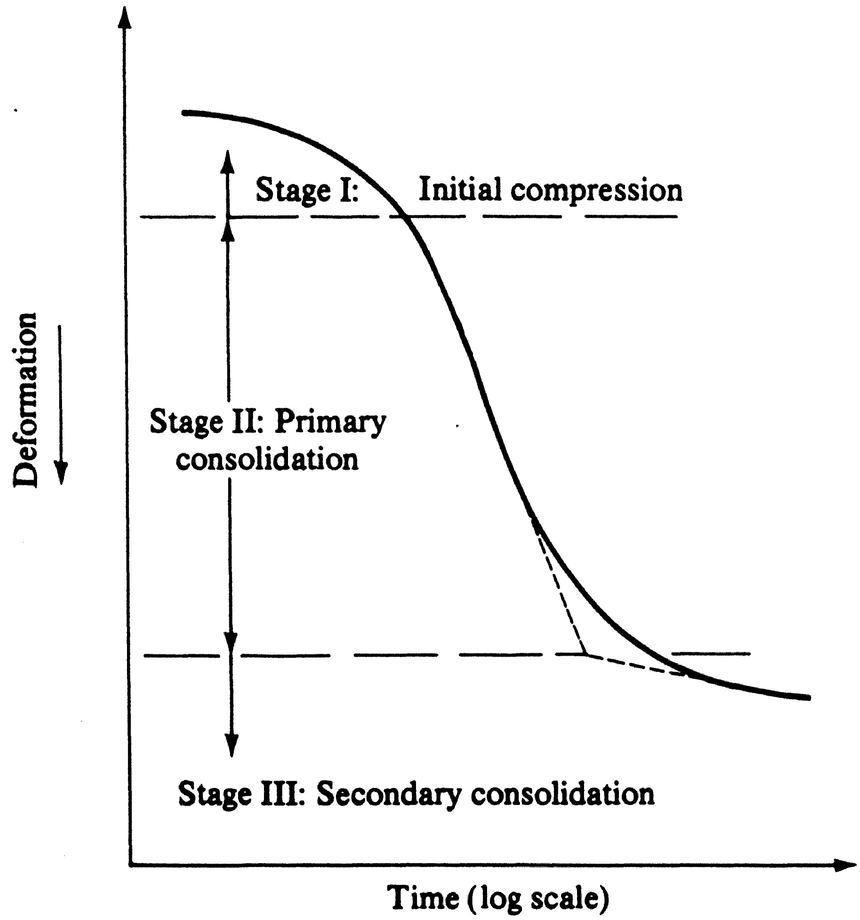

Figure 10. Settlement Over Time
(after Das, 1990)

Also, immediate settlement will occur as the soil deforms elastically. Immediate settlement for any soil may be found by the following equation:

$$\rho_i = p \bullet B \frac{1-\mu^2}{E} I_p \tag{13}$$

where ρ_i = elastic settlement

p = net pressure applied

B = width of the foundation

μ = pressure ratio

E = modulus of elasticity for soil

I_p = nondimensoinal influence factor

The influence factor may be found from Table 2. This method generally leads to a conservative estimate of the initial settlement (9).

Once these are known - primary consolidation, secondary consolidation, and initial elastic settlement - total settlement can be calculated. The total settlement is the sum of the primary consolidation, secondary consolidation, and initial elastic settlement. Consolidation is mainly a problem with clays, where it takes a long time to squeeze the water out of the soil. Sands do not have this problem, as consolidation occurs almost instantaneously. Therefore, consolidation tests are not run on sands, and initial elastic settlement is taken as the total settlement (9).

<u>Settlement Within the Embankment</u> Clough and Woodward (8) developed a method to calculate settlement within a trapezoidal embankment. Their method assumes that the embankment is built in lifts as opposed to being built instantaneously. The classical definition of settlement refers to a fixed datum and assumes instantaneous

		I_p		
		Flexible		
Shape	m_1	Center	Corner	Rigid
Circle	—	1.00	0.64	0.79
Rectangle				
	1	1.12	0.56	0.88
	1.5	1.36	0.68	1.07
	2	1.53	0.77	1.21
	3	1.78	0.89	1.42
	5	2.10	1.05	1.70
	10	2.54	1.27	2.10
	20	2.99	1.49	2.46
	50	3.57	1.8	3.0
	100	4.01	2.0	3.43

Table 2. Table for Influence Factor for Elastic Settlement (after Das, 1990)

creation of the embankment. This displacement is termed the "single lift" displacement. In reality, the embankment is built over time in multiple lifts, and the resulting displacement is termed "observed displacement". These displacements are related as follows:

$$v(z,h) = \rho(z,h) - \rho(z,z) \qquad (14)$$

where $v(z,h)$ = observed displacement,

$\rho(z,h)$ = single lift displacement, and

$\rho(z,z)$ = the single lift displacement of point Z when the the top of the embankment is at level Z, i.e., z above the base.

Figure 11 shows how H, h, Z, and z are defined. Clough and Woodward (8) developed plots to find influence values for vertical displacements, and these are found in figures 12 through 17. The equation for actual displacement is as follows:

$$\rho\left(\frac{z}{H},\frac{h}{H}\right) = I\left(\frac{z}{H},\frac{h}{H}\right)\gamma\frac{H^2}{E} \qquad (15)$$

where I(z/H,h/H) is the influence factor from figures 13 to 18, γ is the unit weight of the embankment, H is the height of the triangle in figure 11, and E is Young's modulus. This method gives the elastic settlement in the embankment itself. This settlement must then be added to the settlement calculated for the foundation soil. Clough and Woodward (8) also investigated the effects of changes in ν and side slope from their standard case. Figure 19 shows how to obtain multipliers to correct displacements for cases where ν and side slope vary from the standard case.

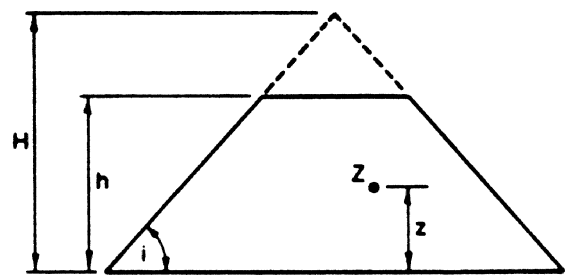

Figure 11. Embankment Dimensions for Clough and Woodward's Method (after Clough and Woodward, 1967)

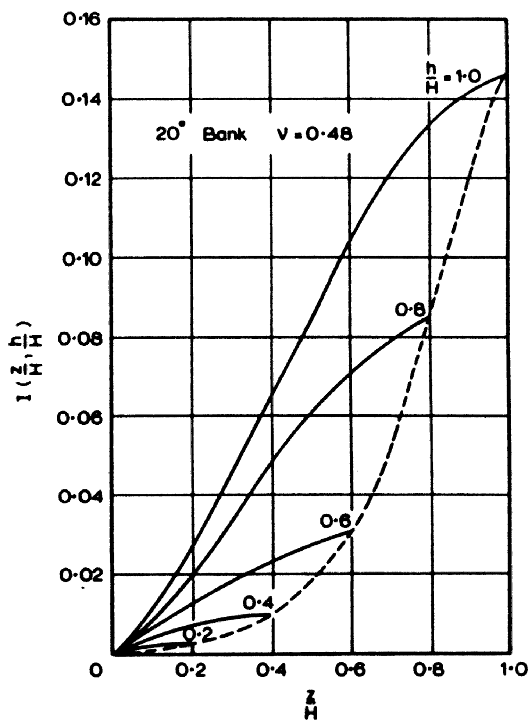

Figure 12. Embankment Vertical Displacement Factors, 20 Degree Slope, $\nu = 0.48$ (after Clough and Woodward, 1967)

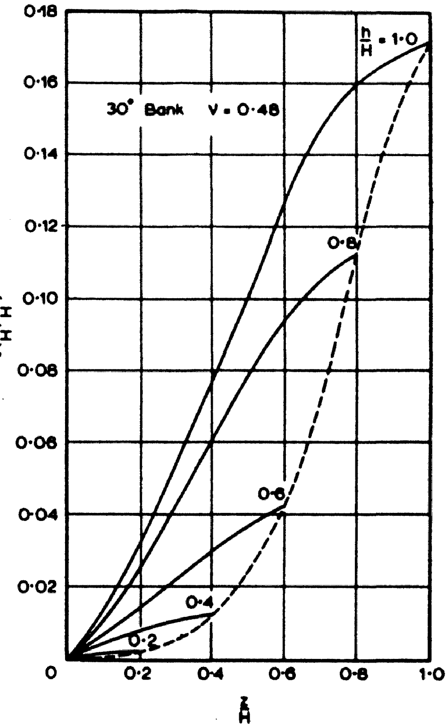

Figure 13. Embankment Vertical Displacement Factors, 30 Degree Slope, ν = 0.48 (after Clough and Woodward, 1967)

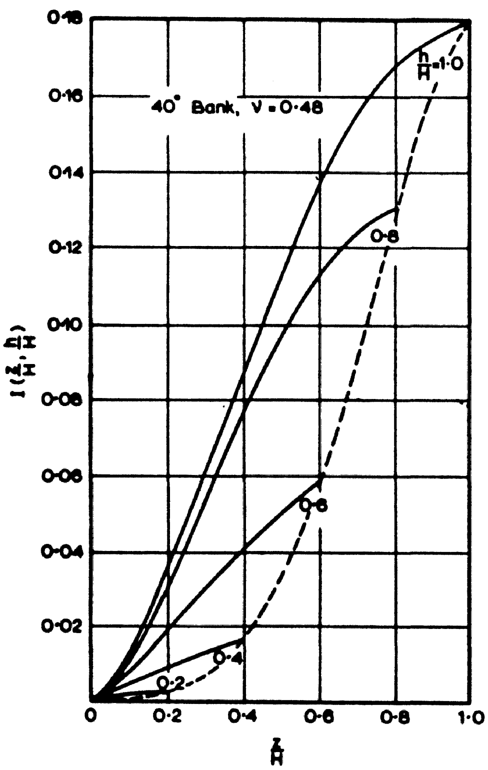

Figure 14. Embankment Vertical Displacement Factors, 40 Degree Slope, ν = 0.48 (after Clough and Woodward, 1967)

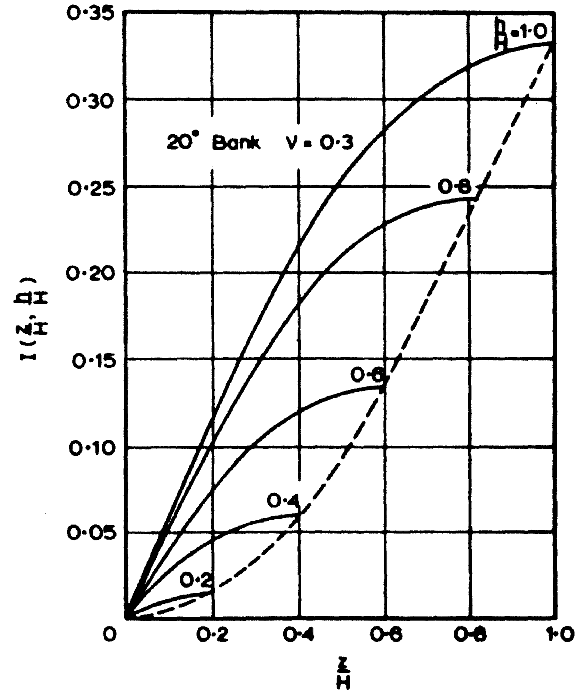

Figure 15. Embankment Vertical Displacement Factors, 20 Degree Slope, ν = 0.30 (after Clough and Woodward, 1967)

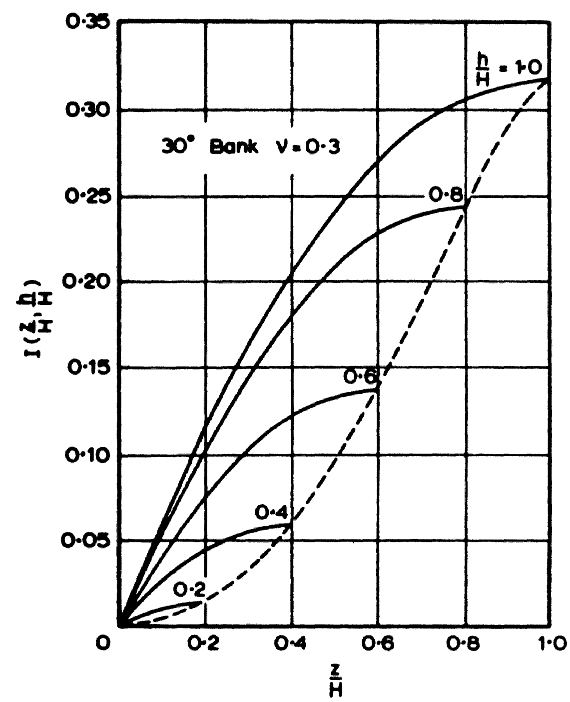

Figure 16. Embankment Vertical Displacement Factors, 30 Degree Slope, ν = 0.3 (after Clough and Woodward, 1967)

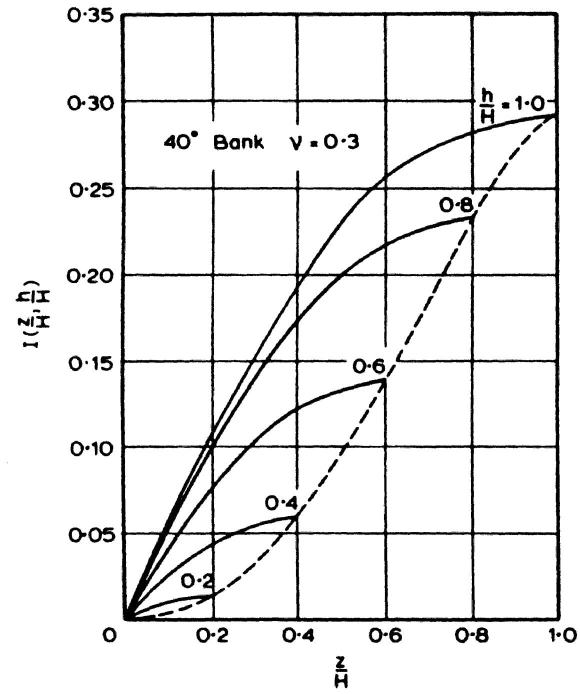

Figure 17. Embankment Vertical Displacement Factors, 40 Degree Slope, $\nu = 0.3$ (after Clough and Woodward, 1967)

Lateral Movement at Wall and Embankment

Little work has been done on calculating the lateral displacement of an abutment wall. The Federal Highway Administration (7) has published some information on this subject. They have developed a way to estimate the amount of wall tilting when the wall tilts toward (into) the embankment. This only happens when the embankment is built on a thick deposit of soft, compressible soil. As the embankment settles, the soft soil moves horizontally, pushing the piles that support the abutment wall outward and causing the wall to tilt into the embankment. In order to determine if tilting can occur, the following equation is used:

$$\gamma_{fill} \times H_{fill} > 3C \tag{16}$$

where γ_{fill} = the unit weight of the fill,

H_{fill} = height of the fill, and

C = cohesion of the foundation soil.

When this equation is satisfied, tilting of the abutment wall into the embankment will be a problem (based on field experience only). If this is a problem, movement of the wall can be estimated by multiplying the fill settlement by 0.25. This, of course, depends on an accurate estimate of the fill settlement, and this relationship also comes from experience in the field. Table 3 shows fill settlement, abutment settlement, and abutment tilting for 9 case histories. This gives some idea of how much the wall will tilt for other abutment walls. To date, there are no methods in the literature for calculating movement of the abutment wall away from the embankment.

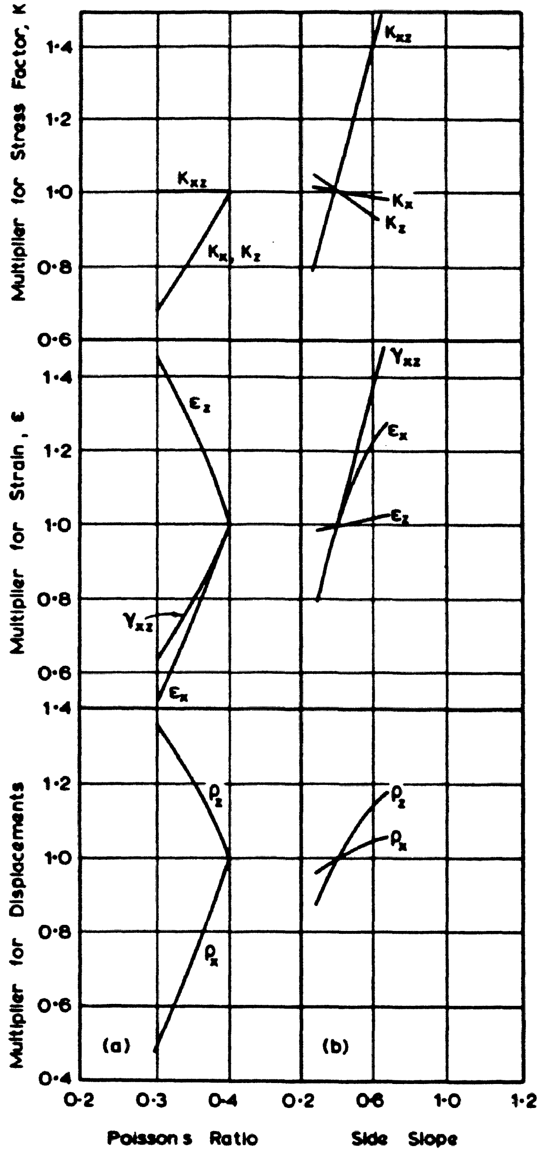

Figure 18, Multipliers to Correct for Variations in ν and Side Slope
(after Clough and Woodward, 1967)

Embankment Settlement Prediction Methods Using Cone Penetration Test Results

Riaund and Miran, of the Federal Highway Administration, published a manual on the cone penetration test in 1992 (18). This manual gives different methods for predicting settlement using Cone Penetration Test results. Two of the commonly used methods are Schmertmann's method, developed in 1970, and Sanglerat's method, developed in 1972. Schmertmann's method assumes that the loading comes from a shallow footing that is either square or rectangular in shape. It also assumes that the foundation soil is sand. The equation for determining settlement is as follows:

$$s = C_1 \times C_2 \times \Delta p \times \Sigma \frac{I_{zi} \times \Delta z_i}{x \times q_{ci}} \tag{17}$$

where

$$C_1 = 1 - 0.5\left(\frac{\sigma_1'}{\Delta p}\right),$$

$$C_2 = 1 + 0.2\log_{10}\left(\frac{t_{yr}}{0.1}\right),$$

s = settlement,

Δp = net foundation pressure increase at the bottom of the footing = q - σ_1 ',

q = bearing pressure,,

σ_1' = previous vertical effective stress at the elevation of the bottom of the footing,

I_{zi} = strain influence factor at the center of the i[th] sublayer,

N = number of sublayers,

Δz_i = thickness of the i[th] sublayer,

t_{yr} = time after the application, in years,

q_{ci} = average value of q_c in the i[th] sublayer,

Foundation	Fill Settlement (in.)	Abutment Settlement (in.)	Abutment Tilting (in.)	Ratio of Abutment Tilting to Fill Settlement
Steel H-piles	16	Unknown	3	0.19
Steel H-piles	30	0	3	0.10
Soil bridge	24	24	4	0.17
Cast-in-place piles	12	3.5	2.5	0.19
Soil bridge	12	12	3	0.25
Steel H-piles	48	0	2	0.06
Steel H-piles	30	0	10	0.33
Steel H-Piles	5	0.4	0.5 to 1.5	0.1 to 0.3
Timber Piles	36	36	12	0.33

Table 3. 9 Case Histories of Lateral Movement of Abutment Walls (after Cheny and Chassie, 1982)

x = modulus factor = 2.5 for square footing

= 3.5 for rectangular footing, and

q_c = CPT tip resistance of cone penetration test.

The distribution of the change in stress due to the footing is found from Figure 5. Schmertmann's method is limited because the footing must have a finite length, and it must be founded on sand. However, Schmertmann's method does allow the engineer to estimate the settlement over varying lengths of time. Sanglerat's method, on the other hand, can be used in any type of soil and on any footing shape. Sanglerat's settlement equation is as follows:

$$s = \Sigma_1^n H_0 \frac{\Delta\sigma}{\alpha q_c} \tag{18}$$

where:

s = total settlement (short and long term),

H_0 = thickness of the soil layer,

α = soil compressibility coefficient, and

q_c = average tip resistance for a soil layer.

The soil compressibility coefficient is chosen from Table 4. Care must be taken when choosing α because this will have a significant effect on the predicted settlement. Doubling the value of α will cut the calculated settlement in half for a given soil layer. The opposite is also true - cutting the value of α in half will double the predicted settlement. It is important that a soil profile be carefully defined using the tip resistances and friction ratios from the Cone Penetration Test. This should be done before predicting settlement so that the proper soil type may be used to determine α (18).

Many methods of calculating stress distribution can be used to find $\Delta\sigma$ in Sanglerat's method. Riaund and Miran, in The Cone Penetration Test, suggests using

q_c (bar)	α	Soil type
$q_c < 7$ $7 < q_c < 20$ $q_c > 20$	$3 < \alpha < 8$ $2 < \alpha < 5$ $1 < \alpha < 2.5$	Clay of low plasticity (CL)
$q_c > 20$ $q_c < 20$	$3 < \alpha < 6$ $1 < \alpha < 3$	Silts of low plasticity (ML)
$q_c < 20$	$2 < \alpha < 6$	Highly plastic silts and clays (MH, CH)
$q_c < 12$	$2 < \alpha < 8$	Organic silts (OL)
$q_c < 7$ $50 < w < 100$ $100 < w < 200$ $w > 200$	 $1.5 < \alpha < 4$ $1 < \alpha < 1.5$ $0.4 < \alpha < 1$	Peat and organic clay (P_t, OH)
$20 < q_c < 30$	$2 < \alpha < 4$	Chalk
$q_c < 50$ $q_c > 100$	$\alpha = 2$ $\alpha = 1.5$	Sand

Table 4. α Values for Sanglerat's Method
(after Sanglerat, 1972)

Boussinesq's equations for circular and rectangular footings (18). This method has already been discussed in the previous section of this chapter. However, Sanglerat's equation only requires that $\Delta\sigma$ be known, it does not specify how to calculate it, so any method will do. Therefore, for approach embankments, it would be logical to use Perloff's method for calculating stresses due to a trapezoidal embankment.

Accuracy of Different Methods

The Federal Highway Administration manual (18) also comments on the accuracy of Schmertmann's and Sanglerat's methods. Schmertmann's method was tested on 37 case histories in 1985 by Briaud (5) The results of these are plotted in Figure 20 using the ratio of predicted settlement to measured settlement versus measured settlement. For these cases, Schmertmann's method overpredicted settlement by 30%. Sanglerat evaluated his own method in 1979 using data from 17 sites in France. The ratio of calculated/measured average settlement had a mean of 1.47 and a standard deviation of 0.53. Therefore, this method also overpredicts settlements for these cases. He determined that the error came from choosing the right α value. This was difficult to do, but it would become easier as one gained experience with using this method on local soils (18).

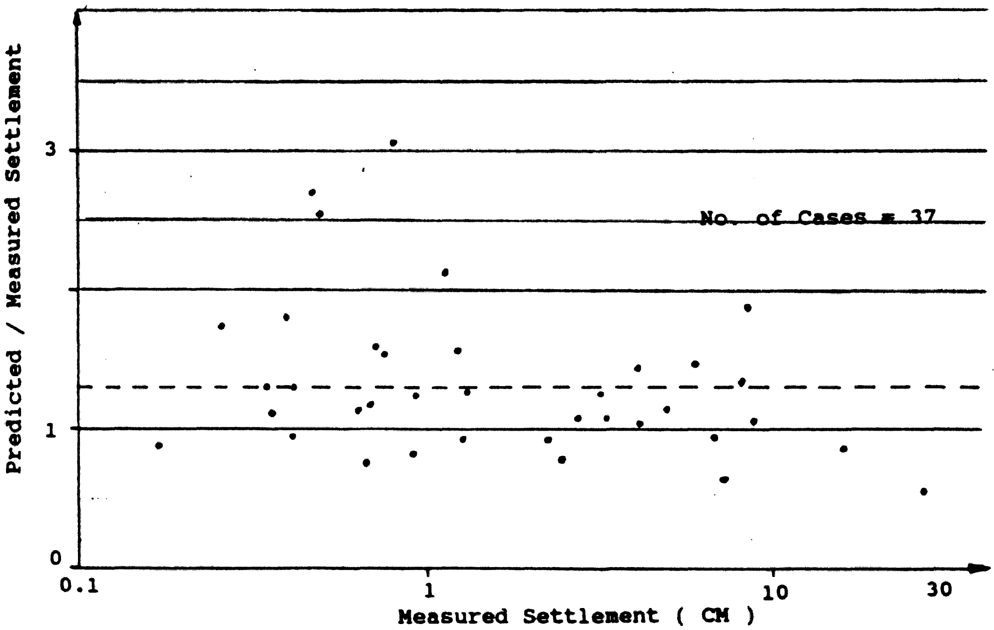

Figure 19. Accuracy of Schmertmann's Method
(after Briaud, 1985)

CHAPTER 3

EVALUATION OF SETTLEMENT PREDICTION METHODOLOGY STUDY

In order to find the most accurate method of predicting settlement, several methods were considered and evaluated. The first method was developed at the University of Oklahoma and published in 1993 (12). This method uses a statistical equation to predict settlement. The other two methods that were tested were Schmertmann's method and Sanglerat's method. In addition, different methods of calculating the stress distribution were used on each prediction method. These two methods were evaluated using Cone Penetration Test data from the sites used in the University of Oklahoma study.

Review of OU Approach Embankment Settlement Study

In 1993, Laguros, Boyd, Zaman, and Jha of the University of Oklahoma published a statistical model for predicting bridge approach settlement. The data used to develop this model came from 25 bridges throughout Oklahoma. Table 5 gives the location and number of each bridge, and table 6 gives the data set that was used to develop the statistical equation (12, 13, 14, 15). For the data tables, the following abbreviations apply:

TST = total measured settlement

TCN = average number of vehicles using the bridge in one day

FND = depth of foundation soil

Site #	Bridge #	County
1	I-40 20-02 X 1072E	Custer
2+	US270 30-12 X 0849	Harper
3	SH152 75-10 X 0849	Washita
4	SH152 75-08 X 2077	Washita
5	SH9 14-11 X 1242	Cleveland
6+	US270 04-20 X 1897	Beaver
7	SH102 41-38 X 1250	Lincoln
8	SH142 10-35 X 0376	Carter
9	SH003 64-12 X 0735	Pushmataha
10	I-35 36-25 X 1241E	Kay
11	SH17A 25-53 X 0087	Garvin
12	US69 18-10 X 0348	Craig
13	SH10 58-24 X 1287	Ottawa
14	US70 12-02 X 1078	Choctaw
15	US59 68-02 X 0000	Sequeah
16	SH20 66-08 X 0674	Rogers
17	US177 41-20 X 0611	Lincoln
18	US62 38-03 X 0213	Kiowa
19	US75 56-04 X 0113	Okmulgee
20	US183 75-06 X 0501	Washita
21	County Bridge (56th. st.)	Tulsa
22	SH15 23-20 X 0922	Ellis
23	US64 30-04 X 1825	Harper
24	US64 76-06 X 0545	Woods
25	SH8 47-18 X 1505	Major

+*CPT test was not conducted at these sites.*

Table 5. Locations and Numbers for Bridges in OU Study
(after Laguros, Boyd, Zaman, and Jha, 1993)

SITE #	TST (in.)	TCN (ADT)	FND (ft.)	EHT (ft.)	AOE (yrs.)	SPT	SPTE	SPTF	FR	TIPR (tsf)	SKEW (deg.)
1	8.0	4800	12	25	34	11	14	6	1.41	33.78	0
2	0.0	1950	40	13	7	13	10	14	N/A	N/A	50
3	18.0	1500	60	22	16	9	10	8	2.19	45.22	0
4	5.0	2500	72	12	21	5	9	4	2.3	17.91	40
5	6.0	5000	50	10	29	12	10	10	2.5	38.92	10
6	0.0	1300	32	9	57	8	6	8	N/A	N/A	0
8	10.0	4700	15	32	34	23	9	48	6.56	44.32	0
9	1.0	3700	26	26	23	10	10	9	4.41	75.33	10
10	6.0	4550	31	35	32	11	8	13	2.16	31.66	50
11	2.8	650	45	20	22	16	9	20	1.53	72.65	40
12	0.0	3000	18	21	5	17	9	23	6.46	44.86	60
13	2.5	13300	5	33	35	11	11	9	3.88	37.8	30
14	2.5	1600	38	36	7	7	7	8	4.19	16.17	0
15	15.0	10000	46	30	24	25	33	18	0.98	147.51	0
16	3.0	4500	20	16	44	6	6	6	4.9	25.04	40
17	5.0	1900	50	13	17	6	6	5	1.93	24.7	60
18	2.0	2500	42	24	16	22	10	29	4.83	41.24	40
19	3.5	6100	9	27	27	10	10	11	4.5	74.63	60
20	2.5	1000	40	15	9	5	5	5	0.84	16.5	0
21	3.0	3100	28	15	56	13	8	14	3.9	42.45	0
22	5.0	1800	50	11	53	20	12	21	1.04	74.07	0
23	2.5	900	40	10	57	13	11	14	2.29	51.11	0
24	2.5	1300	21	13	18	9	5	11	3.72	62.5	0
25	1.5	1600	25	8	38	17	9	21	4.43	55.31	0

Table 6. Data Set for OU Study
(after Laguros, Boyd,
Zaman, and Jha, 1993)

AOE = age of embankment

EHT = embankment height

SPT = weighted average of standard penetration test blow count

SPTE = standard penetration test blow count for embankment

SPTF = standard penetration test blow count for foundation soil

FR = friction ratio from cone penetration test, in percent

TIPR = tip resistance from cone penetration test

SKEW = skew of the approach

Before discussing their statistical model, it is necessary to explain how the data used to develop this model was obtained. First, total settlement was estimated by one or more of the following methods:

1) measuring the movement of the curb between the bridge and approach
2) measuring the thickness of cumulative overlay or patching
3) examining other noticeable evidence at the site
4) interviewing maintenance personnel.

However, specific information on settlement is not routinely kept by the Oklahoma Department of Transportation (ODOT), so this data is at best an estimate. Next, the height of each embankment was measured by shooting the level difference between the top of the embankment and the original ground surface. Age of the embankment was then recorded as the time in years since the bridge was open to traffic. Traffic count was obtained from the ODOT Bridge Division records. Standard Penetration Test and Cone Penetration Test data were obtained in an extensive testing program conducted by ODOT

Materials Division. In this program, two Standard Penetration Tests and one Cone Penetration Test were performed at each site. Figure 20 shows the locations of the two Standard Penetration Tests, and the Cone Penetration Test was performed near the continuous sample bore hole #1. The Standard Penetration Tests were performed using a split spoon sampler driven by a 140 pound hammer dropped 30 inches. The Cone Penetration Test used an electric cone pushed at a constant rate of 2 centimeters per second.

The Standard Penetration Test (SPT) and Cone Penetration Test (CPT) data were corrected for effects of overburden pressure and were each reduced to one single value for each site. The statistical model was then developed using the single SPT and CPT values for each site. A weighted average was taken for the SPT values, and it was calculated as follows:

$$SPT = \frac{N_1 \times h_1 + N_2 \times h_2 + \ldots + N_n \times h_n}{(h_1 + h_2 + \ldots + h_n)} \qquad (19)$$

where: N = SPT blow count for layer n, and

h = thickness of layer n.

Weighted averages were also taken for tip resistance (q_c) and friction ratio (FR) for the cone penetration tests. These are the numbers that appear in table 6 (12).

From this data, several statistical equations were developed to predict settlement of an approach embankment. These may be found in the OU report (12), and they are the only equations that have been specifically developed to predict bridge approach settlement. However, after careful evaluation of several options, it was decided to use classical methods of settlement prediction for the methodology study. These methods give more flexibility to account for variations in the foundation soil profile. Data from the OU

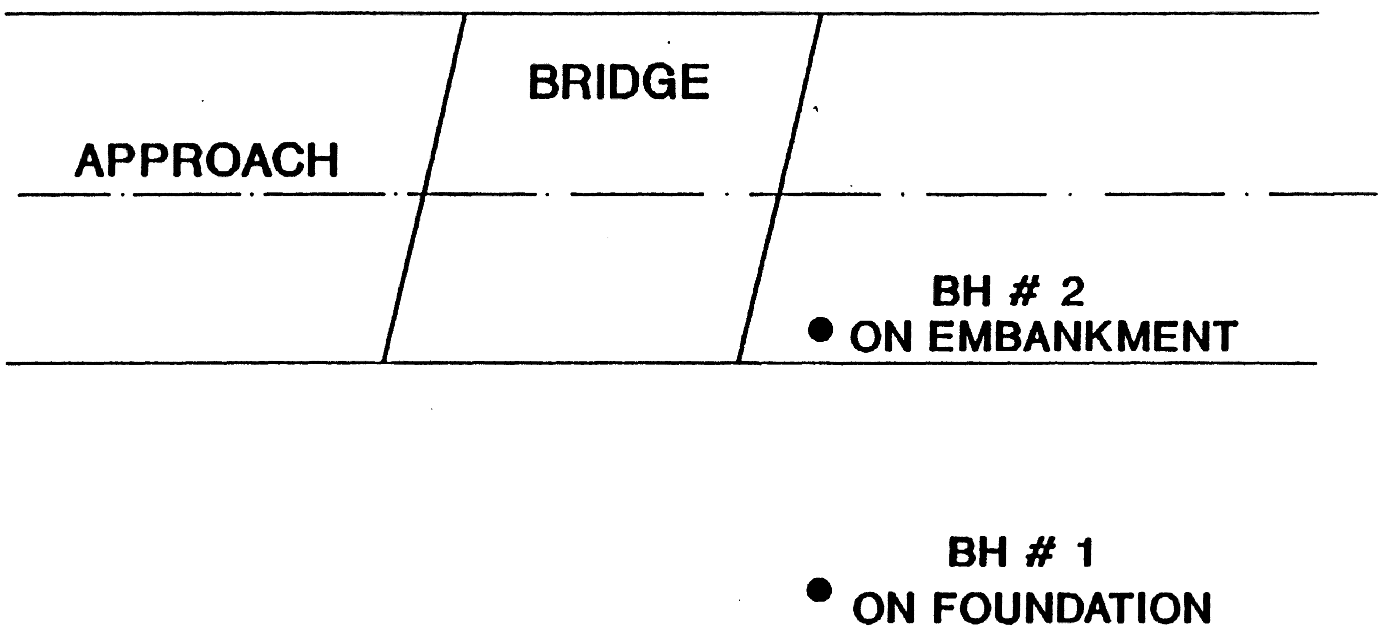

Figure 20. Location of Borings for OU Data (after Laguros, Boyd, Zaman, and Jha, 1993)

study was used for the methodology study, including the raw CPT and SPT data and the measured settlement for each embankment.

Data for Methodology Study

Even though data from the OU study were used for this methodology study, additional data had to be collected. The original CPT plots and SPT results, which were not in the OU report, were on file at ODOT. Jim Nevels, the head geotechnical engineer at ODOT, sent these files for use on this study. Also, the OU report gave no information on the geometry of the embankments (widths at top and bottom and side slopes). To get this information, the as-built cross sections were obtained from ODOT design records. However, some of these records were not available, so a few of the approach embankments had to be surveyed.

Also, the original 25 OU data sites were not all used for the methodology study. Two of the sites lacked Cone Penetration Test data, so they were not used. In addition, the 25 sites were scattered all over the state of Oklahoma. Since some of the sites had to be surveyed, it was not economical to drive to some of the sites. Therefore, a circle with a 120 mile radius was drawn with Stillwater at the center. All of the sites within the circle were used for the methodology study, and the total number of sites used was 12. These included site numbers 3, 4, 5, 7, 10, 11, 16, 17, 19, 20, 24, and 25. Site #21 was not used because it was a county bridge, and there was some difficulty finding records on it.

Calculation of Settlement Using CPT Data

Many options were open for methods of calculating settlement. However, the electric Cone Penetration Test gives a continuous soil profile, and direct correlations have been developed to calculate settlement directly from this test. In addition, there are various methods available for calculation settlement from CPT data. Therefore, it was decided to compare these different methods.

Four steps were required to calculate settlement from the CPT data. First, the data from the field was reduced, and soil profiles were drawn. The soil profiles contained such information as the thickness of each layer, the angle of internal friction, relative density, and soil type. Next, the settlement calculation methods were chosen. This included methods of calculating changes in stress, as well as methods of calculating settlement. Third, the best method was chosen after testing each method on the 12 chosen approach embankments. Finally, the settlement at each of the 12 sites was calculated using the chosen method.

Reduction of Cone Penetration Test Data

Figure 21 shows an example of the Cone Penetration Test data from the field. The electric cone penetrometer measured tip resistance and side friction, then this information is transferred to a computer which plots tip resistance and side friction versus depth. The computer also calculates the friction ratio and plots it versus depth. Once this is plotted, there will be "breaks" in the plot where the average friction ratio and tip resistance change as the soil type changes. These "breaks" indicate approximate boundaries between soil layers. The easiest way to find these breaks is to first find the breaks in the friction ratio-versus-depth plot, then compare that to the tip resistance-versus-depth plot. The breaks on each plot should be at about the same depth, but they should be easier to see on the friction ratio-versus-depth plot. Once this is done for the entire plot, the depth and thickness of each layer can be recorded, as well as the average tip resistance and friction ratio for each layer. Next, the tip resistance for each layer is corrected for the effects of overburden pressure. This is done by the following equation:

$$q_{cl} = q_c[1 - 1.25\log_{10}\sigma'_{vo}] \qquad (20)$$

where q_{cl} = corrected tip resistance,

q_c = measured tip resistance, and

σ_{vo}' = effective overburden pressure.

This corrected tip resistance is then used, along with the average friction ratio of the layer, to determine the soil type, angle of internal friction, and relative density of the profile using Figure 23. The next step was the selection of the settlement calculation methods to be tested.

Selection of Settlement Calculation Methods

There are two methods available for calculating settlement from a CPT test, and there are many methods for calculating changes in stress due to a surcharge. The two methods for calculating settlement are Schmertmann's method and Sanglerat's method were described in Chapter 2. The options for calculating change in stress due to a surcharge are Schmertmann's method, the Boussinesq equations, the equation for an

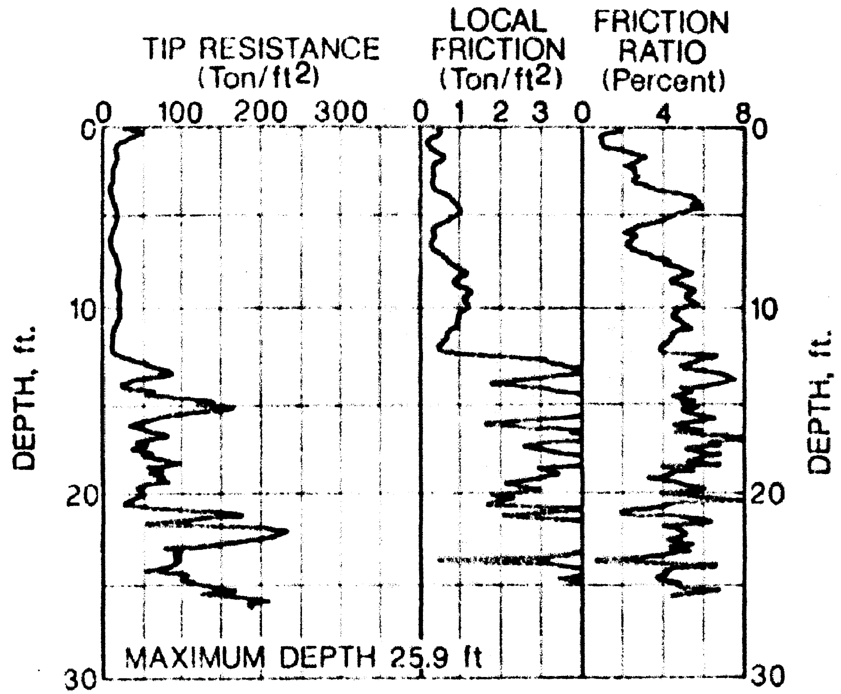

Layer 1: Sandy Silt to Clayey Silt

q_c = 46.61 tsf **FR** = 2.8% D_r = 70% ϕ = 29°

Layer 2: Clayey Silt to Silty Clay

q_c = 37.22 tsf **FR** = 4.2% D_r = ---- ϕ = 0°

Layer 3: Clayey Silt to Silty Clay

q_c = 93.53 tsf **FR** = 5.8% D_r = ---- ϕ = 0°

Layer 4: Clayey Silt to Silty Clay

q_c = 124.23 tsf **FR** = 5.0% D_r = ---- ϕ = 0°

Figure 21. Example CPT Interpretation

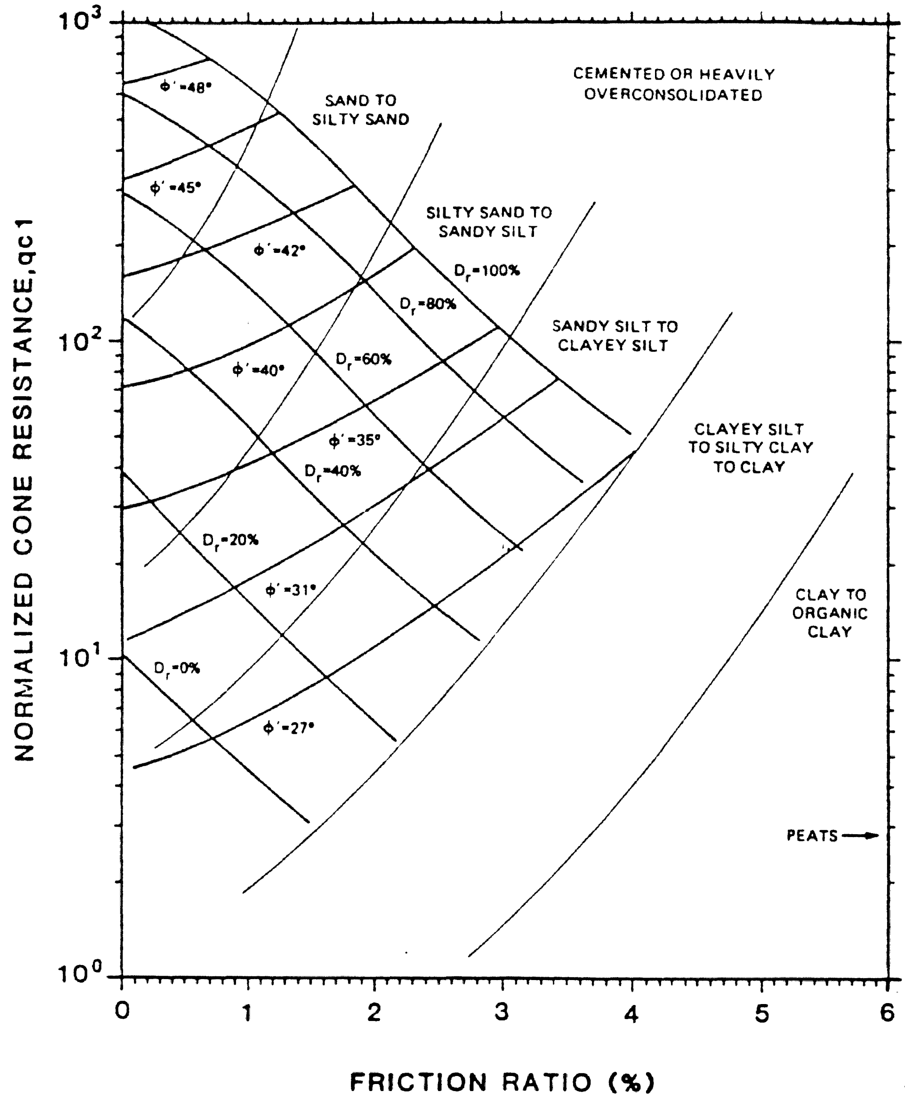

Figure 22. Plot for Finding ϕ and D_r from CPT Data (after Schmertmann, 1972)

infinite strip footing, and Perloff's method for trapezoidal embankments. These were the chosen methods for this study and were described in detail in Chapter 2. Schmertmann's method for settlement was used both with Schmertmann's method for change in stress, the equation for an infinite strip footing, and Perloff's embankment method. Sanglerat's method was used with the Boussinesq equation for a rectangular footing, the equation for an infinite strip footing, and Perloff's method for embankments. Each combination of stress change calculation method and settlement calculation method was performed on the 12 sites, and the calculated settlement was compared with the measured settlement at each site. The most accurate method was chosen, but there were also other factors that were considered in choosing a settlement prediction method.

Final Selection of Settlement Prediction Method

First, Schmertmann's method was used with Schmertmann's method for calculating stress distribution. It was then tried with the strip footing method and then with Perloff's method. However, Schmertmann's method was rejected for the following reasons:

1) It always assumes a finite footing length.
2) It only works on sand foundations.
3) It consistently overpredicted the settlement by as much as 30%.
4) The settlements got farther off as more accurate methods of calculating stress distribution were used. (The rectangular footing was least accurate, and the trapezoidal embankment was most accurate.)

Sanglerat's method was used, with the Boussinesq equation for a rectangular footing and with the infinite strip footing method. These gave more accurate results than Schmertmann's method. However, a static load from a highway approach embankment will not be similar, as far as stress distribution in the foundation, to a rectangular footing. Even assuming that it will resemble an infinite strip footing is not as accurate as modeling the approach as a trapezoidal embankment. Therefore, Sanglerat's method using Perloff's method for calculating stress distribution proved to be the most accurate method of predicting settlement. Also, Sanglerat's method will work in any soil type.

Sample Calculation

The settlement calculations for all of the 12 sites are shown in appendix A, and following is a detailed explanation of the calculation procedures using site 3. The first step is to identify the soil layers, including soil type, depth of the layer, and tip resistance. This is illustrated in Figure 23, and the procedures for doing this have already been explained. Next, Table 7 was constructed as follows:

Layer	H_0 (feet)	q_c (tsf)	α	$\Delta\sigma$	$H_0(\Delta\sigma/\alpha q_c)$
1	3	230.71			
2	11	63.53			
3	8	94.99			
4	20	14.87			
5	4	12.49			
6	11.5	37.51			
7	2.5	54.82			

Table 7. Settlement Calculation

Next, the α values are chosen, according to Table 4 in Chapter 2. For example, the soil type of layer 2 is sandy silt to clayey silt, and the tip resistance (corrected for effects of overburden) is 63.53 tons per square foot (tsf). Looking at Table 4, for silts with a tip resistance of greater than 20 tsf, the α value ranges from 3 to 6. There are no hard and fast rules for determining where in this range the α value might fall. The decision is based on experience from using this method on different soil types; in other words, it is up to the interpretation of the engineer. Once all of the α values are determined, $\Delta\sigma$ is calculated for each layer. First, the change in stress at the ground surface is calculated. This is the embankment height at the center of the embankment multiplied by the unit weight of the embankment soil. For site 3, the embankment height is 22 feet, and the unit weight is 115 pounds per cubic foot (pcf). Therefore, the change in stress at the ground surface is:

$$22(115) = 2530 \text{ psf} = 1.265 \text{ tsf}$$

This is then multiplied by a multiplier found from the plot in Figure 14. To get a multiplier from this plot, find the depth at the middle of the soil layer, z. Divide z by the height of the embankment, H, to get the location on the y axis of the plot. For layer 2, the depth to the middle of the layer is 8.5 feet, so 8.5 divided by 22 is 0.386. The location on the x axis is the horizontal distance from the centerline of the embankment to the point where settlement is to be calculated (x), divided by the height of the embankment. This value is zero, since settlement is being calculated at the centerline of the embankment. The corresponding point is then located on the plot, and the stress contour that it lies on is recorded. This number is multiplied by the stress at the ground surface, so for layer two, 0.386 corresponds to a stress contour of about 0.94. The change in stress in layer 2 is then

$$0.94(1.265) = 1.189 \text{ tsf}$$

The change in stress is calculated for each layer and recorded in the table. The settlement for each layer is then calculated for each layer using Sanglerat's equation, and the table is

Layer (feet)	H_0	q_c (tsf)	α	$\Delta\sigma$ (tsf)	$H_0(\Delta\sigma/\alpha q_c)$ (feet)
1	3	230.71	1	1.27	$1.6*10^{-2}$
2	11	63.53	3	1.19	$6.9*10^{-2}$
3	8	94.99	2	1.16	$4.9*10^{-2}$
4	20	14.87	3	1.09	$48.8*10^{-2}$
5	4	12.49	3	1.01	$10.8*10^{-2}$
6	11.5	37.51	4	0.99	$7.6*10^{-2}$
7	2.5	54.82	3	0.23	$1.4*10^{-2}$
					$\Sigma = 0.82$ ft.

Table 8. Completed Settlement Calculation

completed. To calculate the total settlement under the embankment, the numbers in the last column on the right are added. This gives a total settlement at site 3 of 0.817 feet or 9.8 inches.

Comparison and Discussion of Results

In order to determine the merit of this method of calculating settlement, two factors must be considered - accuracy and reliability. Accuracy, according to Tan and Duncan, is "the average value of calculated settlement divided by measured settlement"

(19). Therefore, the calculated settlement is divided by the measured settlement for each site, and the average of all of these numbers is the accuracy of the method. Perfect accuracy is when this ratio is unity. Reliability, on the other hand, is defined by Tan and Duncan as "the percentage of the cases for which the calculated settlement is greater than the measured settlement" (19). Ideally, an accuracy of 1 and a reliability of 100% is what is desired, but this is generally not possible due to the high variability of soils (19).

However, accuracy and reliability are mutually exclusive. That is, for a given method, the results will either be accurate or reliable, but not both. In Tan and Duncan's work, several methods of calculating the settlement of a footing on sand were tested. Terzaghi and Peck's method, for example, had a reliability of 86% and an accuracy of 3.2. On the other hand, Alpan's method had an accuracy of 1 and a reliability of only 40%. The method chosen to calculate settlement will either be more accurate or more reliable.

Using Sanglerat's method and Perloff's stress distribution method, the results were more accurate than reliable, as shown by Figures 23 and 24. The accuracy was 1.44 with a reliability of 42%. However, the measured settlement on site 20 is probably too low for several reasons. The foundation soil is very deep (89 feet), and the bottom 57 feet of it consists of a loose (5% to 18% relative density) sand with a very low tip resistance (12 to 17 tsf). This low tip resistance will obviously give a high settlement value when used in Sanglerat's equation. Also, the methods used to measure settlement for the OU study were not always accurate (12). Records of measured settlements were not kept by ODOT, so settlements were estimated by interviewing the maintenance personnel and measuring the asphalt overlays placed on the approach pavement. Rarely is the same person in charge of maintaining the bridge over a period of years, so the person interviewed may not have been entirely familiar with the entire maintenance history of the approaches. Also, it is difficult to distinguish between asphalt layers and measure their thickness. Therefore, if site 20 is removed from the study, the accuracy becomes 1.07 and the reliability becomes 36%. This is summarized in table 9 below.

	Reliability	Accuracy
With Site 20	42%	1.44
Without Site 20	36%	1.07

Table 9. Effects of Site 20 on Accuracy and Reliability

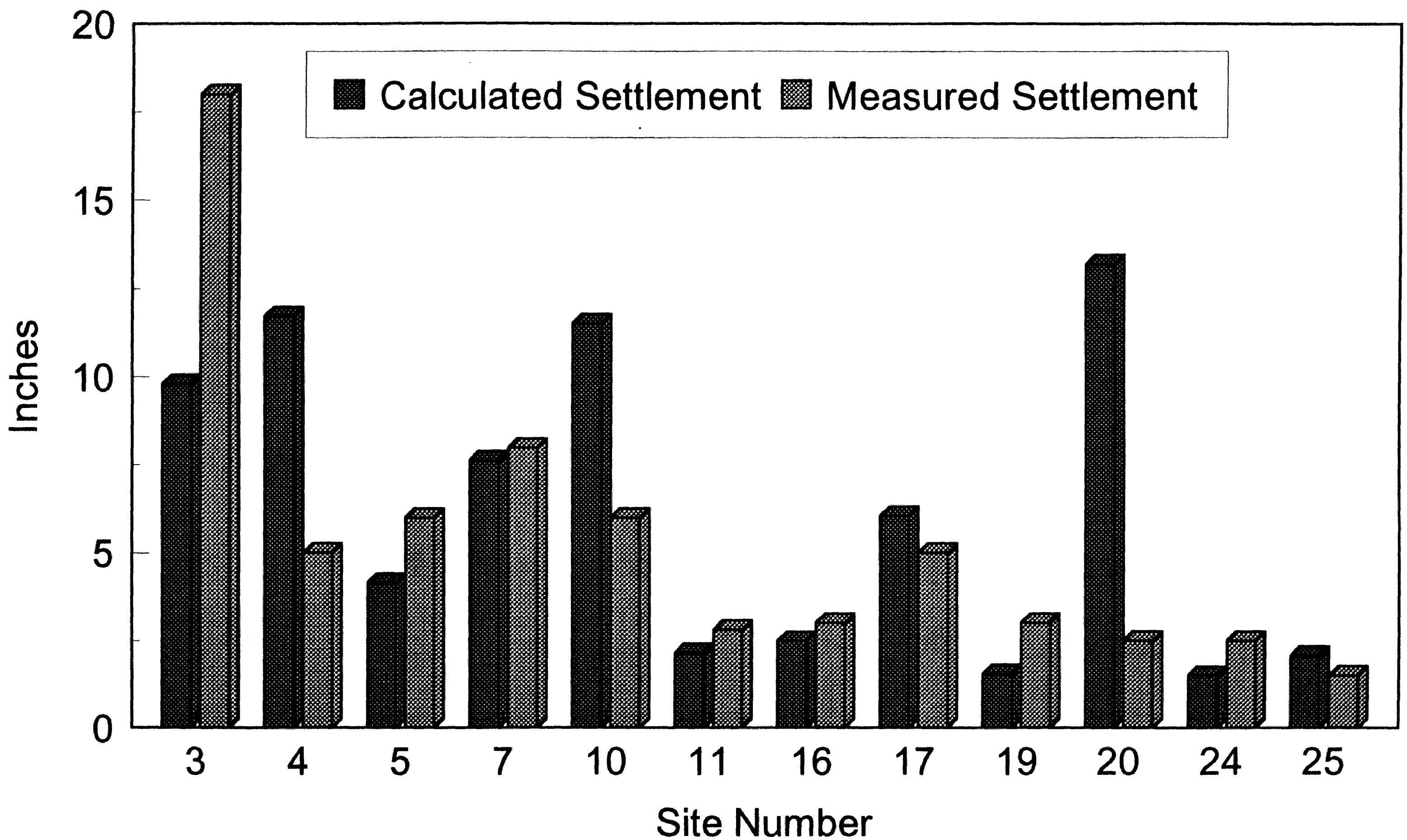

Settlement Data from 12 OU Sites

Figure 23. Comparison of Calculated and Measured Settlement for the 12 OU Sites

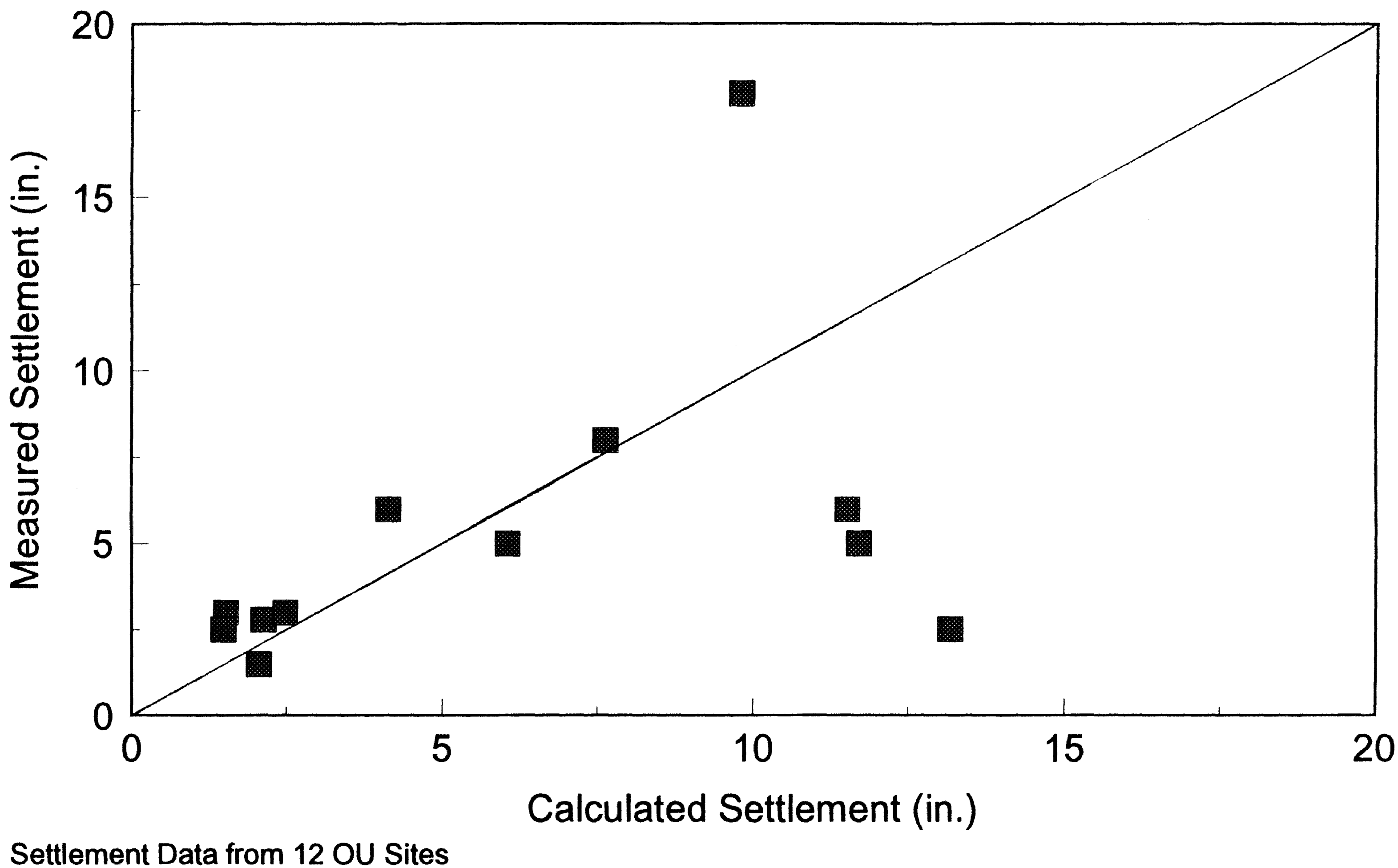

Figure 24. Calculated Versus Measured Settlement for the 12 OU Sites

CHAPTER 4

ESTIMATION OF STRESS AND DEFORMATION PARAMETERS AT SALT FORK RIVER RESEARCH SITE

On US 177 across the Salt Fork River in Noble County, Oklahoma, three new bridges will be built. One of these is over the main river, and the other two bridges are the overflow structures. The bridges are noted as bridge "A", bridge "B", and bridge "C", with "A" being the southernmost bridge and "C" being the northernmost bridge. Five of the six approach embankments on these bridges will be used to study how different embankment construction methods affect the settlement of the embankment. The south approach embankment of bridge A will not be used in this study because of its height. The north abutment of bridge A will be built using unclassified borrow, which is the way most approach embankments are built today. This will be the control embankment. The south approach of bridge B will be built using a geotextile reinforced wall with granular backfill, while the north approach of bridge B will be built using controlled low strength backfill material, which is a mixture of portland cement, fly ash, sand, and water. The south embankment of bridge C will be built using dynamic compaction of the embankment and foundation soil, with granular backfill in the embankment. The north embankment of bridge C will be built with granular backfill and routine construction procedures. Details of the backfill material may be found in appendix B.

This chapter describes the estimation of stress and deformation parameters for these five approach embankments. In order to do this, some background information on the site itself is required. First, the geologic and subsurface profile is described , followed by a description of the boring and in situ testing program for the approaches. Next, the idealized profiles and soil properties are shown, followed by a description of the approach embankment properties. Once this information is known, the stress and deformation parameters can be calculated. These include the lateral earth pressures on the abutment walls and settlement of the embankment.

Description of Geologic and Subsurface Profile Conditions

The soil at this site consists of Quarternary Period alluvium deposits from the Salt Fork of the Arkansas River. These deposits consist of sand, clay, gravel, and silt. The type of material and location of various layers are very uniform across the site. In local areas, gravel deposits may exist which could yield significant water. Wells nearby yield from 20 to 150 gallons per minute, and depth to the water table is shallow, ranging from 2 to 12 feet (14). Also, the ground surface gently slopes upward from an elevation of 905 feet at bridge A to 910 feet at bridge C.

The bedrock underlying this soil consists mostly of shale with a few limestone lenses. The elevation of the top of the bedrock gradually decreases from 888 feet at bridge A to 862 feet at bridge C. The extreme upper part of the bedrock is Permean aged shale of the Wellington formation. This rock is soft, weathered, and reddish brown to light gray. This soft Permean aged shale varies in thickness between the bridges and is thickest under bridge C. As is typical in Permean shales, alternating layers of soft and firm shale zones were encountered. The relative softness of the Permean aged shale can be estimated based on the high Texas Cone Penetration values and the low unconfined compressive strength of the rock cores (14).

Beneath the Wellington formation lies Pennsylvanian Period shale and limestone of the Oscar Group. This Oscar Group is typically described as mainly shale with many layers of limestone and some fine grained Arkosic sandstone. The borings for this project that went into the Oscar Group revealed predominantly dark gray to grayish red shale, silty to clayey. A limestone zone was encountered under bridges A and B at an average depth of 50 feet. This limestone zone occurred as a sequence of interbedded limestone and shale layers and was approximately 10 feet thick. A limestone bed known as the Herrington Limestone Bed is mapped near the bridge sites in geologic references. The limestone encountered in this project could have been the Herrington Limestone Bed. No limestone was found in the borings for bridge C.

Description of Boring and In Situ Testing Program

In order to design the approach embankments, the abutment walls, and the piles to support the bridges, a detailed soil testing plan was developed. This plan was developed by Dr. Jim Nevels, with the ODOT Materials Division. This included 8 electric Cone Penetration Test soundings, 1 Standard Penetration Test boring, 1 Dilatometer test boring. The location of each test is given in Figure 26. The Standard Penetration Test was located beneath the center of the new abutment wall, with Cone Penetration Test 5 located 3 feet west and 2 feet north from the SPT. CPT's 2, 6, 7, and 8 were located on the

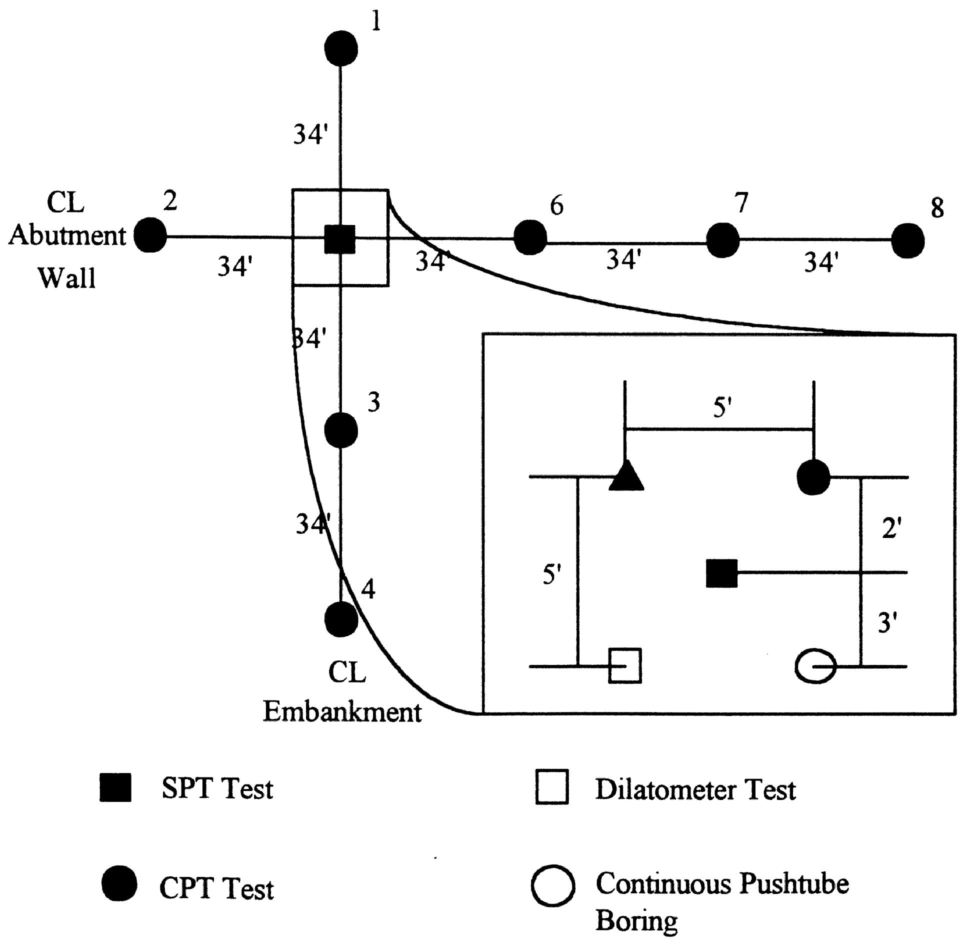

Figure 26. Soil Investigation Plan for Salt Fork River Sites

centerline of the abutment wall, CPT 1 was underneath the approach, and CPT's 3 and 4 were on the opposite side of the abutment wall from the approach. The two vane shear tests were supposed to have been done near the SPT and CPT 7, but the lack of cohesive soils at the site made it impractical to perform these tests. The dilatometer sounding was done near the SPT, and this test was performed in order to have data to which the CPT results could be compared.

Idealized Profiles and Soil Properties

Cone Penetration Test 5 was used to determine the idealized soil profiles for each bridge. This was possible because the soil beneath each bridge was very uniform; the soil type was virtually the same for a given layer across the site, and there was little variation in the location of each soil layer between the different Cone Penetration Tests. Also, CPT-5 was located on the centerline of the embankment, just behind the abutment wall. This is also where the largest settlement of the embankment will likely occur.

Figures 27, 28, 29, 30, and 31 show idealized soil profiles for the foundation soil at each embankment. Notice that the foundation soil is mostly sand with some silt. Relative densities range from 40% to 65%, and the angles of internal friction range from 30 to 40 degrees. The low side friction values from the Cone Penetration Tests show that these soils are not cohesive. Settlement is usually not a big problem in non cohesive soil, and the lack of large clay deposits means that settlement will happen very quickly either during or just after construction.

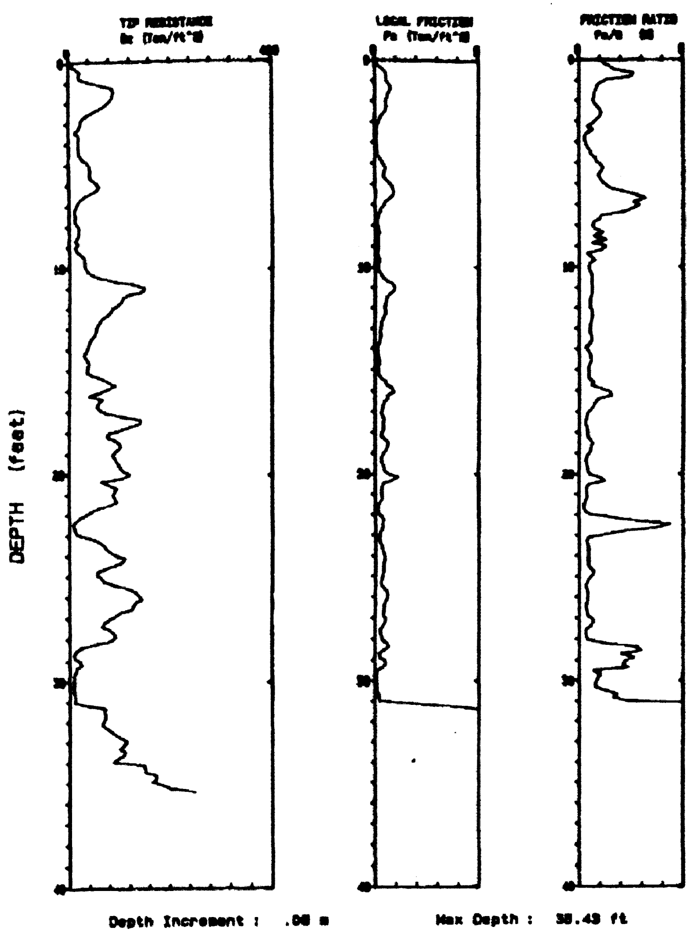

Layer 1: Sand to Silty Sand
D_r = 50% $\phi = 39^0$

Layer 2: Sand to Silty Sand
D_r = 52% $\phi = 40^0$

Layer 3: Sand to Silty Sand
D_r = 52% $\phi = 41^0$

Layer 4: Sand to Silty Sand
D_r = 42% $\phi = 41^0$

Layer 5: Sandy Silt to Clayey Silt
D_r = 27% $\phi = 27^0$

Figure 26. Idealized Soil Profile for North Abutment Bridge A

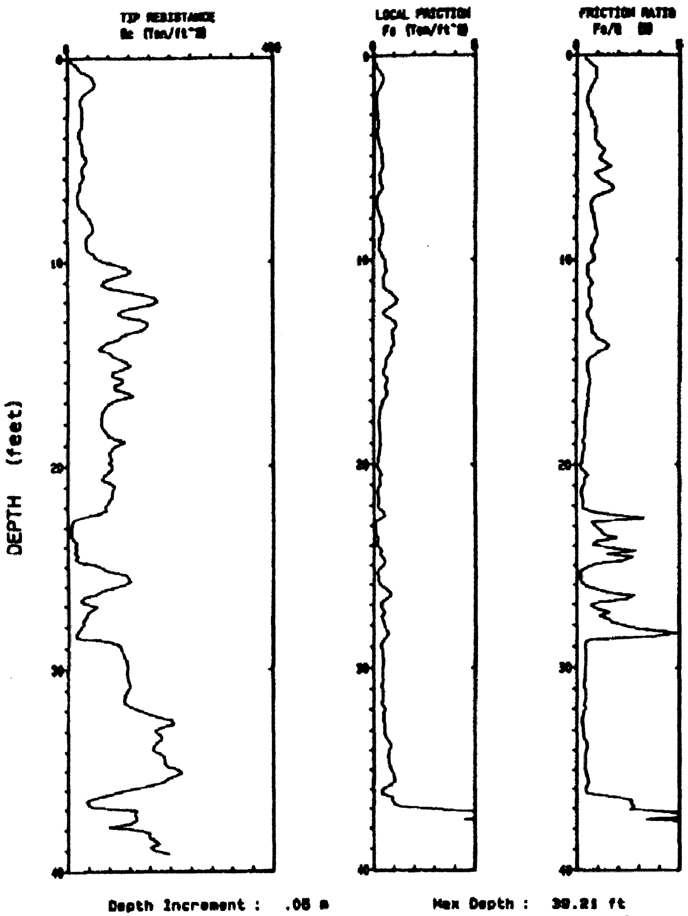

Layer 1: Sand to Silty Sand

D_r = 45% $\phi = 39^{\circ}$

Layer 2: Sand to Silty Sand

D_r = 50% $\phi = 41^{\circ}$

Layer 3: Sandy Silt to Clayey Silt

D_r = 55% $\phi = 29^{\circ}$

Layer 4: Sand to Silty Sand

D_r = 50% $\phi = 41^{\circ}$

Figure 27. Idealized Soil Profile for South Abutment Bridge B

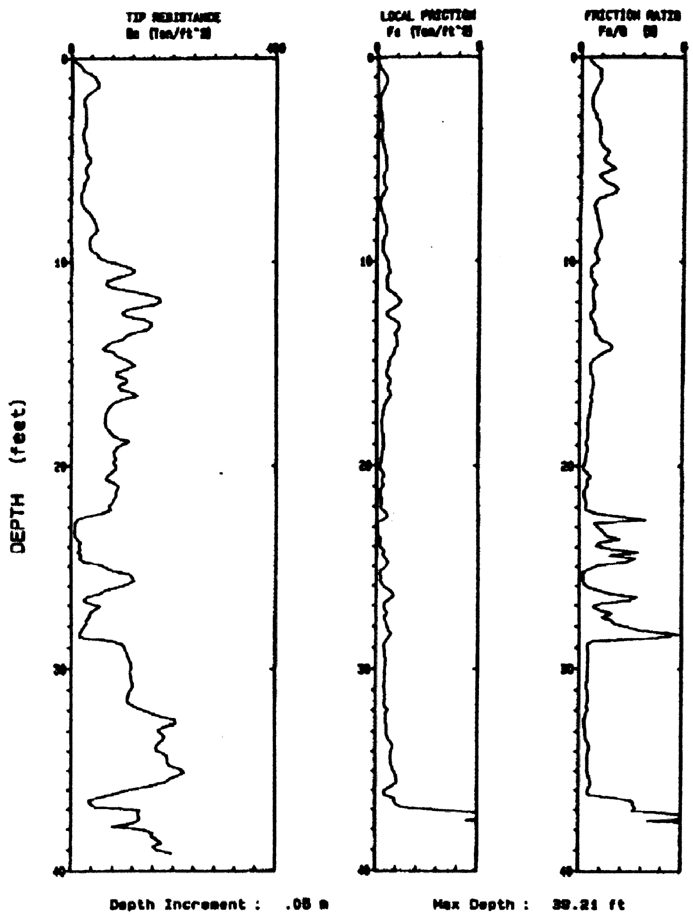

Layer 1: Sand to Silty Sand

D$_r$ = 45% ϕ = 40°

Layer 2: Silty Sand to Sandy Silt

D$_r$ = 45% ϕ = 36°

Layer 3: Sand to Silty Sand

D$_r$ = 50% ϕ = 41°

Layer 4: Silty Sand to Sandy Silt

D$_r$ = 45% ϕ = 35°

Layer 5: Sand to Silty Sand

D$_r$ = 45% ϕ = 41°

Figure 28. Idealized Soil Profile for North Abutment Bridge B

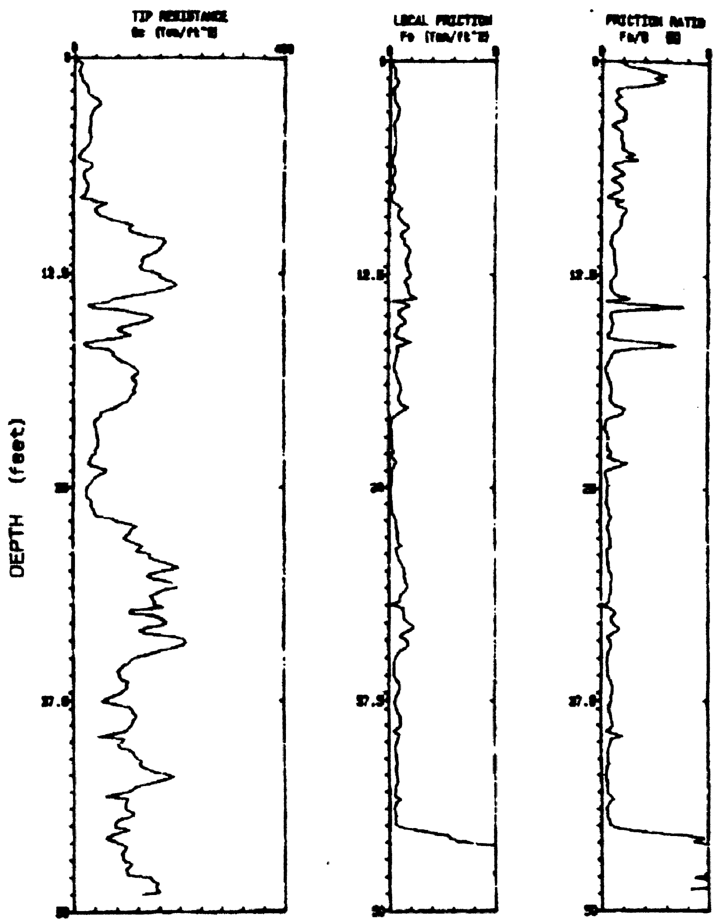

Layer 1: Silty Sand to Sandy Silt

$D_r = 45\%$ $\phi = 36^{\circ}$

Layer 2: Sand to Silty Sand

$D_r = 55\%$ $\phi = 41^{\circ}$

Layer 3: Sand to Silty Sand

$D_r = 30\%$ $\phi = 37^{\circ}$

Layer 4: Sand to Silty Sand

$D_r = 50\%$ $\phi = 41^{\circ}$

Layer 5: Sand to Silty Sand

$D_r = 40\%$ $\phi = 40.5^{\circ}$

Figure 29. Idealized Soil Profile for South Abutment Bridge C

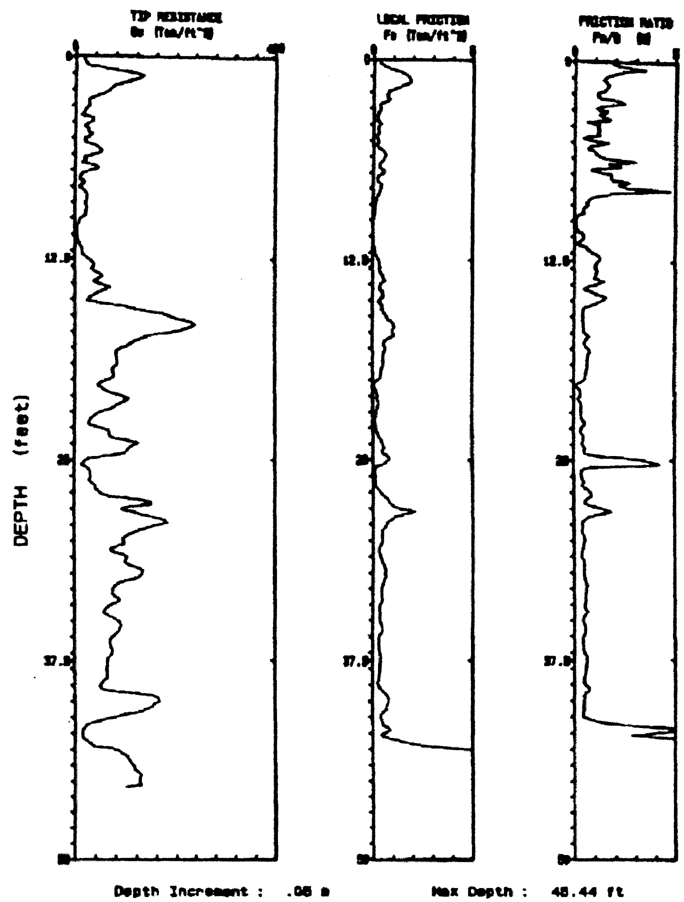

Layer 1: Silty Sand to Sandy Silt

D_r = 70% $\phi = 37^{\circ}$

Layer 2: Sand to Silty Sand

D_r = 50% $\phi = 41^{\circ}$

Layer 3: Sand to Silty Sand

D_r = 45% $\phi = 40.5^{\circ}$

Figure 30. Idealized Soil Profile for South Abutment Bridge C

Properties of Approach Embankment Materials

The angle of internal friction, ϕ, and the unit weight of the embankment material, γ, are the properties which have the most significant impact on the settlement of the embankment and the magnitude of lateral earth pressure on the abutment wall. Settlement is affected by the unit weight of the embankment material, and the angle of internal friction and unit weight both determine the magnitude of lateral earth pressure. These properties had to be estimated for each approach embankment, but this was difficult because the embankments have not yet been constructed.

For the north abutment of bridge A, unclassified borrow will be used to build the embankment. This borrow will probably come from the nearest suitable source, so it is likely that the borrow material will be a silty sand from the Salt Fork River Valley. Therefore, the properties of this soil will be similar the properties of the foundation soil under the five bridge approaches. This would correspond to a unit weight of 115 pounds per cubic foot and a ϕ angle of 39 degrees.

The south abutment of bridge B will be constructed using a geotextile reinforced wall with granular backfill. Given the material specification for granular fill (see appendix B), it was determined that this soil was a "dense, gravelly sand". According to Jumikis, such a soil has a density of 125 pounds per cubic foot (11). The ϕ angle of the soil is 38 degrees, but the lateral earth pressure will likely be carried by the geosynthetic reinforcement. This means that no lateral earth pressure will get to the abutment wall, at least in theory.

The north abutment of bridge B will be constructed using controlled low strength backfill material. This is a mixture of portland cement, water, sand, and fly ash. Such a material can have a wide range of mixtures and therefore a wide range of unit weights. Dr. Michael Ayers, Professor of Civil and Environmental Engineering at Oklahoma State University, was consulted about the unit weight of this material. He said that Dolese in Oklahoma City makes low strength backfill that is 127 pounds per cubic foot. The ϕ angle for the low strength backfill will be 0 degrees when it is poured, since it will flow like a liquid. After it sets, the low strength backfill should act as one mass. In other words, the largest lateral pressure will likely occur just after the backfill is poured.

The south abutment of bridge C will be constructed using dynamic compaction of the foundation and embankment materials, and granular backfill will be used for the embankment. Given the properties of the granular backfill in appendix B, the unit weight of this material should approximate 125 pounds per cubic foot as this is the approximate unit weight given by Jumikis for a dense sand with gravel (8). The ϕ angle will probably be 40 degrees, which also corresponds to a dense sand (3).

The north abutment of bridge C will be built using granular backfill and conventional construction. The unit weight of this material was estimated to be about 120 pounds per cubic foot, and the ϕ angle was estimated to be about 38 degrees. This is reasonable, given that this material will be a sand with some gravel, but it will probably not be as densely compacted as the material for the south abutment of bridge C.

Estimation of Stress and Deformation Parameters

There were two stress and deformation parameters that were calculated for the five approach embankments. The first was settlement of the embankment, which was calculated using Sanglerat's method and Perloff's method for finding stress under a trapezoidal embankment. Lateral earth pressure was calculated using Coulomb's theory, with 17 degrees being used as the interface friction angle between the wall and backfill. This was the value given for a concrete wall holding back a fine, silty sand (3). Also, the slope of the stem face (β) will be 0 degrees, and the slope of the backfill surface will also be 0 degrees. Rankine's method was considered, but it is only applicable where the wall friction angle is equal to the slope of the backfill surface. The log spiral analysis was not used because it gave results that were very close to Rankine's method. Figures 32 through 42 show the soil profiles, calculated and measured settlements, and the active lateral earth forces on the abutment wall for each of the five bridge approaches.

NORTH ABUTMENT BRIDGE A
SALT FORK RIVER

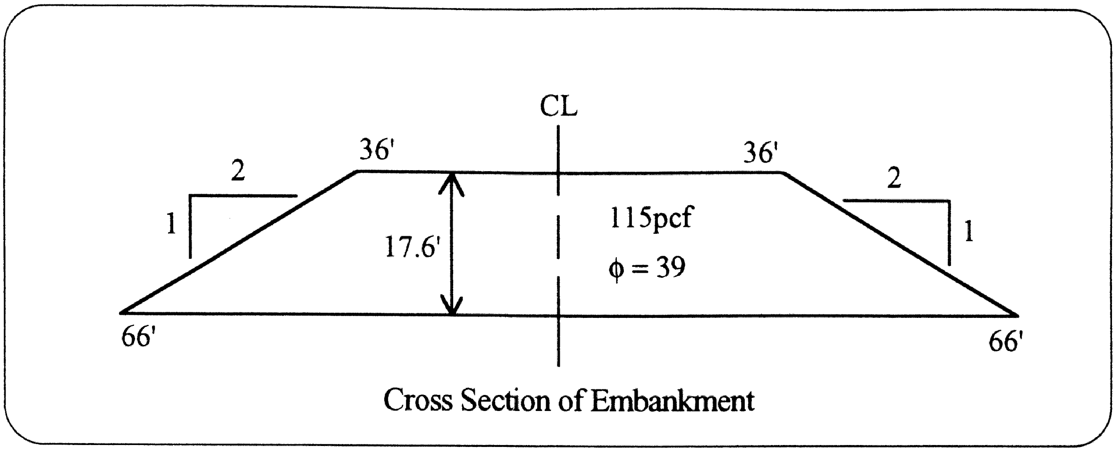

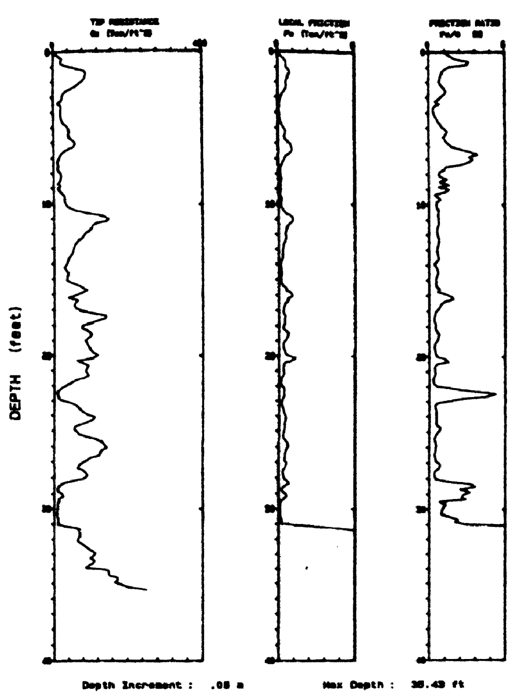

Layer 1: Sand to Silty Sand
H_0 = 6.6 ft. q_c = 81.57 tsf α = 3.0 $\Delta\sigma$ = 0.977 tsf

Layer 2: Sand to Silty Sand
H_0 = 9.0 ft. q_c = 92.20 tsf α = 3.0 $\Delta\sigma$ = 0.941 tsf

Layer 3: Sand to Silty Sand
H_0 = 7.5 ft. q_c = 101.59 tsf α = 1.5 $\Delta\sigma$ = 0.911 tsf

Layer 4: Sand to Silty Sand
H_0 = 4.9 ft. q_c = 90.49 tsf α = 3.0 $\Delta\sigma$ = 0.870 tsf

Layer 5: Sandy Silt to Clayey Silt
H_0 = 3.3 ft. q_c = 10.55 tsf α = 2.0 $\Delta\sigma$ = 0.850 tsf

Calculated Settlement: 3.00 in.
Active Lateral Earth Pressure: 423 psf

Figure 31. Settlement and Lateral Earth Pressure Calculations for North Abutment Bridge A

SOUTH ABUTMENT BRIDGE B
SALT FORK RIVER

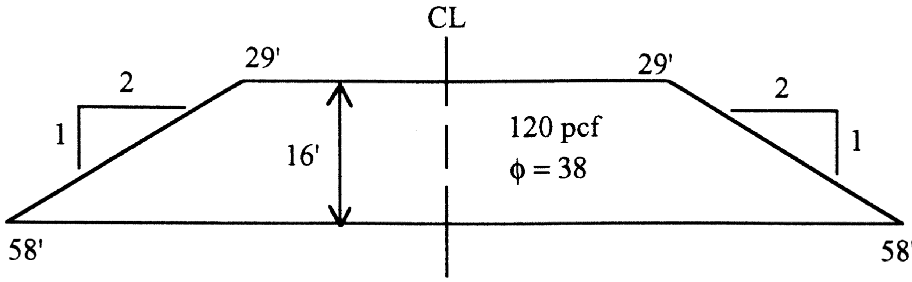

Cross Section of Embankment

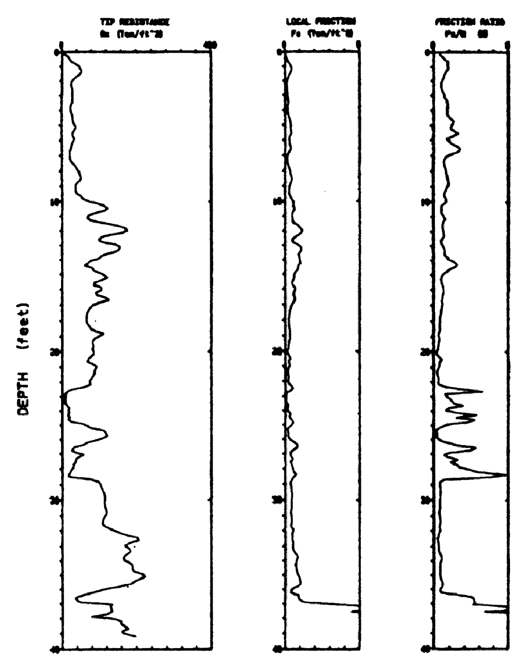

Layer 1: Sand to Silty Sand

H_0 = 12.0 ft. **q_c** = 77.73 tsf **α** = 3.0 **$\Delta\sigma$** = 0.912 tsf

Layer 2: Sand to Silty Sand

H_0 = 6.2 ft. **q_c** = 130.40 tsf **α** = 1.5 **$\Delta\sigma$** = 0.869 tsf

Layer 3: Sandy Silt to Clayey Silt

H_0 = 9.9 ft. **q_c** = 28.68 tsf **α** = 3.0 **$\Delta\sigma$** = 0.826 tsf

Layer 4: Sand to Silty Sand

H_0 = 5.1 ft. **q_c** = 154.35 **α** = 1.5 **$\Delta\sigma$** = 0.787 tsf

Calculated Settlement: 2.24 in.
Active Lateral Earth Pressure: 0.00 psf.

Figure 32. Settlement and Lateral Earth Pressure Calculations for South Abutment Bridge B

NORTH ABUTMENT BRIDGE B
SALT FORK RIVER

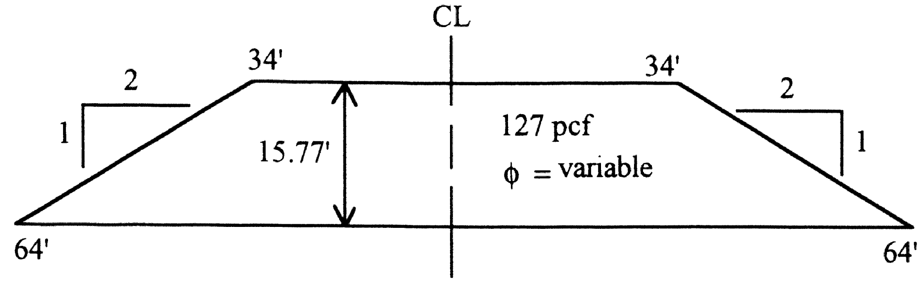

Cross Section of Embankment

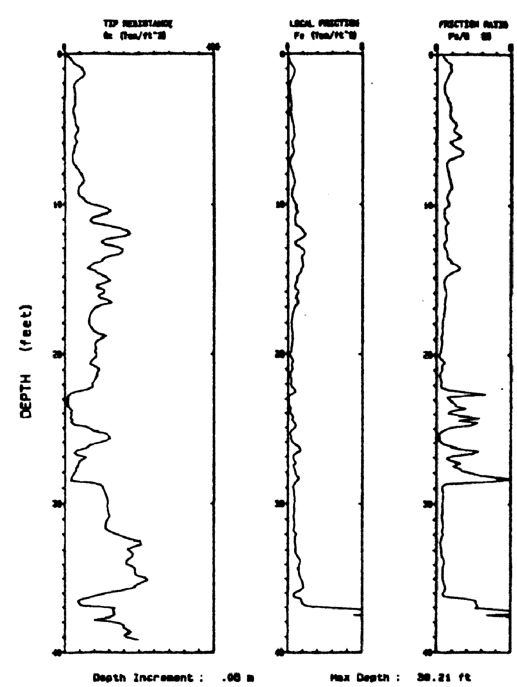

Layer 1: Sand to Silty Sand

H_0 = 4.2 ft. q_c = 75.17 tsf α = 3.0 $\Delta\sigma$ = 0.969 tsf

Layer 2: Silty Sand to Sandy Silt

H_0 = 3.0 ft. q_c = 48.17 tsf α = 2.0 $\Delta\sigma$ = 0.951 tsf

Layer 3: Sand to Silty Sand

H_0 = 14.8 ft. q_c = 98.73 tsf α = 3.0 $\Delta\sigma$ = 0.921 tsf

Layer 4: Silty Sand to Sandy Silt

H_0 = 6.9 ft. q_c = 37.51 tsf α = 2.0 $\Delta\sigma$ = 0.850 tsf

Layer 5: Sand to Silty Sand

H_0 = 7.1 ft. q_c = 119.72 tsf α = 1.5 $\Delta\sigma$ = 0.800 tsf

Calculated Settlement: 2.44 in.
Fluid Pressure From Wet Backfill: 2003 psf

Figure 33. Profile and Settlement Calculations for North Abutment Bridge B

SOUTH ABUTMENT BRIDGE C
SALT FORK RIVER

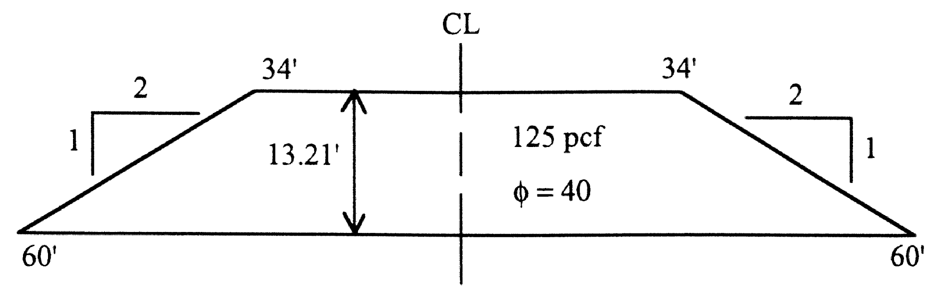

Cross Section of Embankment

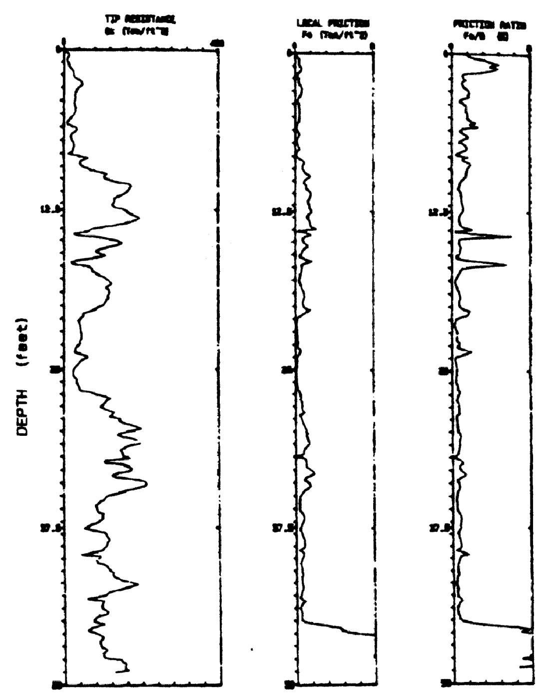

Layer 1: Silty Sand to Sandy Silt

H_0 = 8.0 ft. **q_c** = 49.08 tsf **α** = 3.0 **$\Delta\sigma$** = 0.790tsf

Layer 2: Sand to Silty Sand

H_0 = 13.0 ft. **q_c** = 141.91 tsf **α** = 1.5 **$\Delta\sigma$** = 0.743 tsf

Layer 3: Sand to Silty Sand

H_0 = 5.6 ft. **q_c** = 44.03 tsf **α** = 2.0 **$\Delta\sigma$** = 0.686 tsf

Layer 4: Sand to Silty Sand

H_0 = 8.4 ft. **q_c** = 138.89 tsf **α** = 1.5 **$\Delta\sigma$** = 0.644 tsf

Layer 5: Sand to Silty Sand

H_0 = 9.8 ft. **q_c** = 87.71 tsf **α** = 3.0 **$\Delta\sigma$** = 0.578 tsf

Calculated Settlement: 2.15 in.
Active Lateral Earth Pressure: 394 psf

Figure 34. Settlement Calculation and Lateral Earth Pressures for South Abutment Bridge C

NORTH ABUTMENT BRIDGE C
SALT FORK RIVER

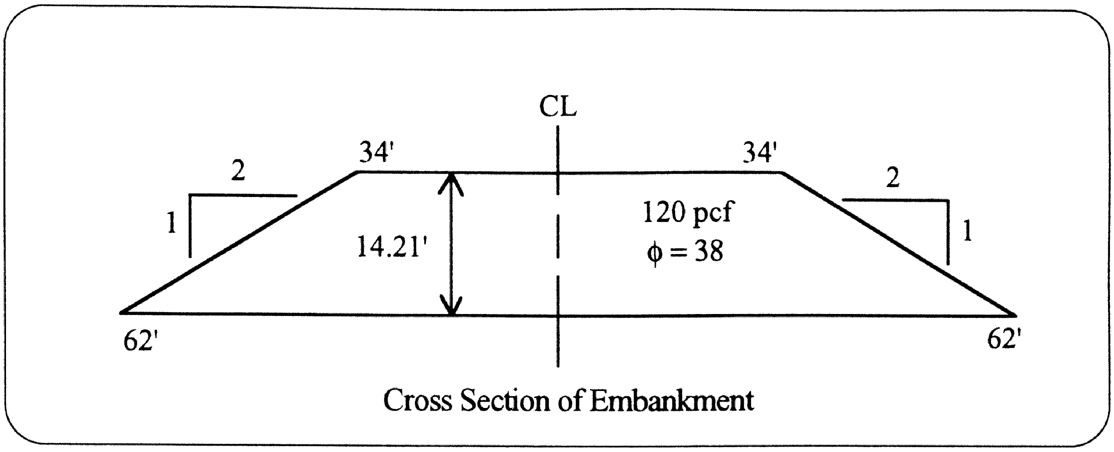

Cross Section of Embankment

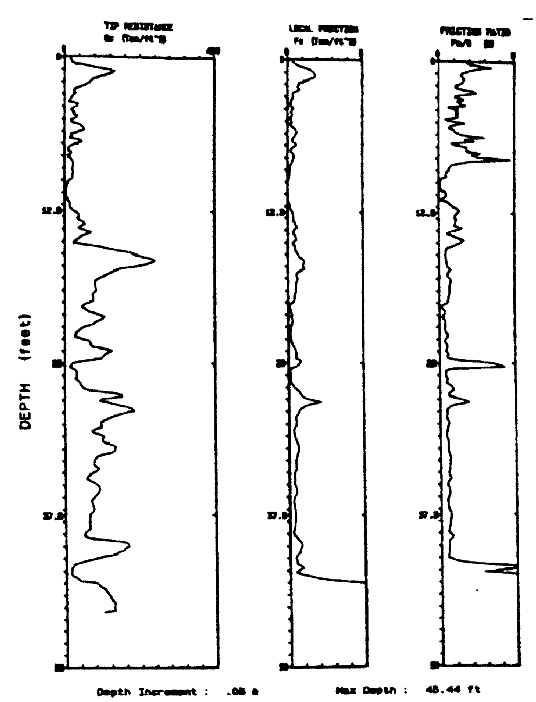

Layer 1: Silty Sand to Sandy Silt

$\mathbf{H_0}$ = 8.8 ft. $\mathbf{q_c}$ = 91.06 tsf $\boldsymbol{\alpha}$ = 3.0 $\boldsymbol{\Delta\sigma}$ = 0.815 tsf

Layer 2: Sand to Silty Sand

$\mathbf{H_0}$ = 16.2 ft. $\mathbf{q_c}$ = 91.06 tsf $\boldsymbol{\alpha}$ = 1.5 $\boldsymbol{\Delta\sigma}$ = 0.768 tsf

Layer 3: Sand to Silty Sand

$\mathbf{H_0}$ = 16.0 ft. $\mathbf{q_c}$ = 97.66 tsf $\boldsymbol{\alpha}$ = 3.0 $\boldsymbol{\Delta\sigma}$ = 0.665 tsf

Calculated Settlement: <u>1.71 in.</u>
Active Lateral Earth Pressure: <u>372 psf</u>

Figure 35 . Settlement and Lateral Earth Pressure Calculations for North Abutment Bridge C

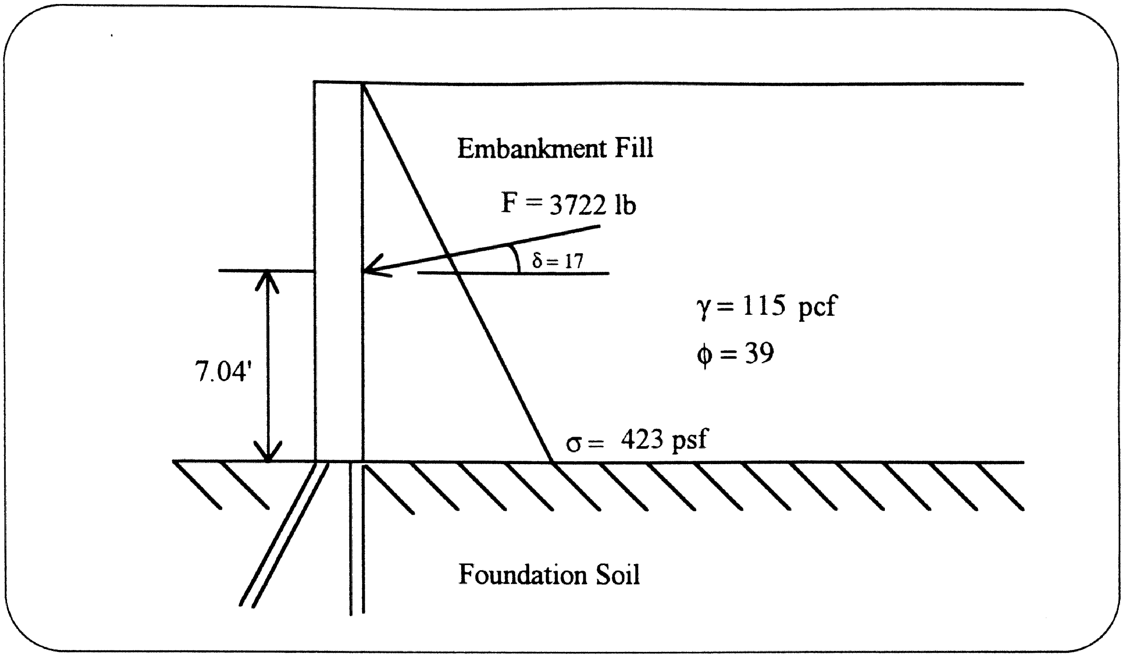

Figure 36. Lateral Earth Pressure, North Abutment Bridge A

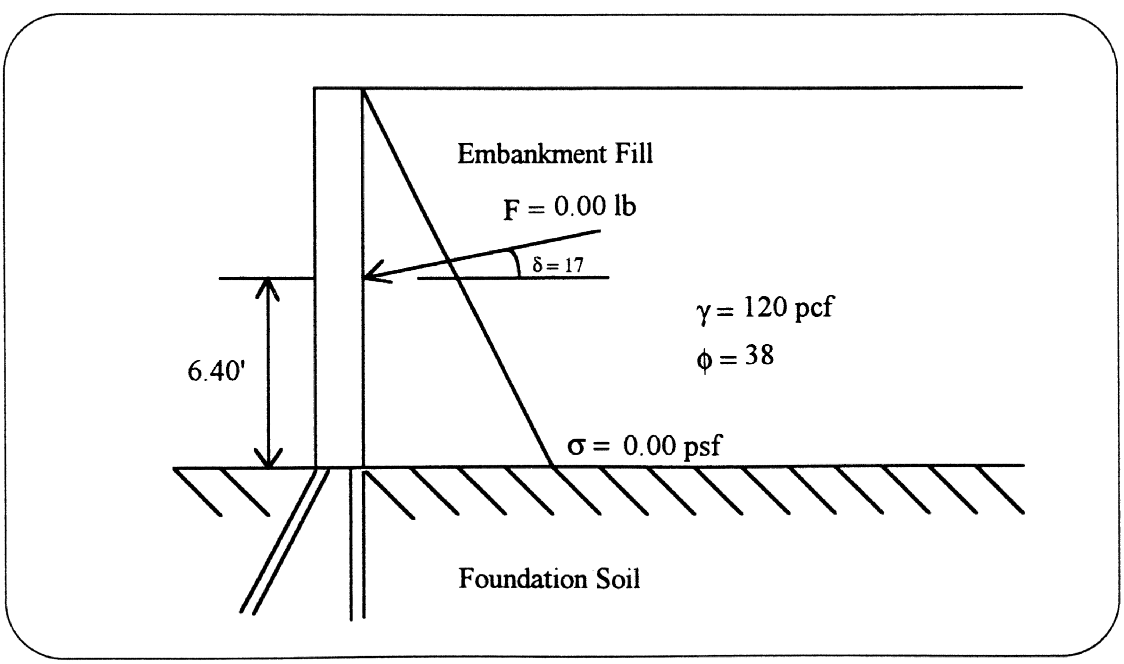

Figure 37. Lateral Earth Pressure, South Abutment Bridge B

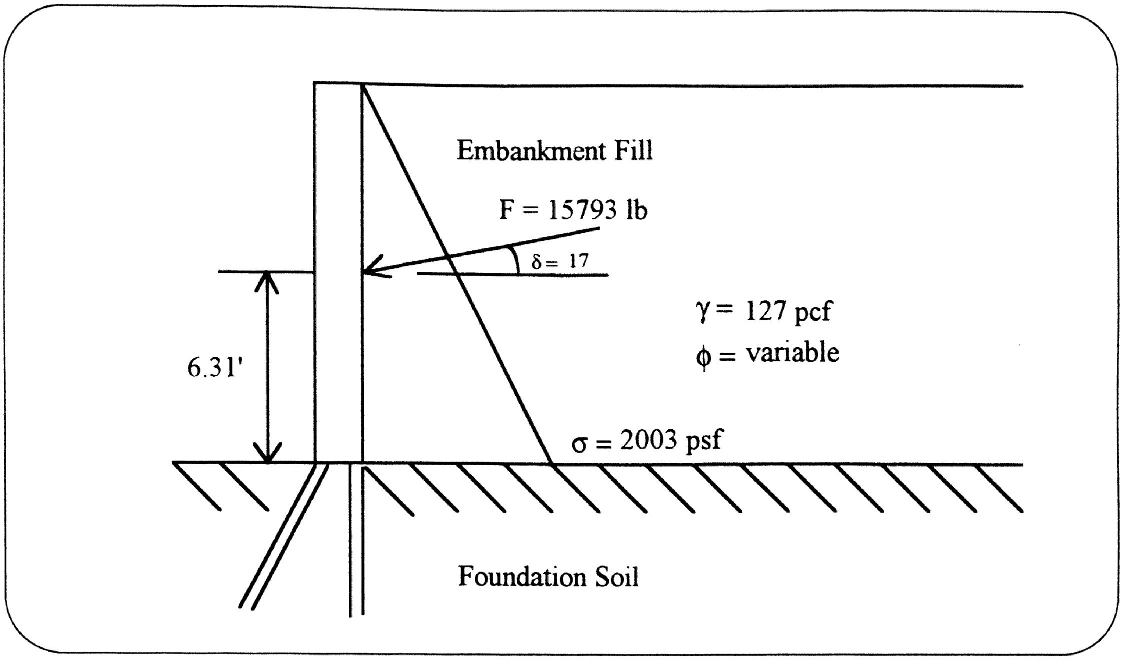

Figure 38. Lateral Earth Pressure, North Abutment Bridge B

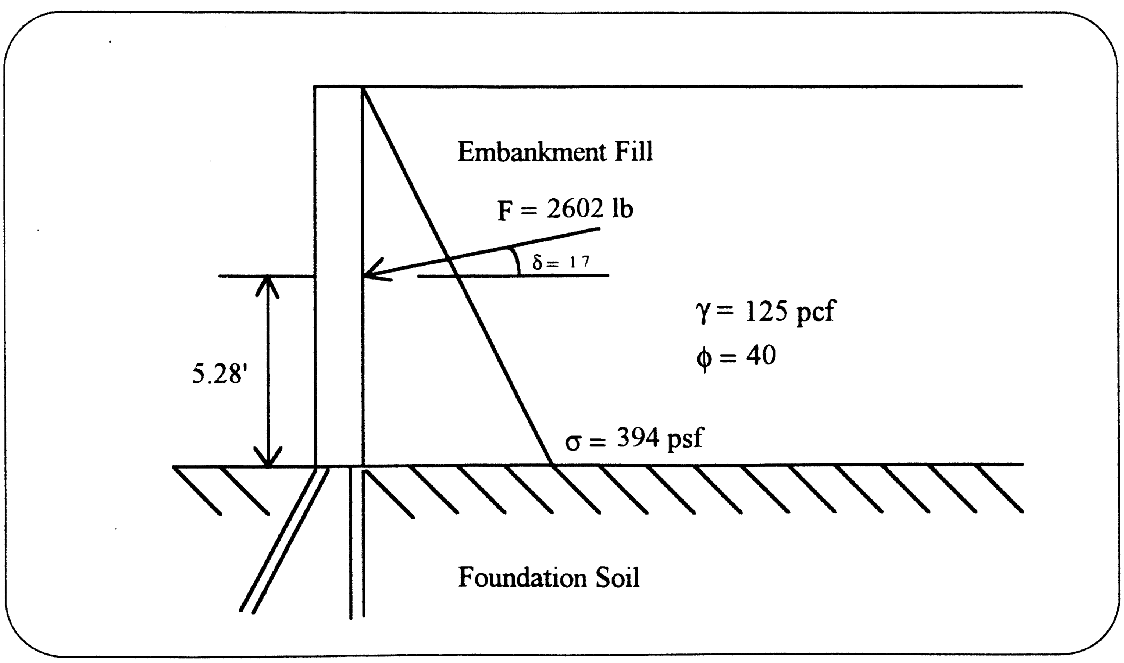

Figure 39. Lateral Earth Pressure, South Abutment Bridge C

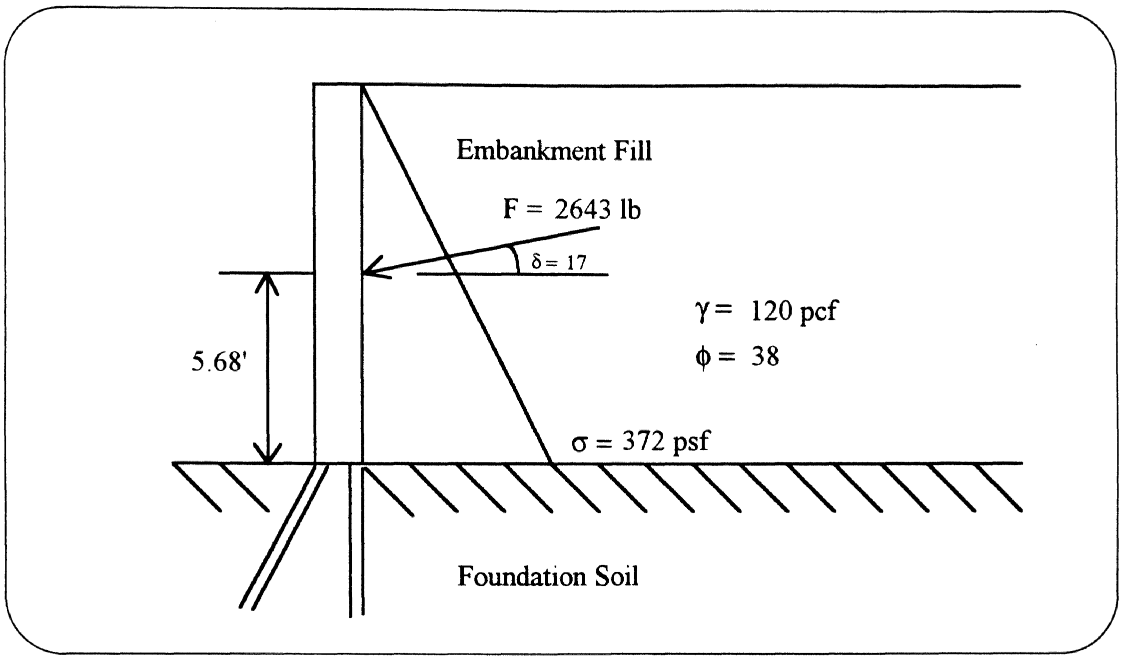

Figure 40. Lateral Earth Pressure, North Abutment Bridge C

CHAPTER 5

DISCUSSION OF RESULTS

The purpose of this paper was to estimate the settlement and lateral earth pressure at the abutment wall for five approach embankments at the Salt Fork River. The first step in doing this was to search the literature for methods for calculating settlement and lateral earth pressure. The next step was to perform a methodology study on some of the settlement calculation methods on 12 bridge approaches where the settlement had already been measured. Once the best settlement calculation method was chosen, it was used to calculate settlement of the Salt Fork River bridges.

Discussion of the Settlement Prediction Methodology Study

Since there was already Cone Penetration Test data available for the 12 sites where settlement had been measured, it was decided to use methods for predicting settlement directly from this data. Therefore, Schmertmann's method and Sanglerat's method were tested using various methods for estimating the change in stress under each embankment. It turned out that Sanglerat's method used with Perloff's method for change in stress under an embankment was the most accurate method of predicting settlement for an embankment. However, even though this method gave results that were close to the measured settlements for the 12 sites, the majority of these calculated settlements were less than the measured settlements and were therefore nonconservative. Schmertmann's method, though not nearly as accurate as Sanglerat's method, usually gave very conservative results. Therefore, this method was more reliable. In selecting a method for predicting settlement, one must choose between an accurate method and a reliable one, and in this case, the more accurate method was chosen.

Despite the accuracy of Sanglerat's method in this study, there were some factors in this study which were up to the judgment of an engineer. For example, the measured settlement on the 12 bridges from the OU site was at times subjective, even though the people who obtained the data did their best to obtain accurate data. The settlements of the approaches were often obtained by measuring the thickness of the various asphalt overlays that had been placed on the pavement surface. It is often difficult to tell where one layer stops and another starts. Also, they interviewed maintenance personnel to get this information, but it is rare to find a bridge where the same person has been in charge of maintenance since the bridge was constructed. Another example is that two engineers can take the same CPT data and each will have his or her own interpretation of the data. Also, choosing the α value in Sanglerat's equation is up to the judgment of the engineer. This number will have a significant impact on the amount of calculated settlement. Therefore, another engineer could (and probably would) come up with a different interpretation of the CPT data. The point of this is that the results of this study are by no means absolute, and different engineers performing the same study will get slightly different results.

Calculation of Settlement and Lateral Earth Pressures at Salt Fork River Bridges

With this in mind, the settlement was calculated at each of the approach embankments on the Salt Fork River Research site. The calculated settlements ranged from 3.00 inches at the north abutment of bridge A to 1.71 inches at the north abutment of bridge C. These settlements seem to be in line with the foundation soil types found at this site - the foundation soils are mostly sand and silt with very little cohesive soils. Judging from the output of nearby wells, water flows quite easily through these soils, indicating that consolidation will not be a problem. Again, these are not absolute values, but they should be within a reasonable range of the settlement that will occur, and they should be good enough to design the embankments and choose the instrumentation for the embankments.

Lateral earth pressure (on the abutment wall) was calculated using Coulomb's theory, and there is not much to say about this, as it is a well established method. Active pressures were calculated, as the lateral earth pressures will likely be close to these values. The soil underneath these abutment walls is a sand and silt mixture which will not likely expand laterally enough to push the piles out away from the embankment and push the wall into the embankment. Other than this, there is no other mechanism by which passive pressure can be developed behind the abutment wall. It was especially difficult, though, to determine how the controlled low strength backfill would behave, and the maximum lateral pressure was taken to be the fluid pressure of the wet backfill just after being poured. Once the backfill sets, it will probably exert no lateral pressure on the abutment

REFERENCES

1. Ardani, A., Bridge Approach Settlement, Report No. CDOH-DTP-R-87-06, Colorado Department of Highways (1987), pp 55.

2. Ayers, M., Personal Correspondence.

3. Barker, R., Duncan, J., Roijiani, K., Ooi, P., Tan, C., and Kim, S., Manuals for the Design of Bridge Foundations, Transportation Research Board, Washington, D.C. (1991), pp

4. Bowles, J., Foundation Analysis and Design, Mc Graw - Hill, New York (1988), pp. 471-525.

5. Briaud, J., and Tucker, L. "Evaluation of Cone Penetration Test Methods Using 98 Load Tests", Proceedings of the First International Symposium on Penetration Testing, ISOPT-I, Orlando, 20-24 March, 1988, pp. 687-697.

6. Caquot, A., and Kerisel, J., Tables for the Calculation of Passive Pressure, Active Pressure, and Bearing Capacity of Foundations, Gauthier-Villars, Imprimeur-Librarie, Librarie du Bureau des Longitudes, de L'Ecole Polytechnique, Paris (1988), 120 pp.

7. Cheny, R., and Chassie, R., Soils and Foundations Workshop Manual, Federal Highway Administration, Washington, D.C. (1982), pp. 113-115.

8. Clough, R., and Woodward, R., Analysis of Embankment Stresses and Deformations, Journal of Soil Mechanics and Foundations Division, ASCE, Vol. 93, No. SM4, pp. 529-549.

9. Das, B., Principles of Geotechnical Engineering, PWS-Kent, Boston (1990) pp.179-268.

10. Holtz, R., Treatment of Problem Foundations for Highway Embankments, Transportation Research Board, Washington, D.C. (1982).

11. Jumikis, A., Soil Mechanics, Robert E. Krieger, Inc., Malabar, Fl. (1984).

12. Laguros, J., Boyd, D., Zaman, M., and Jha, R., Statistical Models for Identification of Problematic Bridge Sites and Estimation of Approach Settlements, Study 2188, ORA 125-064, Oklahoma Department of Transportation, Oklahoma City (1993).

13. Laguros, J., Zaman, M., Evaluation of Causes of Excessive Settlements of

Pavements Behind Bridge Abutments and their Remedies - Phase III, Study 2163, ORA 157-293, Oklahoma Department of Transportation, Oklahoma City (1990).

14. Laguros, J., Zaman, M, and Mahmood, I., Evaluation of Causes of Excessive Settlements of Pavements Behind Bridge Abutments and their Remedies - Phase II, Study 86-04-2, ORA 157-293, Oklahoma Department of Transportation, Oklahoma City (1990).

15. Laguros, J., Boyd, D., Zaman, M., and Mahmood, I., Evaluation of Causes of Excessive Settlements of Pavement Behind Bridge Abutments and their Remedies - Phase I, Study 84-12-2, Oklahoma Department of Transportation, Oklahoma City (1986).

16. Nevels, J., Bridge Foundation Investigation, Project No. BRF-52B(202), State Job No. 08127(04), Structures A, B, and C, Noble and Kay Counties, Project No. 44750, Oklahoma Department of Transportation, Oklahoma City (1994).

17. Perloff, W., Baladi, G., and Haar, M., Stress Distribution Within and Under Long Elastic Embankments, High. Res. Record No. 181. (1967) p. 12.

18. Riaund, J, and Miran, J., The Cone Penetration Test, Publication No. FHWA-SA-91-043, Federal Highway Administration, Washington, D.C. (1992).

19. Tan, C., and Duncan, J., Settlement of Footings on Sands - Accuracy and Reliability, Geotechnical Engineering Congress 1991, Geotechnical Special Publication No. 27, Vol. 1, June, 1991, pp. 446-455.

20. Wahls, H., Design and Construction of Bridge Approaches, Transportation Research Board, Washington, D.C. (1986).

APPENDIX A
PROFILE AND PROPERTIES FOR OU RESEARCH STUDY SITES

SITE # 3, WASHITA COUNTY
STATE HIGHWAY 152

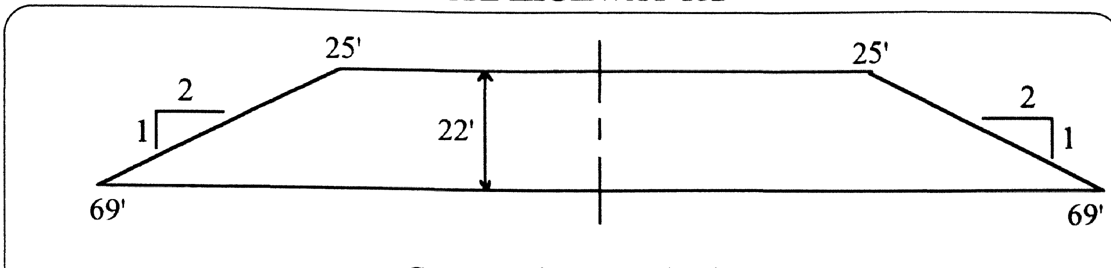

Cross Section of Embankment

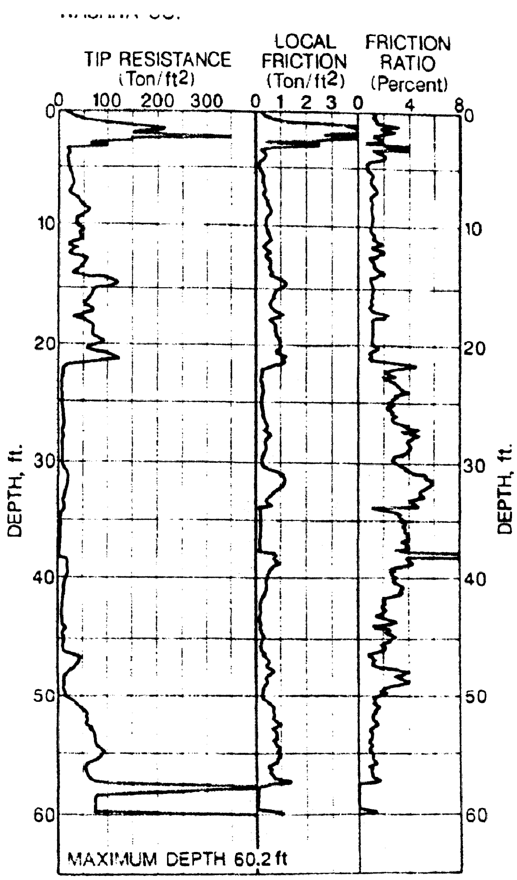

LAYER 1: Sandy Silt to Clayey Silt
H_0 = 3.0 ft. q_c=230.71 tsf α =1.0 $\Delta\sigma$ =1.265 tsf

LAYER 2: Sandy Silt to Clayey Silt
H_0 = 11.0 ft. q_c = 63.53 tsf α = 3.0
$\Delta\sigma$ = 1.189 tsf

LAYER 3: Silty Sand to Sandy Silt
H_0 = 8.0 ft. q_c = 94.99 tsf α = 2.0
$\Delta\sigma$ = 1.164 tsf

LAYER 4: Clay to Organic Clay
H_0 = 20.0 ft. q_c = 14.87 tsf α = 3.0
$\Delta\sigma$ = 1.088 tsf

LAYER 5: Clayey Silt to Silty Clay
H_0 = 4.0 ft. q_c =12.49 tsf α = 3.0 $\Delta\sigma$ =1.012 tsf

LAYER 6: Sandy Silt to Clayey Silt
H_0 = 11.5 ft. q_c = 37.51 tsf α = 4.0
$\Delta\sigma$ = 0.987 tsf

LAYER 7: Silty Sand to Sandy Silt
H_0 = 2.5 ft. q_c = 54.82 tsf α = 3.0
$\Delta\sigma$ = .923 tsf

Calculated Settlement: 9.8 in.
Measured Settlement: 18.0 in.

SITE # 4, WASHITA COUNTY
STATE HIGHWAY 152

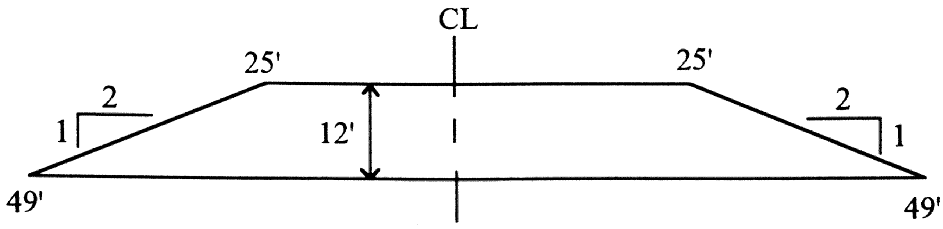

Embankment Cross Section

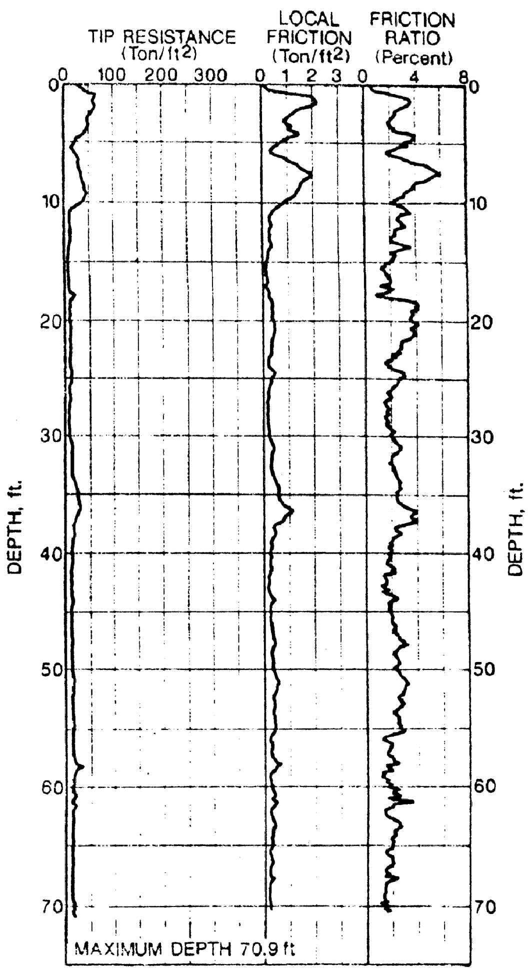

LAYER 1: Sandy Silt to Clayey Silt

H_0 = 11 ft. **q_c** = 68.78 tsf **α** = 4.0
$\Delta\sigma$ = 0.705 tsf

LAYER 2: Sandy Silt to Clayey Silt
H_0 = 7 ft. **q_c** = 13.27 tsf **α** = 3.0 **$\Delta\sigma$** = 0.675 tsf

LAYER 3: Sandy Silt to Clayey Silt

H_0 = 19 ft. **q_c** = 10.25 tsf **α** = 3.0 **$\Delta\sigma$** = 0.585 tsf

LAYER 4: Sandy Silt to Clayey Silt

H_0 = 10 ft. **q_c** = 12.21 tsf **α** = 3.0 **$\Delta\sigma$** = 0.488 tsf

LAYER 5: Sandy Silt to Clayey Silt

H_0 = 9 ft. **q_c** = 10.65 tsf **α** = 3.0 **$\Delta\sigma$** = 0.435 tsf

LAYER 6: Sandy Silt to Clayey Silt

H_0 = 15 ft. **q_c** = 9.03 tsf **α** = 3.0 **$\Delta\sigma$** = 0.383 tsf

Calculated Settlement: 11.71 in.
Measured Settlement: 5.0 in.

SITE # 5, CLEVELAND COUNTY
STATE HIGHWAY 9

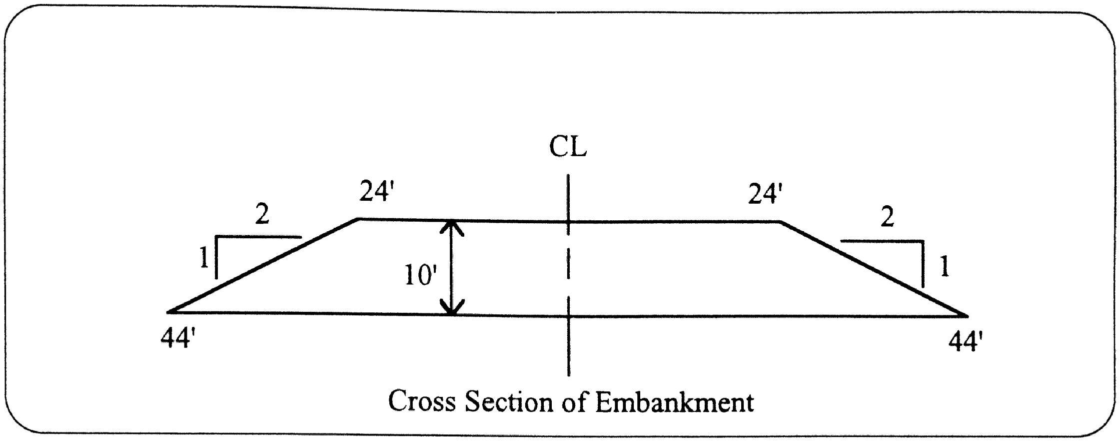

Cross Section of Embankment

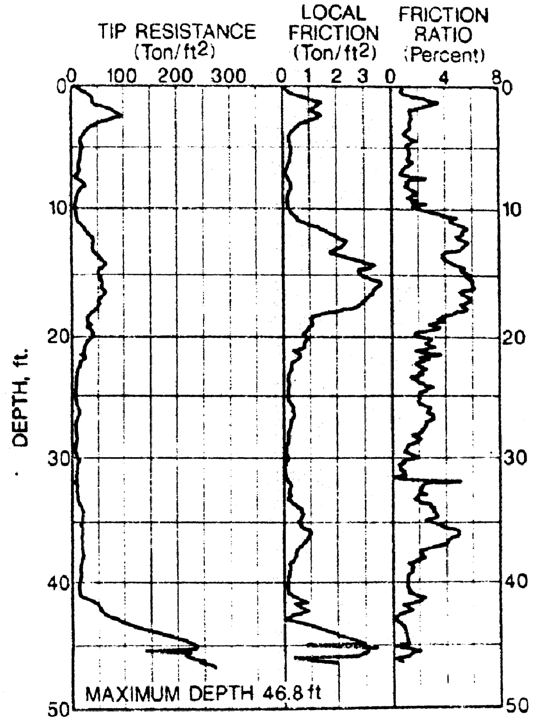

Layer 1: Silty Sand to Sandy Silt
H_0 = 10 ft. **q_c** = 44.50 tsf **α** = 2.0
$\Delta\sigma$ = 0.570 tsf

Layer 2: Clayey Silt to Silty Clay
H_0 = 10 ft. **q_c** = 60.71 tsf **α** = 1.0
$\Delta\sigma$ = 0.516 tsf

Layer 3: Sandy Silt to Clayey Silt
H_0 = 12 ft. **q_c** = 21.86 tsf **α** = 2.0
$\Delta\sigma$ = 0.444 tsf

Layer 4: Sandy Silt to Clayey Silt
H_0 = 6 ft. **q_c** = 23.69 tsf **α** = 2.0
$\Delta\sigma$ = 0.390 tsf

Layer 5: Sand to Silty Sand
H_0 = 9 ft. **q_c** = 106.28 tsf **α** = 1.5
$\Delta\sigma$ = 0.348 tsf

Calculated Settlement: 4.14 in.
Measured Settlement: 6.00 in.

SITE # 7, LINCOLN COUNTY
STATE HIGHWAY 102

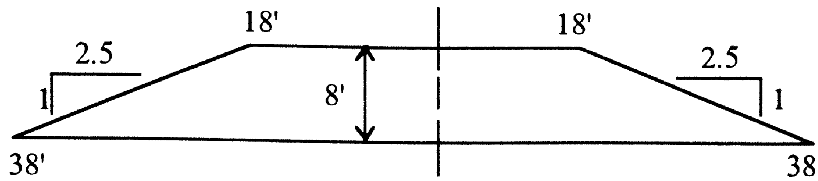

Cross Section of Embankment

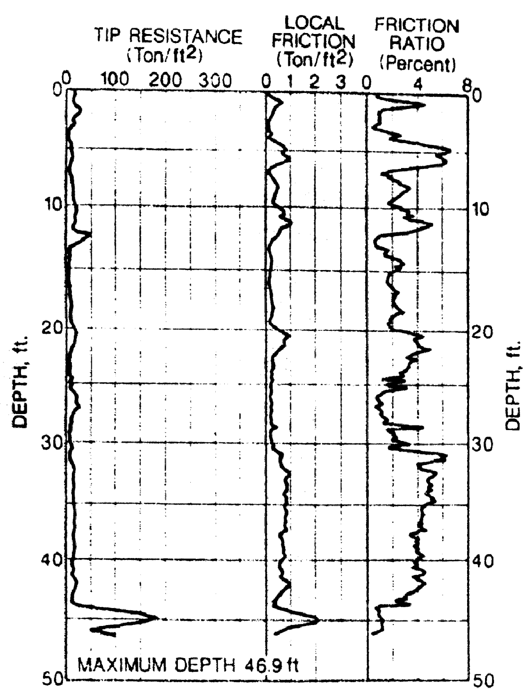

Layer 1: Sandy Silt to Clayey Silt

H_0 = 12.0 ft. **q_c** = 34.36 tsf **α** = 3.0
$\Delta\sigma$ = 0.460 tsf

Layer 2: Sandy Silt to Clayey Silt
H_0 = 7.5 ft. **q_c** = 13.27 tsf **α** = 1.0
$\Delta\sigma$ = 0.400 tsf

Layer 3: Sandy Silt to Clayey Silt
H_0 = 6.5 ft. **q_c** = 17.36 tsf **α** = 1.0 **$\Delta\sigma$** = 0.360 tsf

Layer 4: Silty Sand to Sandy Silt
H_0 = 4.0 ft. **q_c** = 21.14 tsf **α** = 3.0 **$\Delta\sigma$** = 0.325 tsf

Layer 5: Clayey Silt to Silty Clay

H_0 = 13.5 ft. **q_c** = 18.46 tsf **α** = 1.0
$\Delta\sigma$ = 0.275 tsf

Calculated Settlement: 7.63 in.
Measured Settlement: 8.0 in.

SITE # 10, KAY COUNTY
INTERSTATE 35

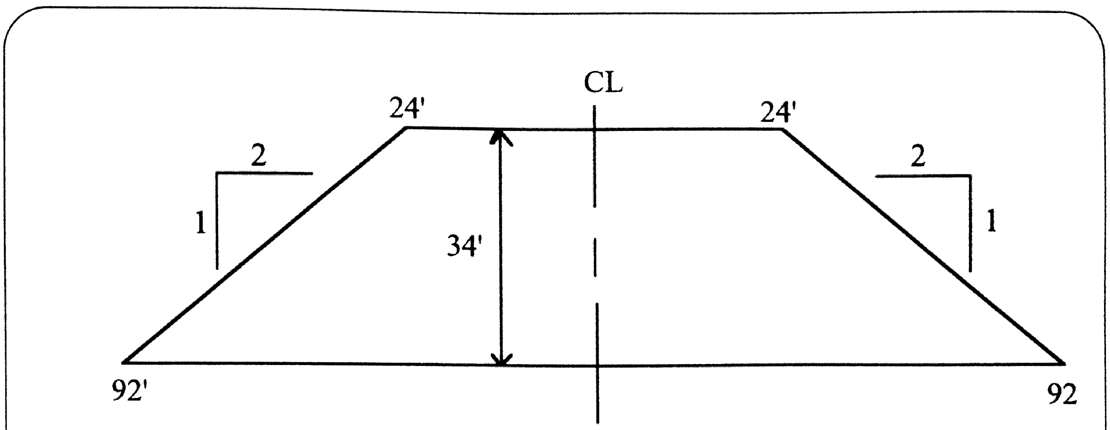

Cross Section of Embankment

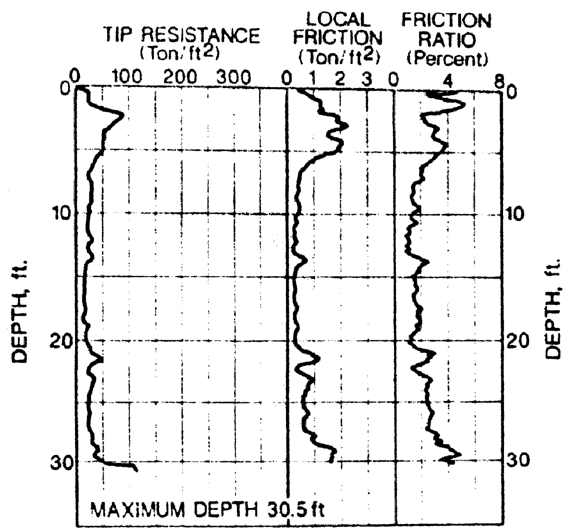

LAYER 1: Sandy Silt to Clayey Silt
H_0 = 7.0 ft. **q_c** = 73.69 tsf **α** = 3.0
$\Delta\sigma$ = 2.14 tsf

LAYER 2: Silty Sand to Sandy Silt
H_0 = 7.0 ft. **q_c** = 43.06 tsf **α** = 2.0
$\Delta\sigma$ = 2.11 tsf

LAYER 3: Silty Sand to Sandy Silt
H_0 = 8.0 ft. **q_c** = 23.84 tsf **α** = 2.0
$\Delta\sigma$ = 2.08 tsf

LAYER 4: Sandy Silt to Clayey Silt
H_0 = 5.0 **q_c** = 31.32 tsf **α** = 3.0 **$\Delta\sigma$** = 2.04 tsf

LAYER 5: Clayey Silt to Silty Clay
H_0 = 5.0 ft. **q_c** = 38.11 tsf **α** = 1.0
$\Delta\sigma$ = 2.01 tsf

Calculated Settlement: 11.52 in.
Measured Settlement: 6.00 in.

SITE # 11, GARVIN COUNTY
STATE HIGHWAY 174

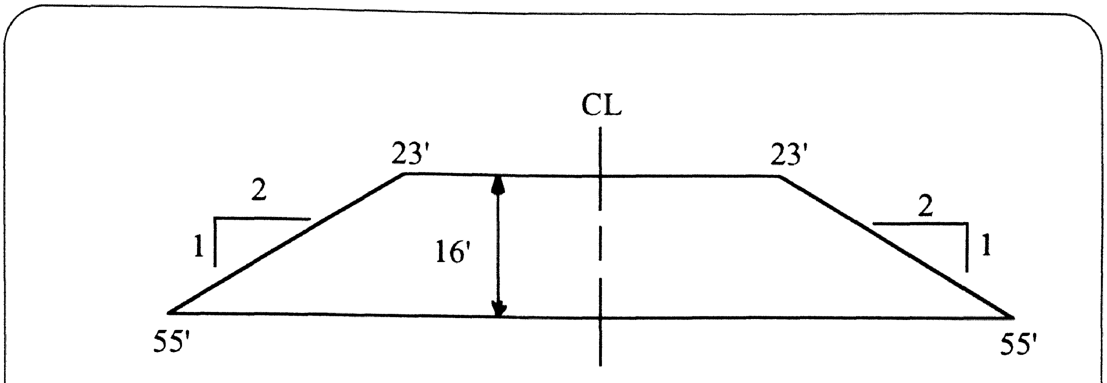

Cross Section of Embankment

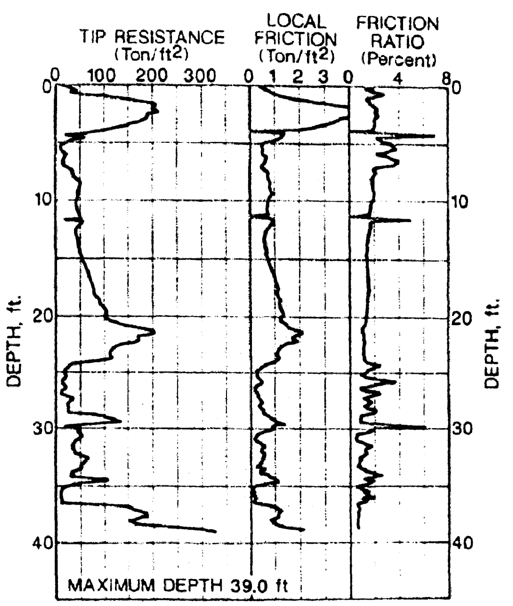

LAYER 1: Sand to Silty Sand
H_0 = 4.0 ft. q_c = 380.47 tsf α = 1.5 $\Delta\sigma$ = 0.901 tsf

LAYER 2: Sandy Silt to Clayey Silt
H_0 = 3.5 ft. q_c = 52.92 tsf α = 2.0 $\Delta\sigma$ = 0.864 tsf

LAYER 3: Sand to Silty Sand
H_0 = 16.5 ft. q_c = 102.59 tsf α = 1.5
$\Delta\sigma$ = 0.781 tsf

LAYER 4: Silty Sand to Sandy Silt
H_0 = 4.0 ft. q_c = 45.47 tsf α = 2.0 $\Delta\sigma$ = 0.643 tsf

LAYER 5: Silty Sand to Sandy Silt
H_0 = 10.0 ft. q_c = 57.42 tsf α = 2.0
$\Delta\sigma$ = 0.496 tsf

Calculated Settlement: 2.28 in.
Measured Settlement: 2.80 in.

SITE # 16, ROGERS COUNTY
STATE HIGHWAY 20

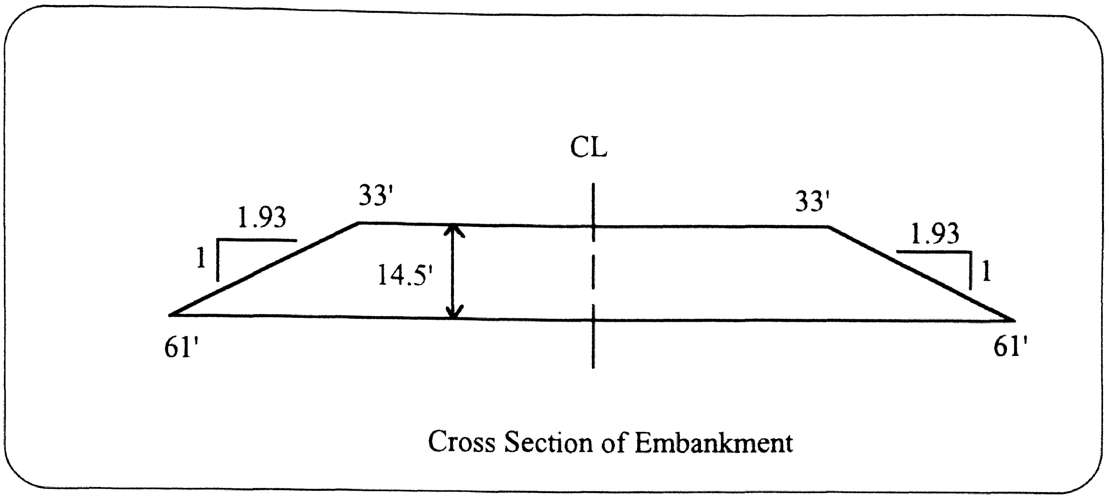

Cross Section of Embankment

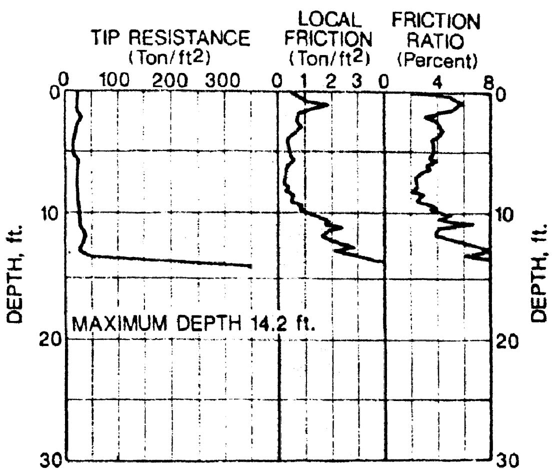

Layer 1: Clay to Organic Clay
H_0 = 2.3 ft. q_c=60.73 tsf α = 1.0 $\Delta\sigma$= 0.888 tsf

Layer 2: Clayey Silt to Silty Clay
H_0 = 6.9 ft. q_c=34.07 tsf α = 1.5 $\Delta\sigma$= 0.860 tsf

Layer 3: Clayey Silt to Silty Clay
H_0 = 3.0 ft. q_c=43.80 tsf α = 1.5 $\Delta\sigma$= 0.834 tsf

Layer 4: Organic Clay or Peat
H_0 = 1.6 ft. q_c=68.79 tsf α = 1.0 $\Delta\sigma$= 0.824 tsf

Calculated Settlement: 2.48 in.
Measured Settlement: 3.0 in.

SITE # 17, LINCOLN COUNTY
U.S. HIGHWAY 177

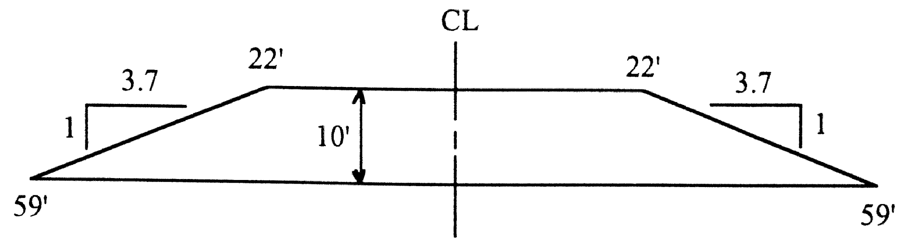

Cross Section of Embankment

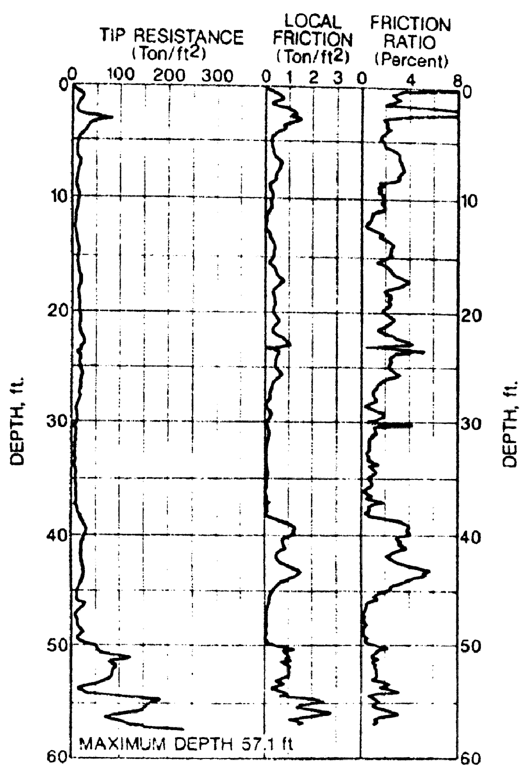

LAYER 1: Clayey Silt to Silty Clay
H_0 = 3.5 ft. q_c = 43.60 tsf α = 1.5 $\Delta\sigma$ = 0.631 tsf

LAYER 2: Silty Sand to Sandy Silt
H_0 = 7.5 ft. q_c = 31.76 tsf α = 2.0 $\Delta\sigma$ = 0.598 tsf

LAYER 3: Silty Sand to Sandy Silt
H_0 = 16.0 ft. q_c = 29.16 tsf α = 2.0
$\Delta\sigma$ = 0.533 tsf

LAYER 4: Silty Sand to Sandy Silt
H_0 = 11.0 ft. q_c = 31.76 tsf α = 2.0
$\Delta\sigma$ = 0.442 tsf

LAYER 5: Sandy Silt to Clayey Silt
H_0 = 8.0 ft. q_c = 23.25 tsf α = 3.0 $\Delta\sigma$ = 0.377 tsf

LAYER 6: Silty Sand to Sandy Silt
H_0 = 3.5 ft. q_c = 10.64 tsf α = 2.0 $\Delta\sigma$ = 0.358 tsf

LAYER 7: Sand to Silty Sand
H_0 = 3.5 ft. q_c = 50.49 tsf α = 2.0 $\Delta\sigma$ = 0.352 tsf

LAYER 8: Silty Sand to Sandy Silt
H_0 = 4.0 ft. q_c = 85.95 tsf α = 3.0 $\Delta\sigma$ = 0.325 tsf

Estimated Settlement: <u>6.05 in.</u>

Measured Settlement: <u>5.00 in.</u>

SITE # 19, OKMULGEE COUNTY
US HIGHWAY 75

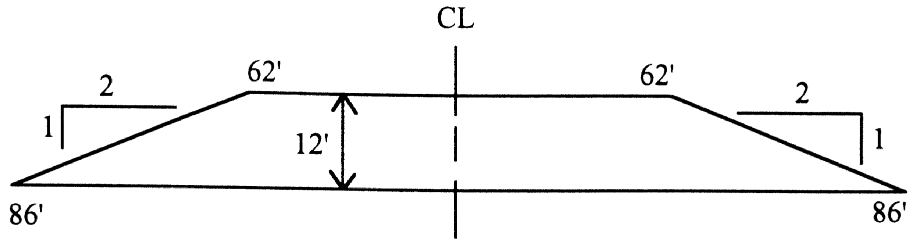

Cross Section of Embankment

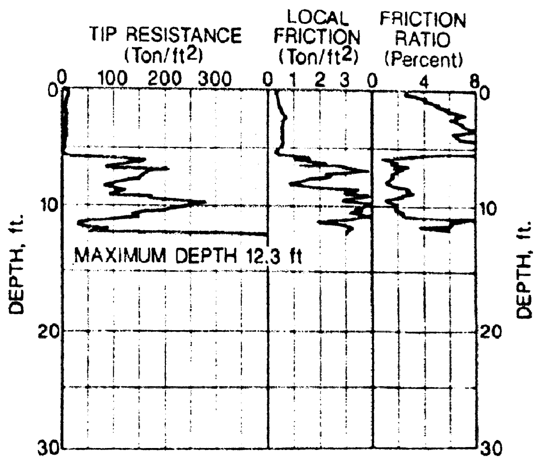

Layer 1: Organic Clay to Clay
H_0 = 6.0 ft. q_c = 18.04 tsf α = 2.0 σ = 0.749 tsf

Layer 2: Sand to Silty Sand
H_0 = 5.0 ft. q_c= 210.71 tsf α = 1.5 $\Delta\sigma$=0.718 tsf

Layer 3: Clay to Organic Clay
H_0 = 1.5 ft. q_c = 77.50 tsf α = 4.0
$\Delta\sigma$ = 0.710 tsf

Calculated Settlement: 1.53 in.
Measured Settlement: 3.00 in.

SITE # 20, WASHITA COUNTY
US HIGHWAY 183

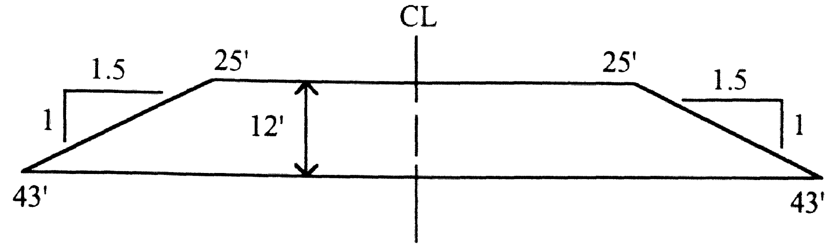

Cross Section of Embankment

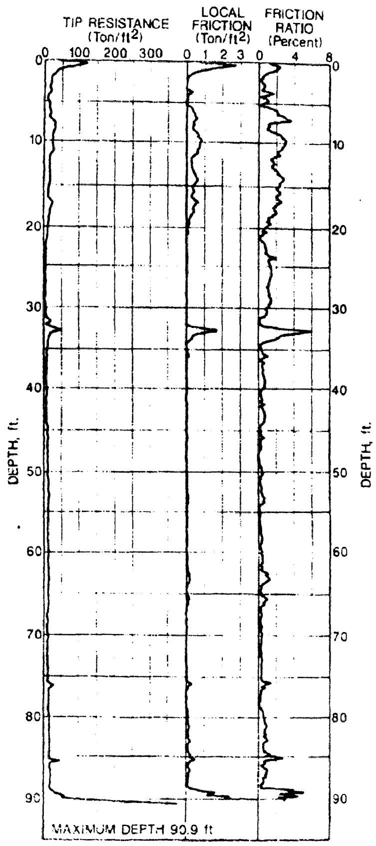

Layer 1: Sand to Silty Sand
H_0 = 5.5 ft. **q_c** = 79.00 tsf **α** = 3.0 **$\Delta\sigma$** = 0.664 tsf

Layer 2: Silty Sand to Sandy Silt
H_0 = 16.0 ft. **q_c** = 35.88 tsf **α** = 2.0 **$\Delta\sigma$** = 0.621 tsf

Layer 3: Silty Sand to Sandy Silt
H_0 = 10.5 ft. **q_c** = 11.23 tsf **α** = 2.0 **$\Delta\sigma$** = 0.538 tsf

Layer 4: Sandy Silt to Clayey Silt
H_0 = 2.5 ft. **q_c** = 25.44 tsf **α** = 3.0 **$\Delta\sigma$** = 0.504 tsf

Layer 5: Silty Sand to Sandy Silt
H_0 = 28.0 ft. **q_c** = 16.59 tsf **α** = 2.0 **$\Delta\sigma$** = 0.414 tsf

Layer 6: Silty Sand to Sandy Silt
H_0 = 7.5 ft. **q_c** = 13.40 tsf **α** = 2.0 **$\Delta\sigma$** = 0.393 tsf

Layer 7: Silty Sand to Sandy Silt
H_0 = 9.0 ft. **q_c** = 12.19 tsf **α** = 2.0 **$\Delta\sigma$** = 0.311 tsf

Layer 8: Silty Sand to Sandy Silt
H_0 = 10.0 ft. **q_c** = 13.68 tsf **α** = 2.0 **$\Delta\sigma$** = 0.297 tsf

Calculated Settlement: 13.18 in.
Measured Settlement: 2.50 in.

SITE # 24, WOODS COUNTY
US HIGHWAY 64

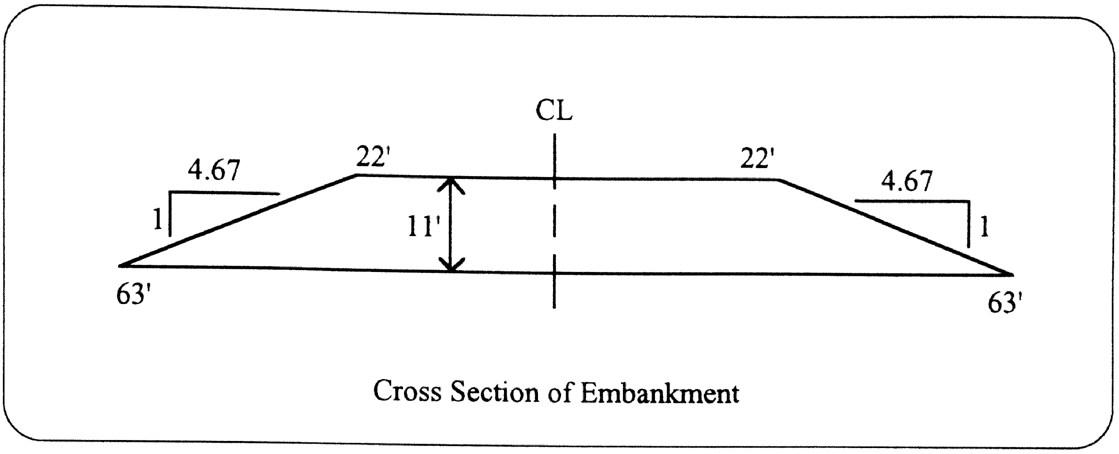

Cross Section of Embankment

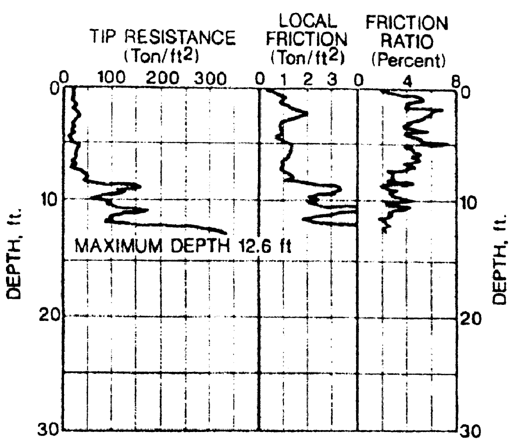

Layer 1: Clayey Silt to Silty Clay
H_0 = 7.5 ft. **q_c** = 45.53 tsf **α** = 1.0 **$\Delta\sigma$** = 0.681 tsf

Layer 2: Silty Sand to Sandy Silt
H_0 = 5.0 ft. **q_c** = 174.74 tsf **α** = 1.5 **$\Delta\sigma$** = 0.658 tsf

Calculated Settlement: 1.49 in.
Measured Settlement: 2.5 in.

SITE # 25, MAJOR COUNTY
STATE HIGHWAY 8

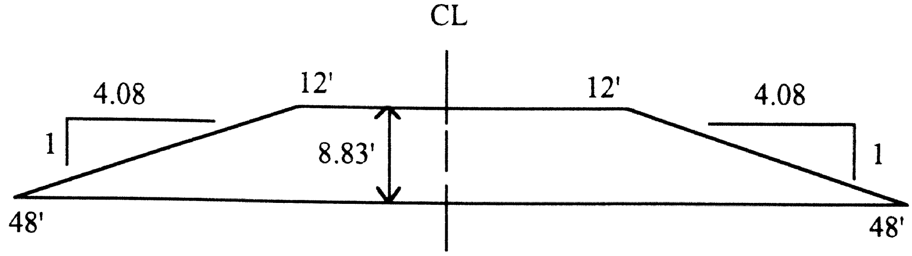

Cross Section of Embankment

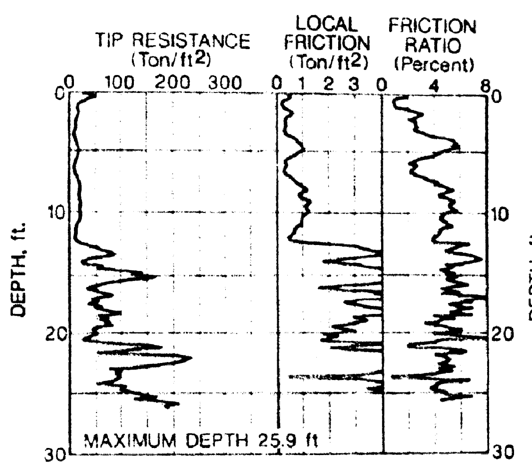

Layer 1: Sandy Silt to Clayey Silt
H_0 = 6.5 ft. **q_c** = 46.61 tsf **α** = 1.0
$\Delta\sigma$= 0.545 tsf

Layer 2: Clayey Silt to Silty Clay
H_0 = 5.5 ft. **q_c** = 37.22 tsf **α** = 1.0 **$\Delta\sigma$**= 0.516 tsf

Layer 3: Clayey Silt to Silty Clay
H_0 = 6.0 ft. **q_c** = 93.52 tsf **α** = 2.5 **$\Delta\sigma$**= 0.487 tsf

Layer 4: Clayey Silt to Silty Clay
H_0 = 5.0 ft. **q_c** = 124.23 tsf **α** = 2.5
$\Delta\sigma$ = 0.435 tsf

Calculated Settlement: 2.06 in.
Measured Settlement: 1.5 in.

APPENDIX B
DETAILS OF VARIOUS APPROACH EMBANKMENT OPTIONS

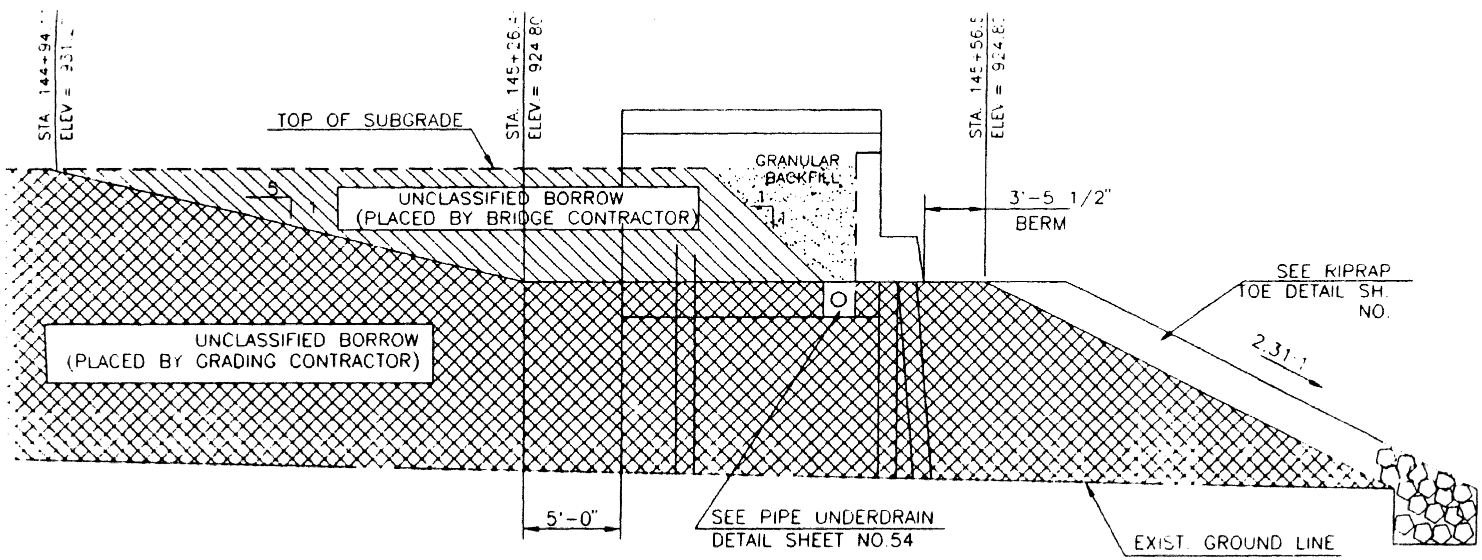

BRIDGE HEADER BEHIND SOUTH ABUTMENT BRIDGE "A"

(UNCLASSIFIED BORROW)

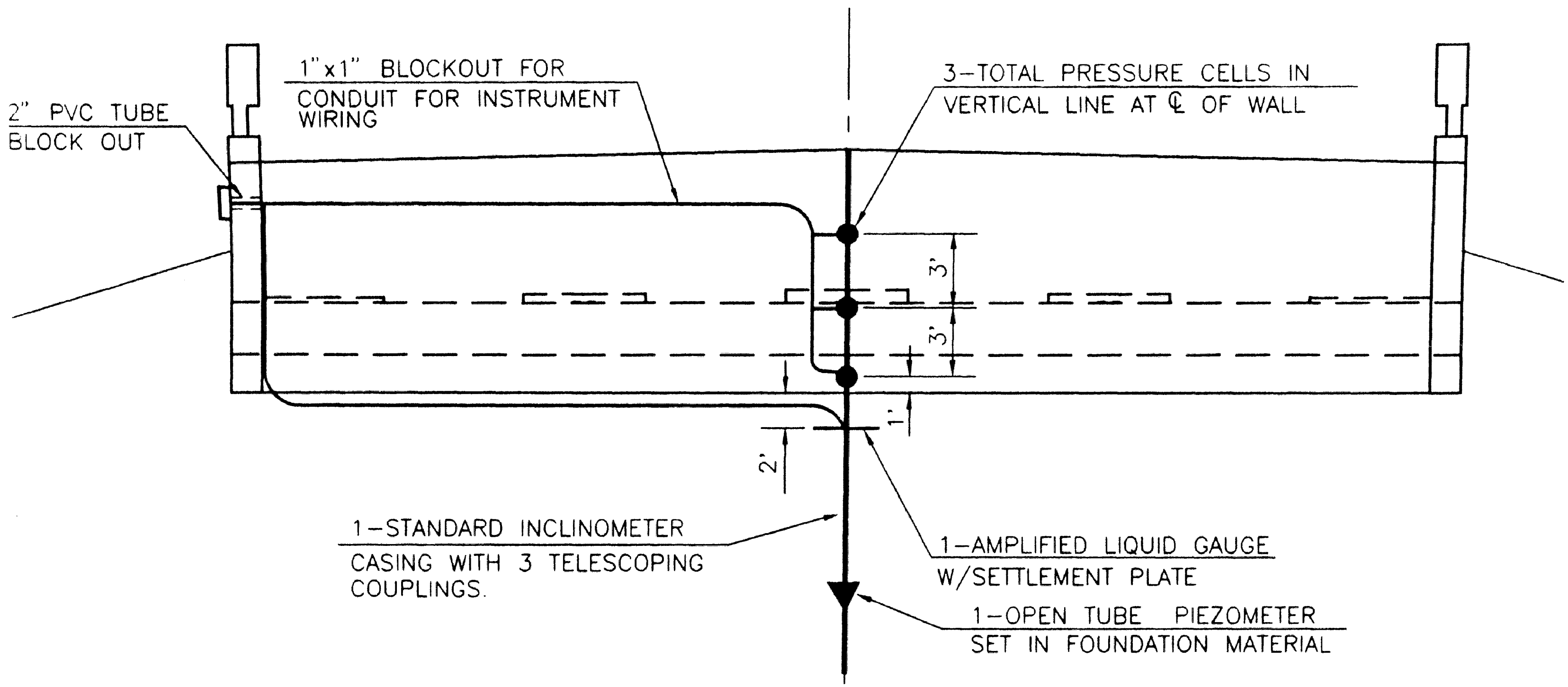
1"x1" BLOCKOUT FOR
CONDUIT FOR INSTRUMENT WIRING
2" PVC TUBE
BLOCK OUT
3-TOTAL PRESSURE CELLS IN
VERTICAL LINE AT ℄ OF WALL
3'
3'
1'
2'
1-STANDARD INCLINOMETER
CASING WITH 3 TELESCOPING COUPLINGS.
1-AMPLIFIED LIQUID GAUGE
W/SETTLEMENT PLATE
1-OPEN TUBE PIEZOMETER
SET IN FOUNDATION MATERIAL

ELEVATION

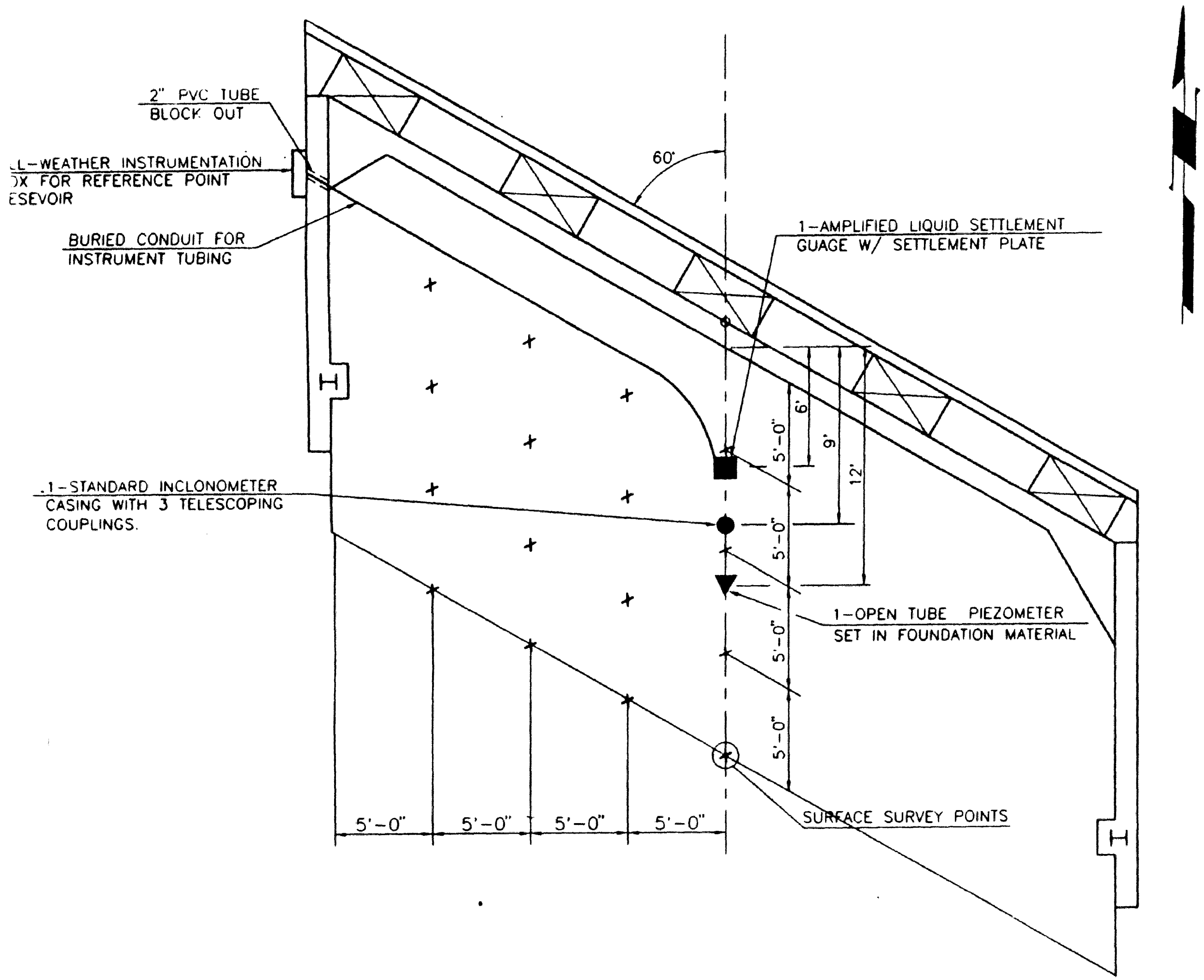

PLAN VIEW OF SOUTH ABUTMENT BRIDGE "A"

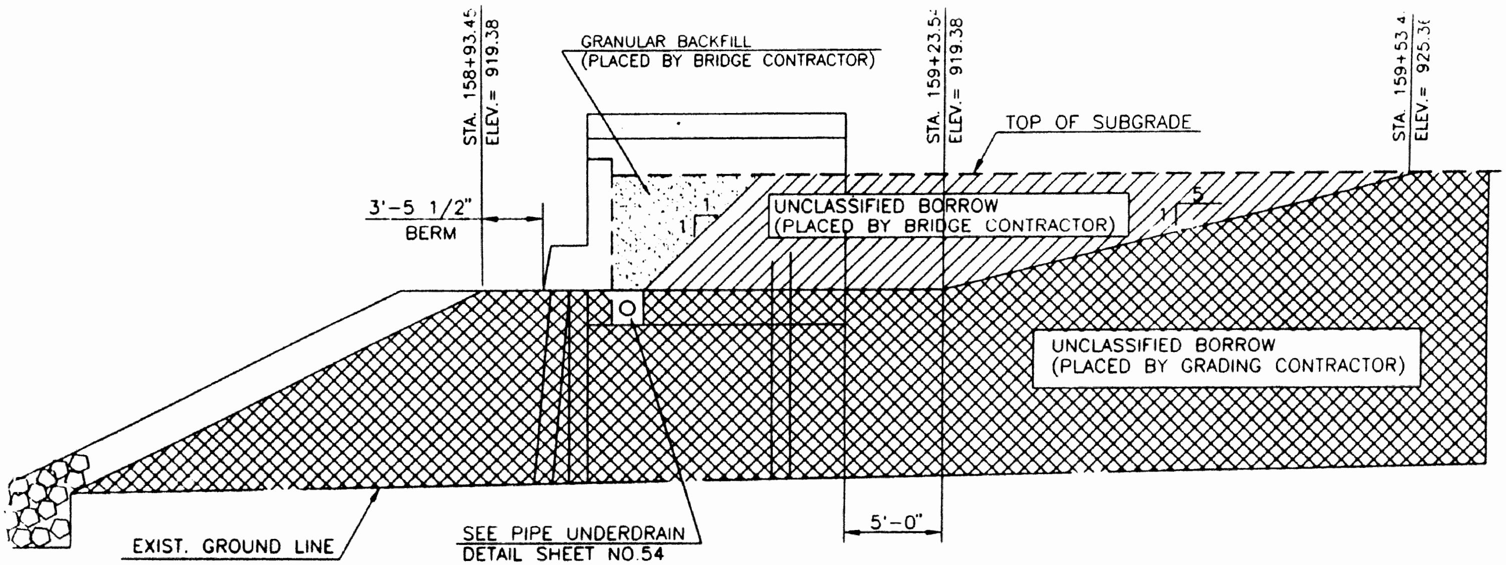

BRIDGE HEADER BEHIND NORTH ABUTMENT BRIDGE "A"

(UNCLASSIFIED BORROW)

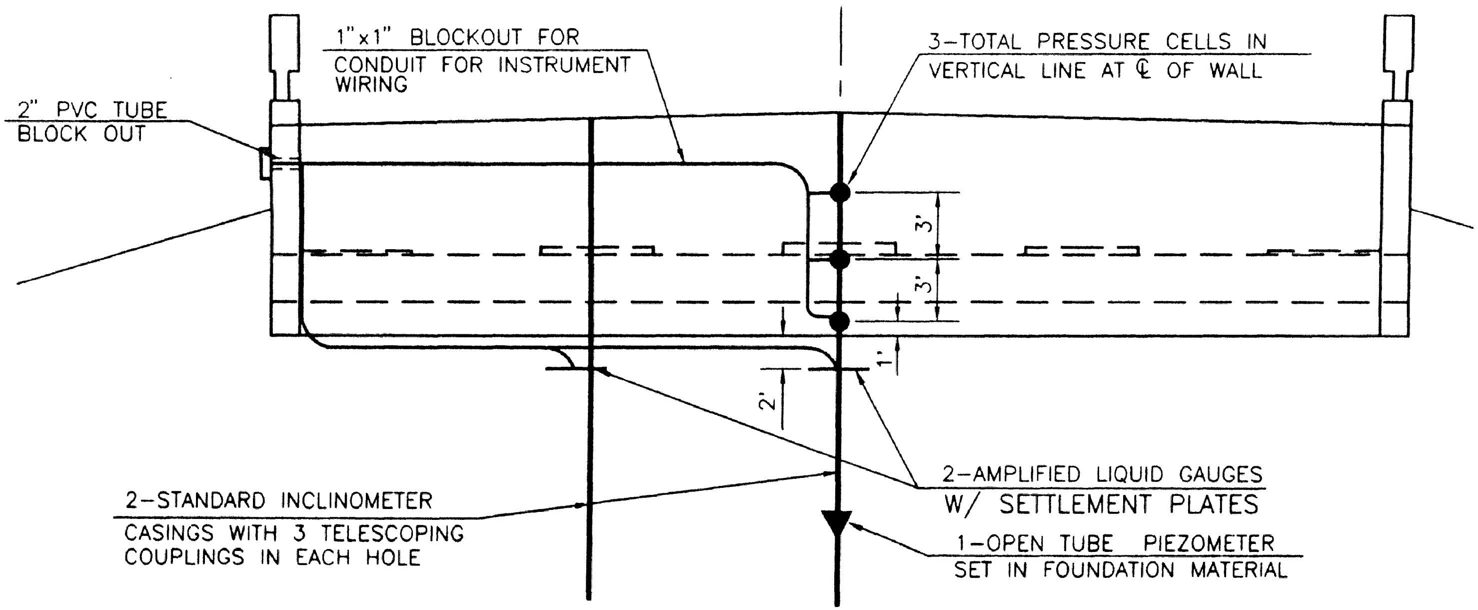
1"x1" BLOCKOUT FOR
CONDUIT FOR INSTRUMENT
WIRING
3–TOTAL PRESSURE CELLS IN
VERTICAL LINE AT ℄ OF WALL
2" PVC TUBE
BLOCK OUT
3'
3'
1'
2'
2–AMPLIFIED LIQUID GAUGES
W/ SETTLEMENT PLATES
2–STANDARD INCLINOMETER
CASINGS WITH 3 TELESCOPING
COUPLINGS IN EACH HOLE
1–OPEN TUBE PIEZOMETER
SET IN FOUNDATION MATERIAL

ELEVATION

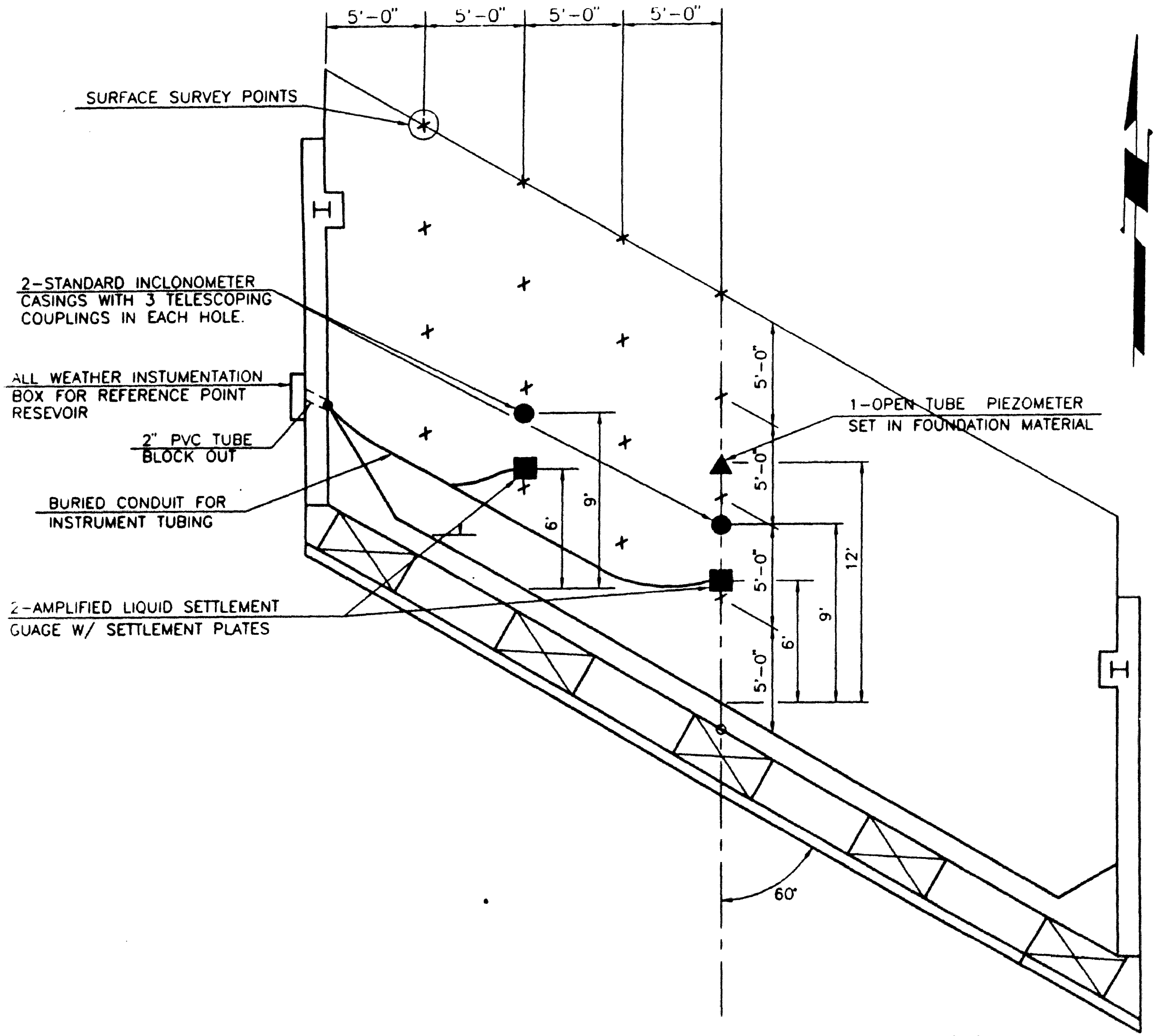

PLAN VIEW OF NORTH ABUTMENT BRIDGE "A"

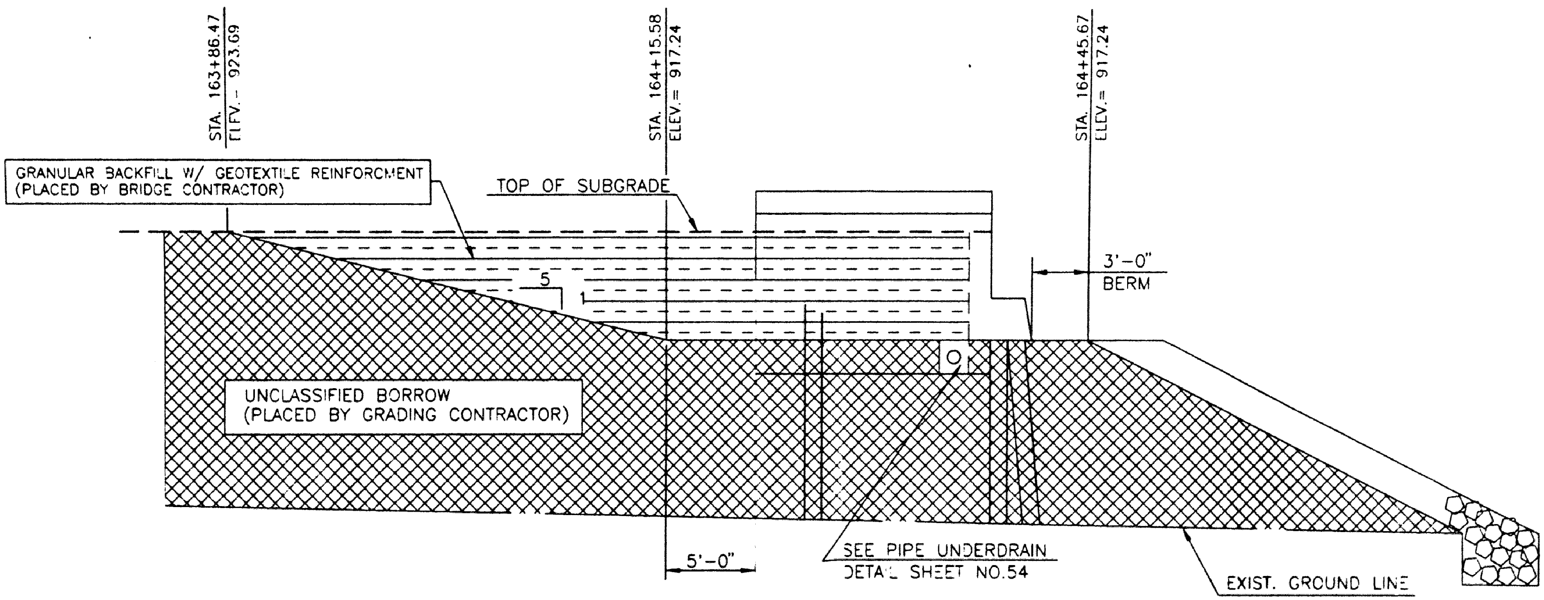

BRIDGE HEADER BEHIND SOUTH ABUTMENT BRIDGE "B"

(GEOTEXTILE REINFORCED APPROACH EMBANKMENT)
SEE SPECIAL PROVISIONS

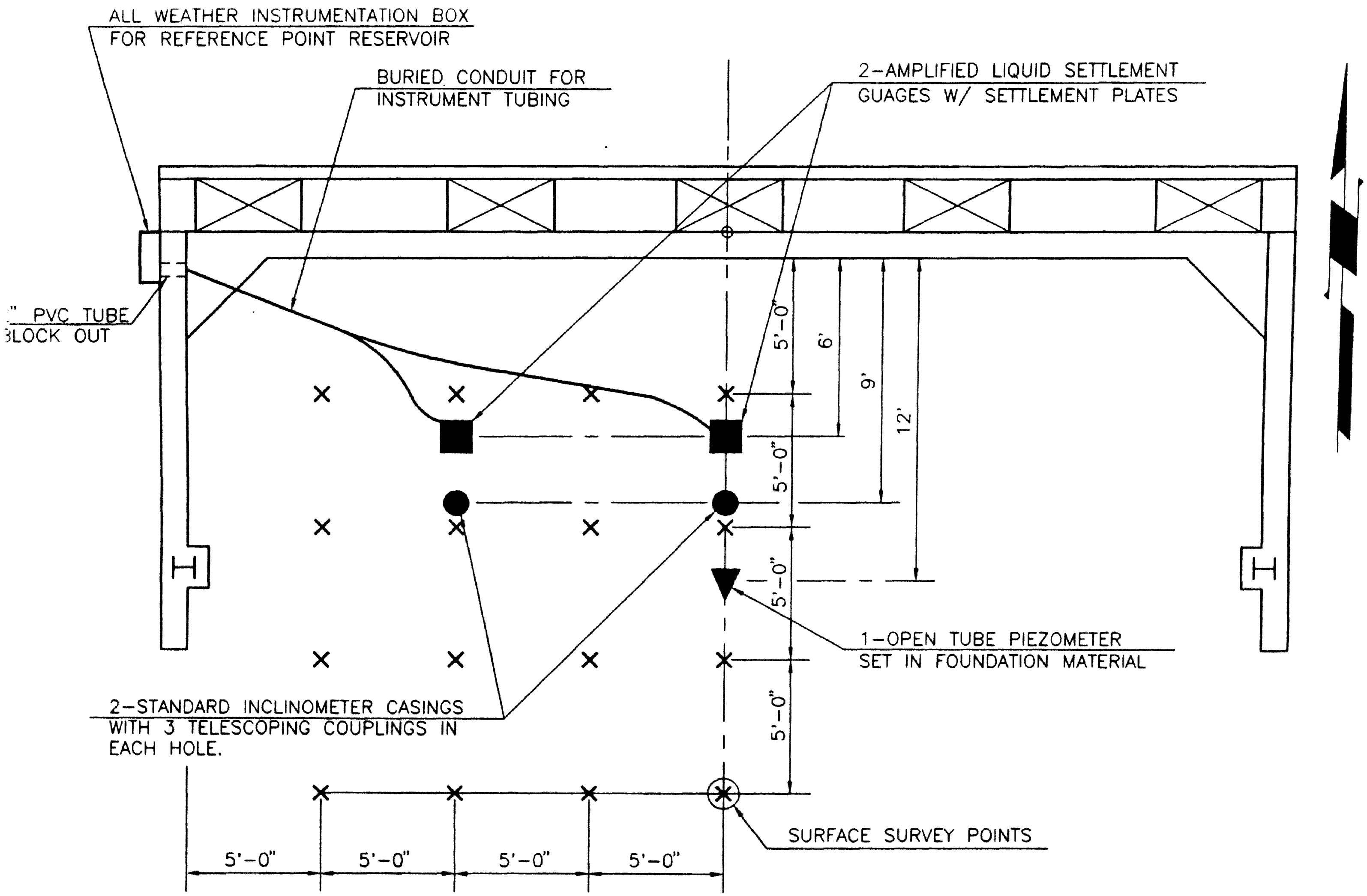

PLAN VIEW OF SOUTH ABUTMENT BRIDGE "B"

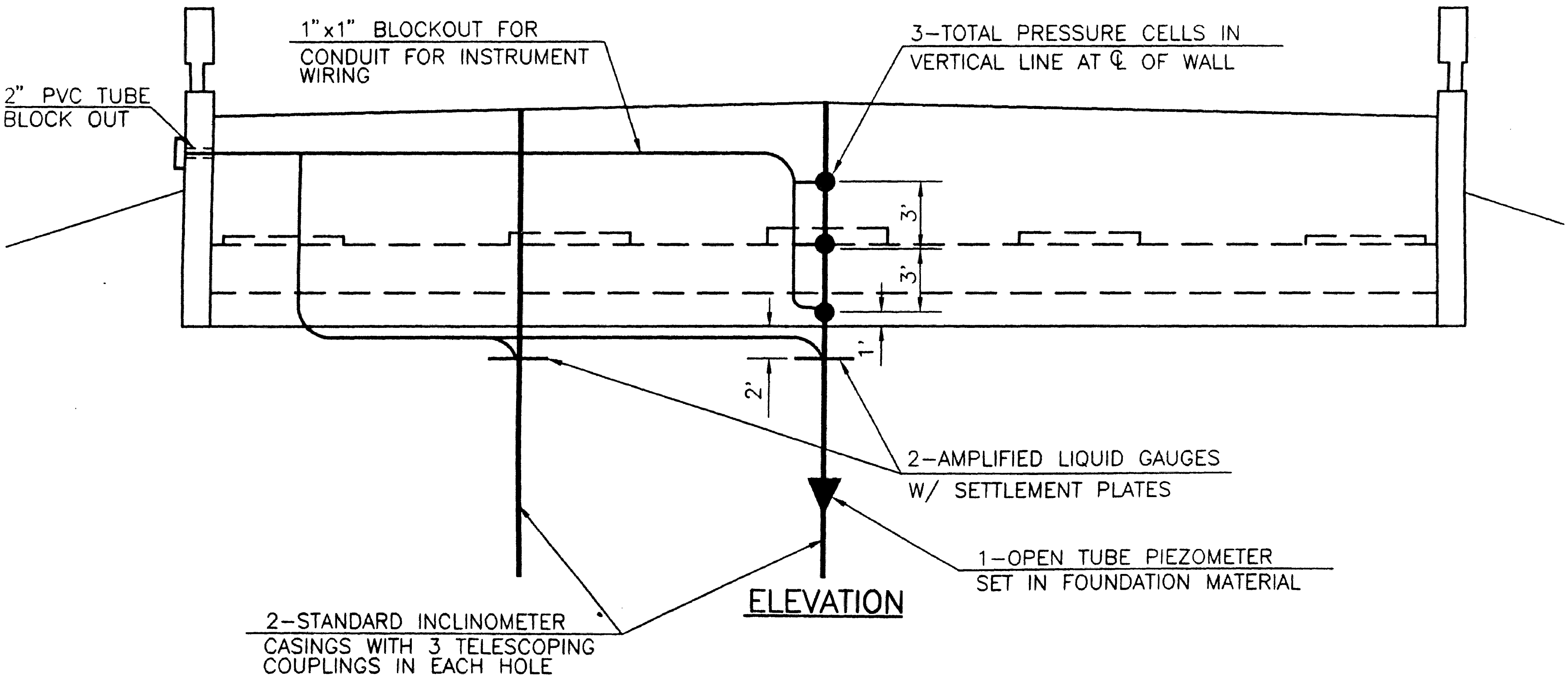
1"x1" BLOCKOUT FOR
CONDUIT FOR INSTRUMENT WIRING
3-TOTAL PRESSURE CELLS IN
VERTICAL LINE AT ℄ OF WALL
2" PVC TUBE
BLOCK OUT
3'
3'
1'
2'
2-AMPLIFIED LIQUID GAUGES
W/ SETTLEMENT PLATES
1-OPEN TUBE PIEZOMETER
SET IN FOUNDATION MATERIAL
2-STANDARD INCLINOMETER
CASINGS WITH 3 TELESCOPING
COUPLINGS IN EACH HOLE

ELEVATION

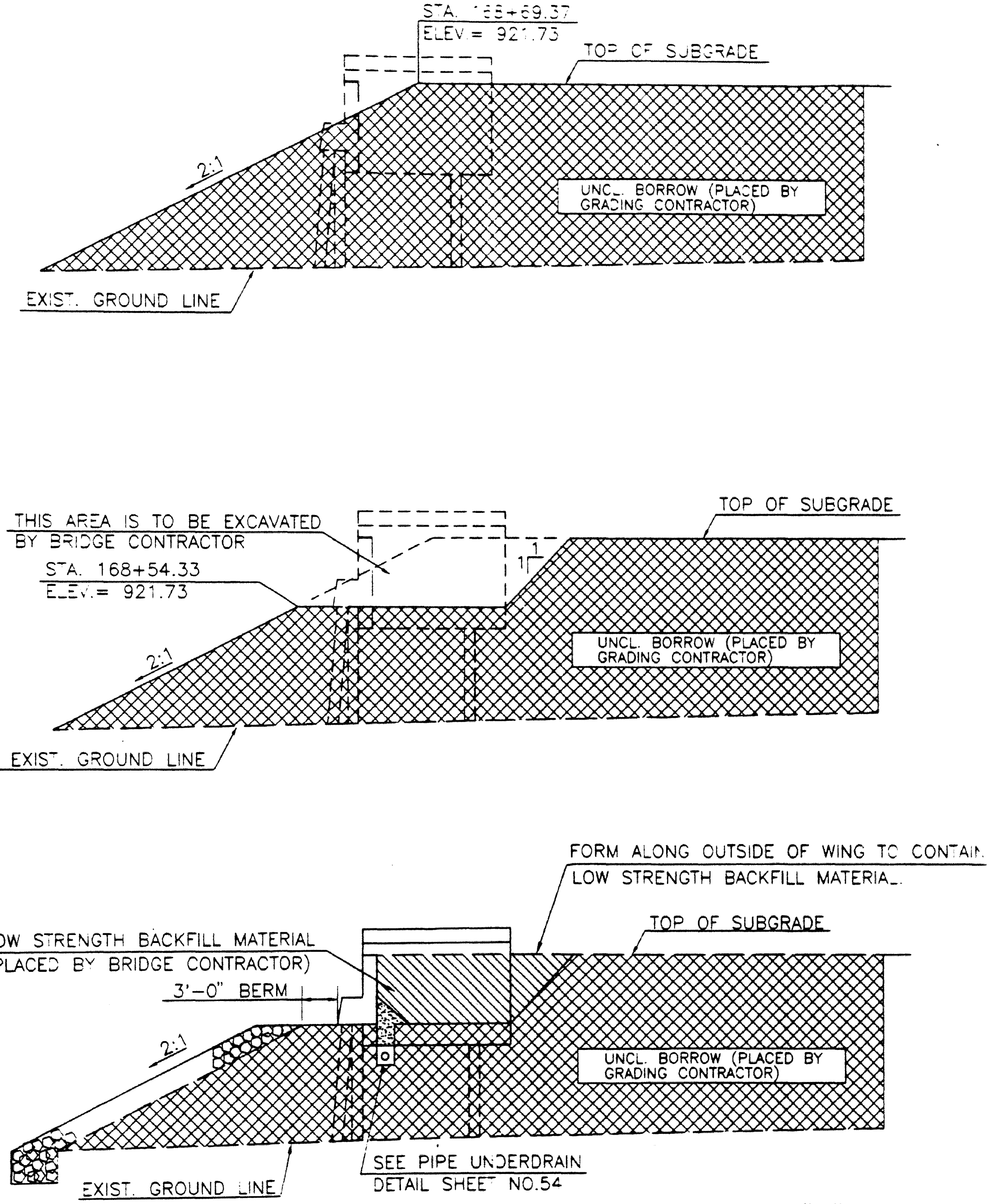

BRIDGE HEADER BEHIND NORTH ABUTMENT BRIDGE "B"

(LOW STRENGTH BACKFILL MATERIAL)

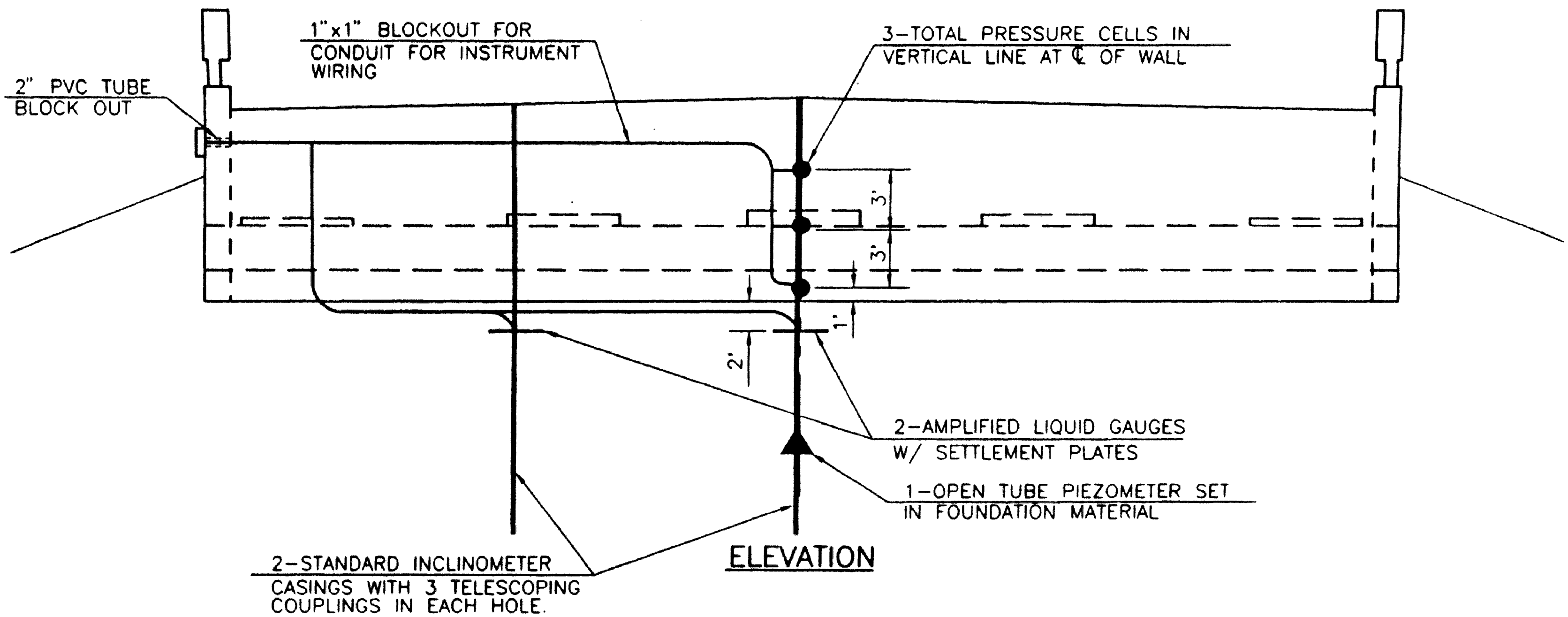
1"x1" BLOCKOUT FOR
CONDUIT FOR INSTRUMENT
WIRING
3-TOTAL PRESSURE CELLS IN
VERTICAL LINE AT ℄ OF WALL
2" PVC TUBE
BLOCK OUT
3'
3'
1'
2'
2-AMPLIFIED LIQUID GAUGES
W/ SETTLEMENT PLATES
1-OPEN TUBE PIEZOMETER SET
IN FOUNDATION MATERIAL
ELEVATION
2-STANDARD INCLINOMETER
CASINGS WITH 3 TELESCOPING
COUPLINGS IN EACH HOLE.

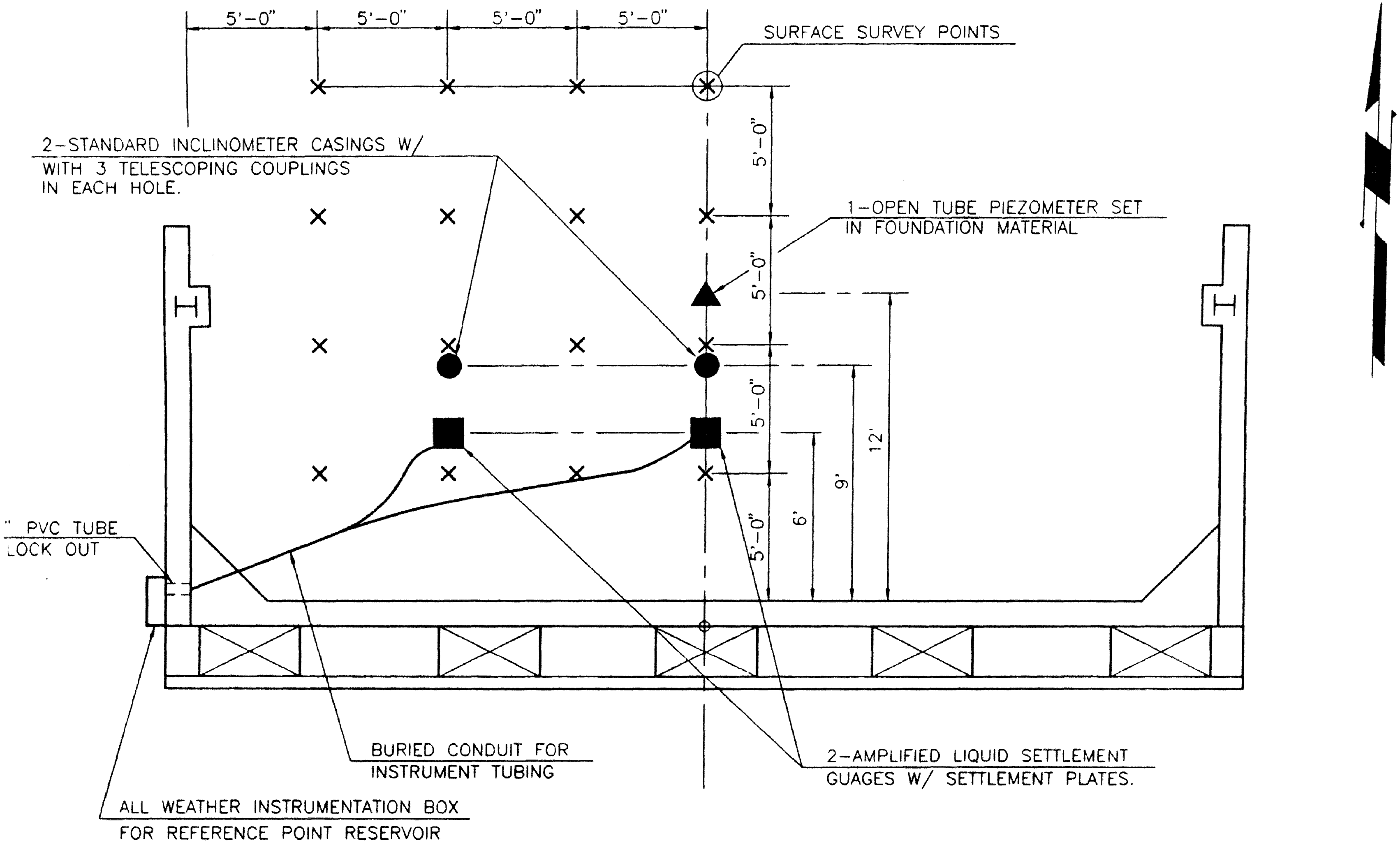

PLAN VIEW OF NORTH ABUTMENT BRIDGE "B"

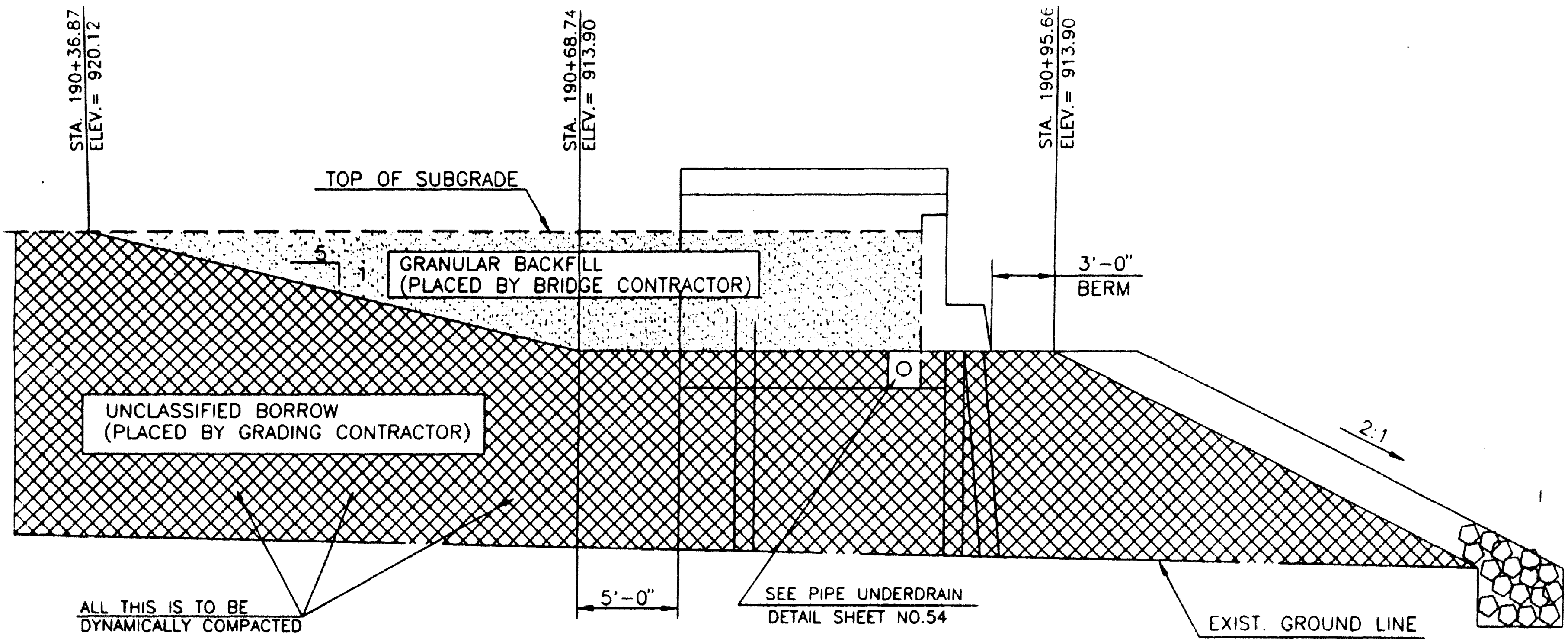

BRIDGE HEADER BEHIND SOUTH ABUTMENT BRIDGE "C"

(DYNAMIC COMPACTION)

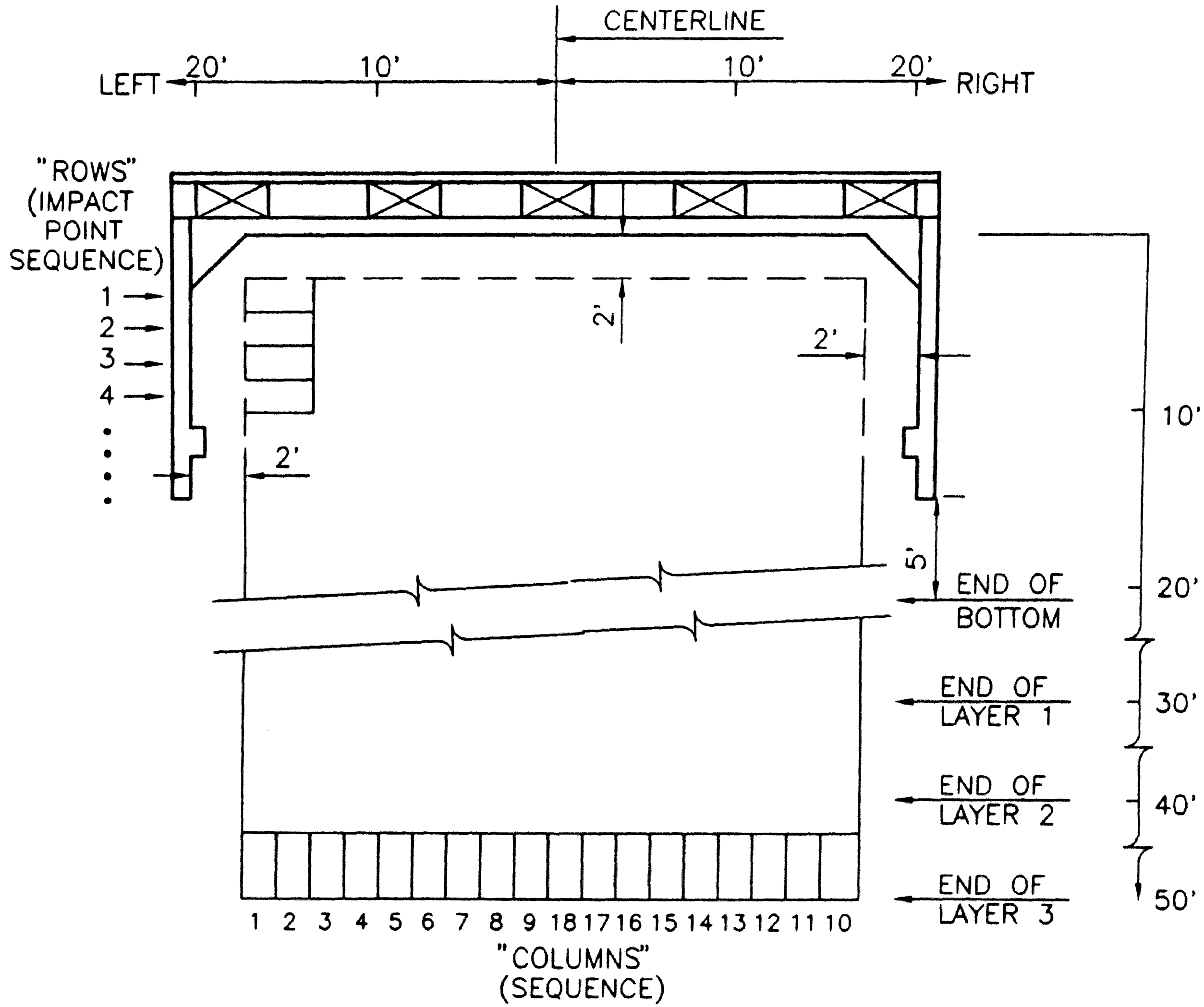

IMPACT SEQUENCE DIAGRAM

SEE SEPECIAL PROVISIONS

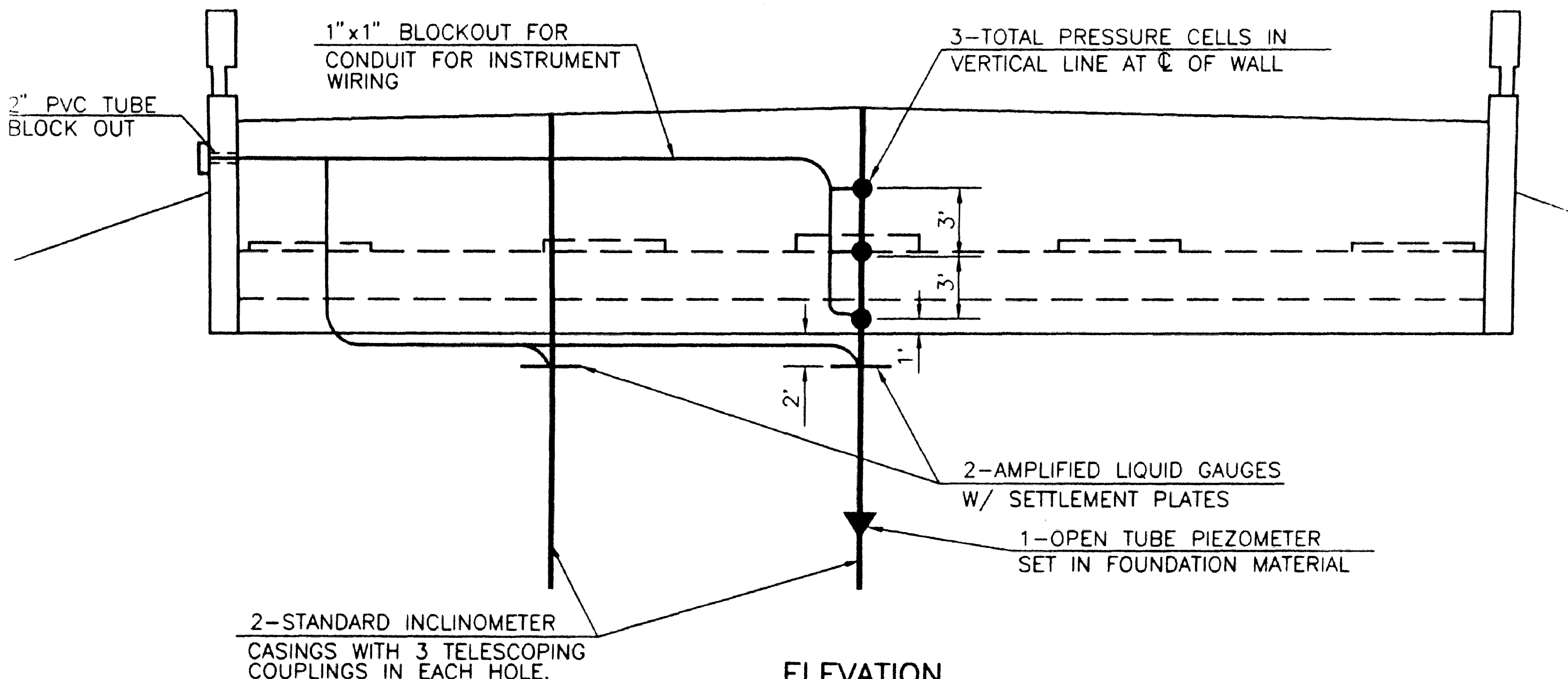
1"x1" BLOCKOUT FOR
CONDUIT FOR INSTRUMENT
WIRING
3–TOTAL PRESSURE CELLS IN
VERTICAL LINE AT ℄ OF WALL
2" PVC TUBE
BLOCK OUT
3'
3'
1'
2'
2–AMPLIFIED LIQUID GAUGES
W/ SETTLEMENT PLATES
1–OPEN TUBE PIEZOMETER
SET IN FOUNDATION MATERIAL
2–STANDARD INCLINOMETER
CASINGS WITH 3 TELESCOPING
COUPLINGS IN EACH HOLE.

ELEVATION

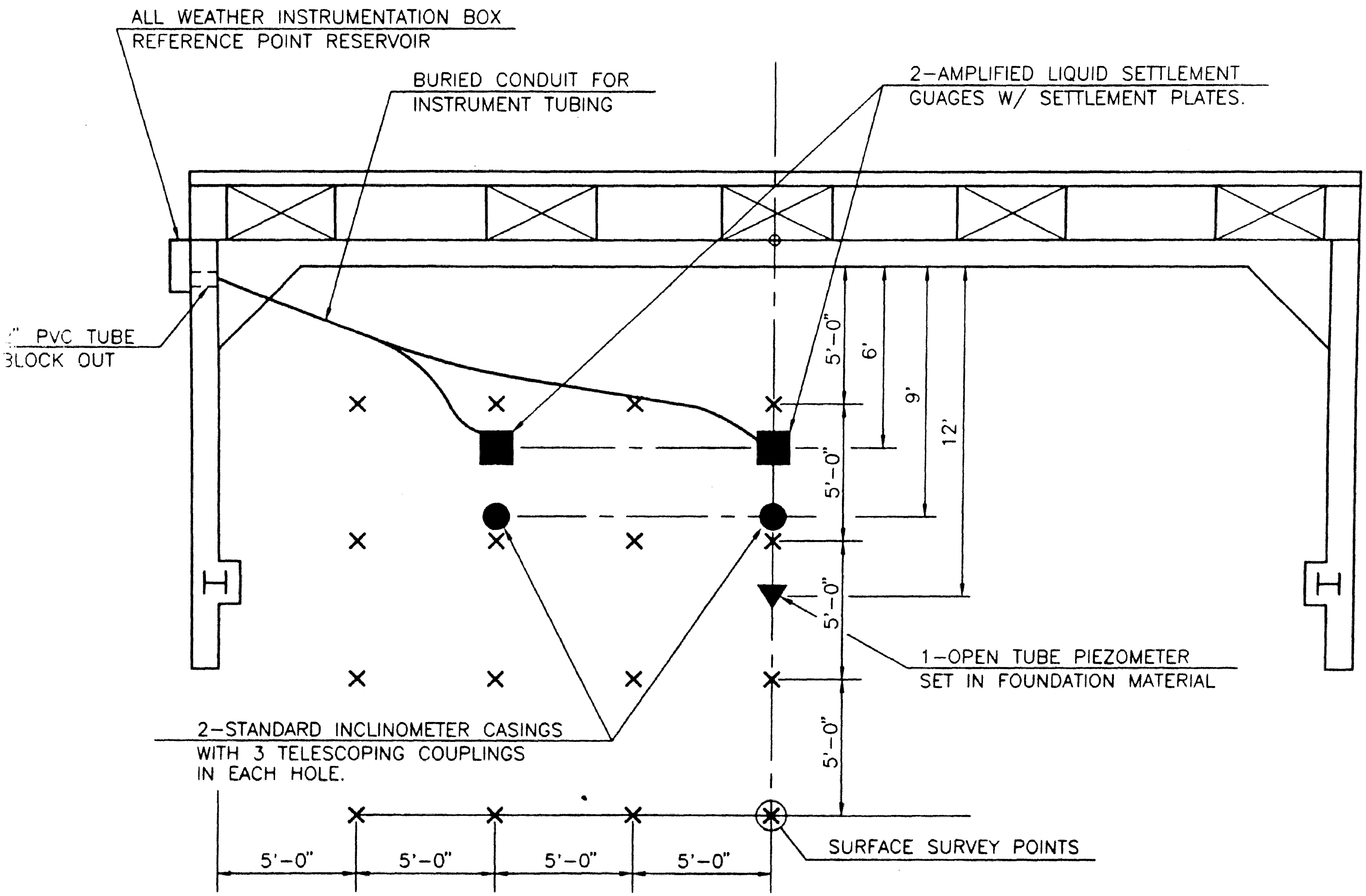

PLAN VIEW OF SOUTH ABUTMENT BRIDGE "C"

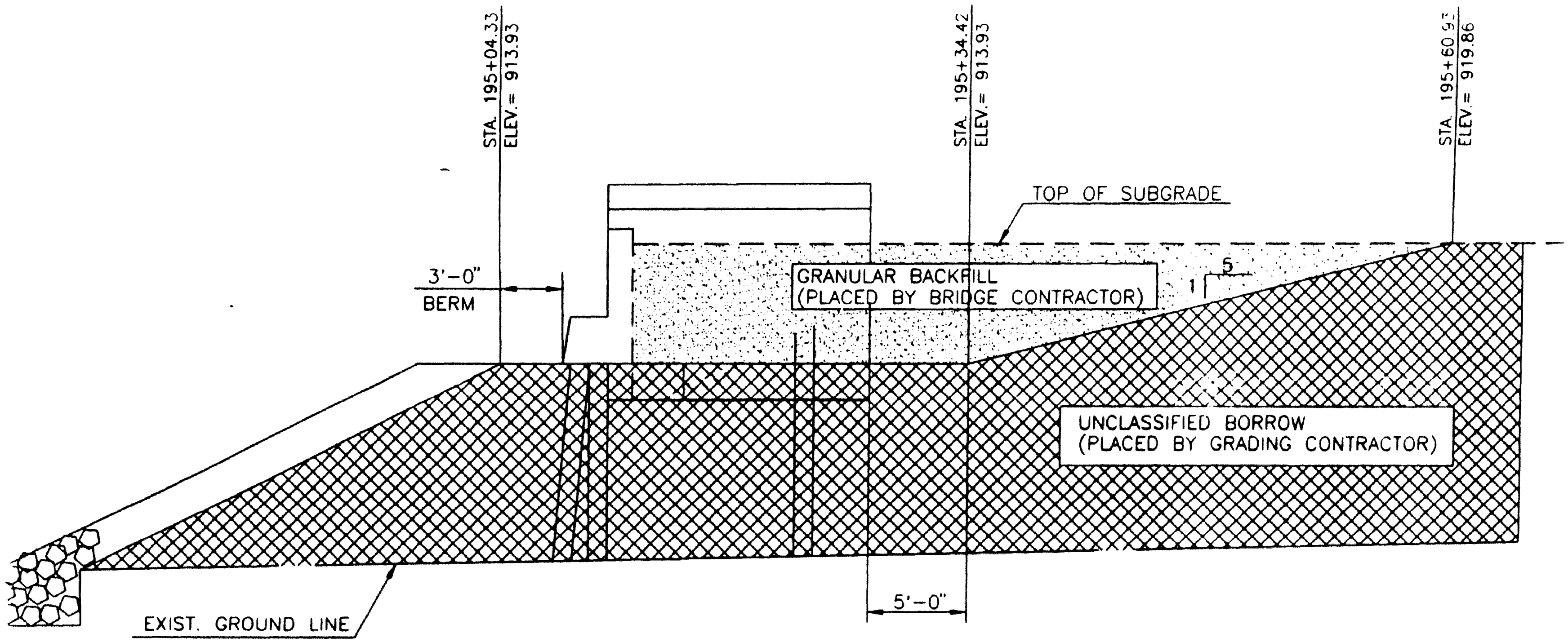

BRIDGE HEADER BEHIND NORTH ABUTMENT BRIDGE "C"

(GRANULAR BACKFILL EMBANKMENT)

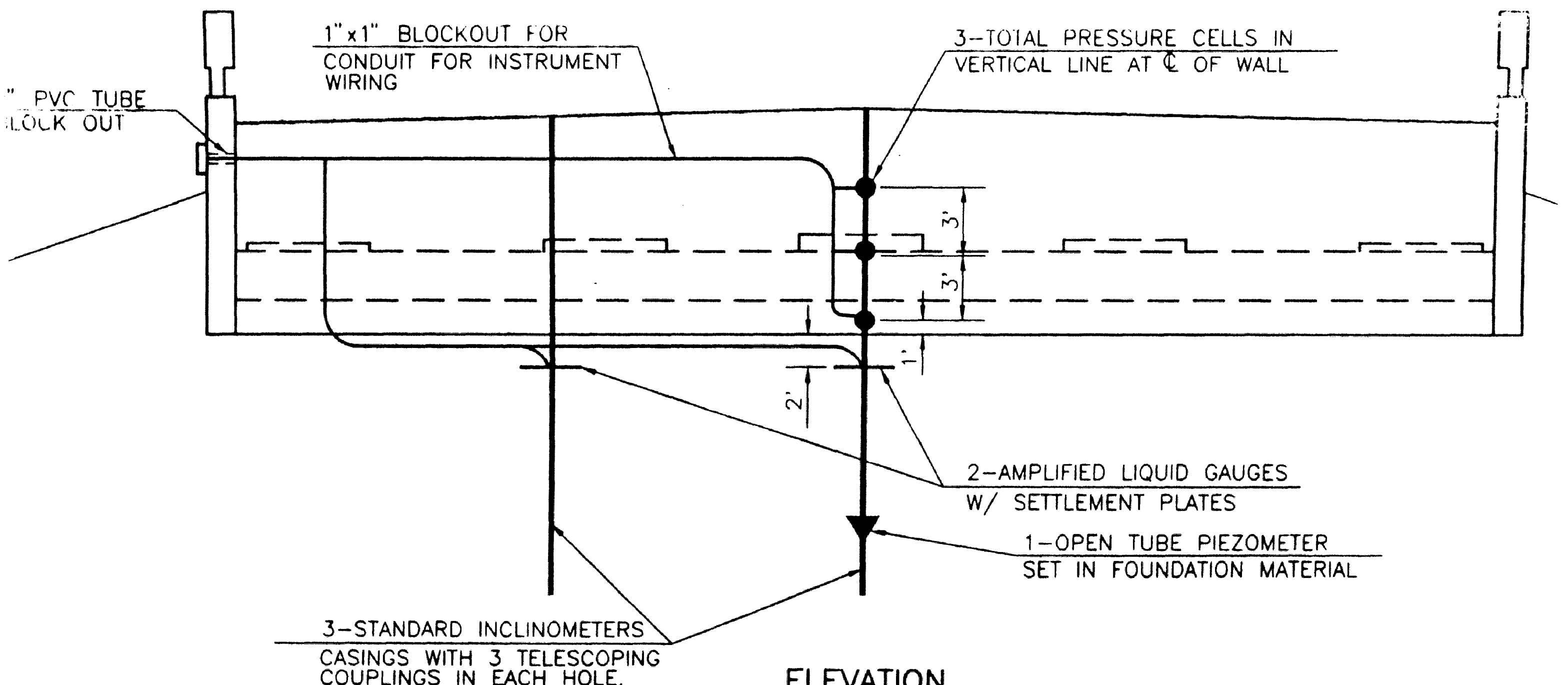
" PVC TUBE
LOCK OUT
1"x1" BLOCKOUT FOR
CONDUIT FOR INSTRUMENT
WIRING
3–TOTAL PRESSURE CELLS IN
VERTICAL LINE AT ℄ OF WALL
3'
3'
1'
2'
2–AMPLIFIED LIQUID GAUGES
W/ SETTLEMENT PLATES
1–OPEN TUBE PIEZOMETER
SET IN FOUNDATION MATERIAL
3–STANDARD INCLINOMETERS
CASINGS WITH 3 TELESCOPING
COUPLINGS IN EACH HOLE.

ELEVATION

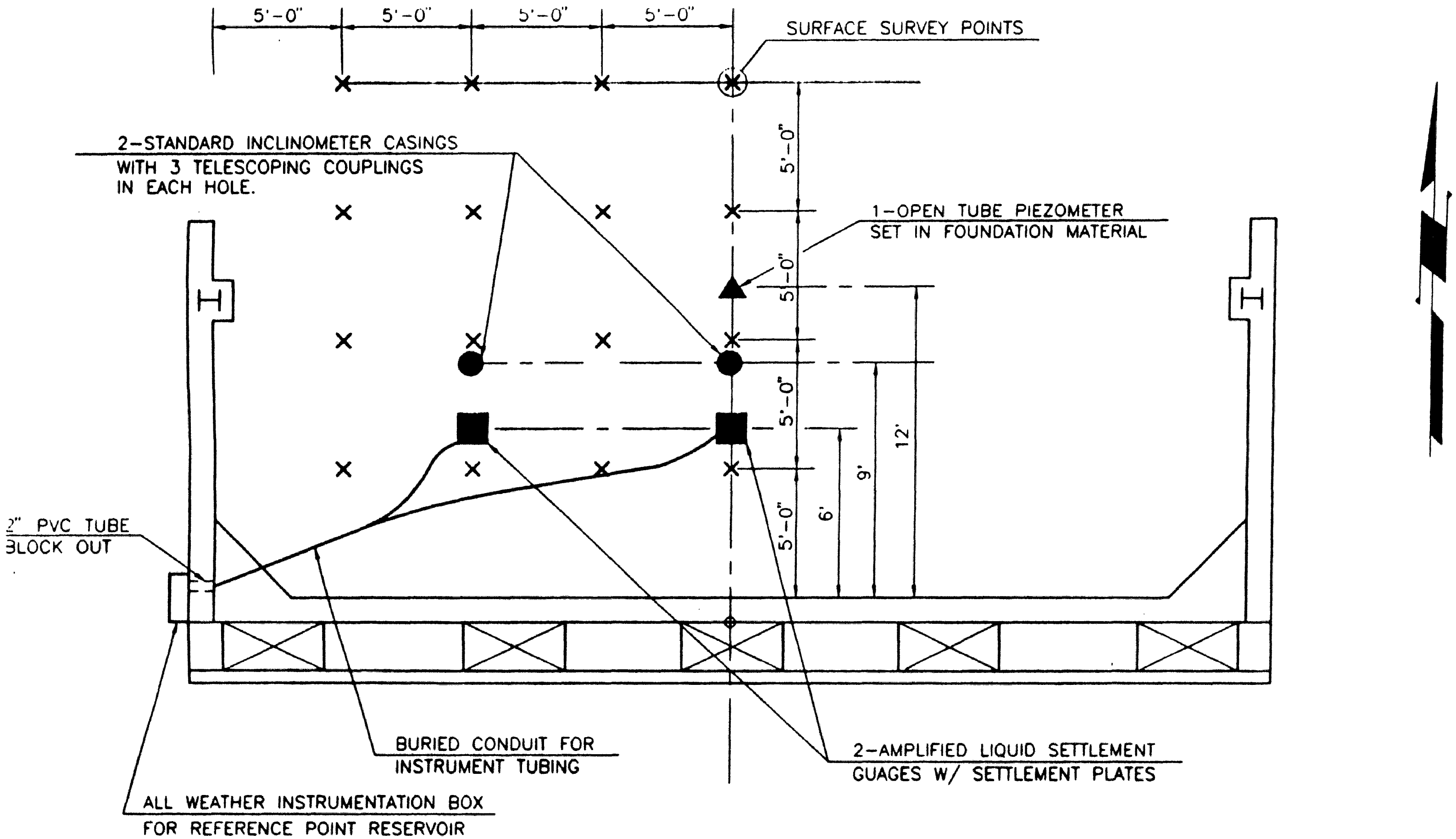

PLAN VIEW OF NORTH ABUTMENT BRIDGE "C"

2

VITA

Arthur J. Schwidder

Candidate for the Degree of

Master of Science

Thesis: ESTIMATION OF STRESS AND DEFORMATION PARAMETERS AT SALT FORK RIVER BRIDGES ON US 177

Major Field: Civil Engineering

Biographical:

Personal Data: Born in Oak Park, Illinois, on June 6, 1970, son of Jack and Jean Schwidder.

Education: Graduated from Edmond Memorial High School, Edmond, Oklahoma in May 1988; received Bachelor of Science degree in Civil Engineering from Oklahoma State University, Stillwater, Oklahoma in May 1993. Completed the requirements for the Master of Science Degree with a major in Civil Engineering at Oklahoma State University, July 1994.

Experience: Employed by Oklahoma State University as a laboratory instructor for the Surveying I and II classes, 1992 to 1993; employed by Oklahoma State University as a graduate research assistant, 1993 to present.

Professional Memberships: American Society of Civil Engineers